

For Reference

NOT TO BE TAKEN FROM THIS ROOM

Ex LIBRIS
UNIVERSITATIS
ALBERTAEENSIS



THE UNIVERSITY OF ALBERTA

RELEASE FORM

NAME OF AUTHOR	MAN KWONG LAWRENCE LEUNG
TITLE OF THESIS	A STUDY OF PHOTOGRAPHIC GAMMA RAY DOSIMETRY IN THE DETERMINATION OF DEPTH DOSES AND ISODOSE DISTRIBUTIONS
DEGREE FOR WHICH THESIS WAS PRESENTED	M. Sc.
YEAR THIS DEGREE GRANTED	FALL, 1977

Permission is hereby granted to THE UNIVERSITY OF ALBERTA LIBRARY to reproduce single copies of this thesis and to lend or sell such copies for private, scholarly or scientific research purposes only.

The author reserves other publication rights, and neither the thesis nor extensive extracts from it may be printed or otherwise reproduced without the author's written permission.

THE UNIVERSITY OF ALBERTA
A STUDY OF PHOTOGRAPHIC GAMMA RAY
DOSIMETRY IN THE DETERMINATION OF
DEPTH DOSES AND ISODOSE DISTRIBUTIONS

by



MAN KWONG LAWRENCE LEUNG

A THESIS

SUBMITTED TO THE FACULTY OF GRADUATE STUDIES AND RESEARCH
IN PARTIAL FULFILMENT OF THE REQUIREMENTS FOR THE DEGREE
OF MASTER OF SCIENCE

DEPARTMENTPHYSICS.....

EDMONTON, ALBERTA

FALL, 1977



Digitized by the Internet Archive
in 2019 with funding from
University of Alberta Libraries

<https://archive.org/details/Leung1977>

THE UNIVERSITY OF ALBERTA
FACULTY OF GRADUATE STUDIES AND RESEARCH

The undersigned certify that they have read, and
recommend to the Faculty of Graduate Studies and Research,
for acceptance, a thesis entitled .A Study of Photographic
Gamma Ray Dosimetry in the Determination of Depth Doses
and Isodose Distributions
submitted by .Man Kwong Lawrence Leung
in partial fulfilment of the requirements for the degree
of Master of .Science

DEDICATED TO MY PARENTS

ABSTRACT

In this project, the main consideration has been the evaluation of the usefulness of, and the difficulties associated with photographic gamma ray dosimetry.

The advantage of using a photographic method is that it facilitates the extraction of the comprehensive isodose curves of radiation fields.

However, several difficulties involving the photographic method can seriously affect the accuracy of the results thus obtained, one such difficulty being the energy dependence of film. To explain the effect of energy dependence on the accuracy of this photographic method, a model of film response to radiation in a semi-infinite phantom is proposed. The other difficulties lie in the angular dependence of the film and the conditions under which it is developed.

Methods by which individual films can be evaluated are considered so that the selection of an appropriate film for measuring the isodose curves can be made. The elimination of scattering materials can be considered as a useful method for controlling the response of the film. Good approximations to the tabulated results obtained by other measuring methods can be procured by using this elimination method. If precise results are preferred, the usefulness of the photographic method is severely limited. However, in such circumstances, a method combining LiF and film has proved acceptable.

ACKNOWLEDGEMENT

I would sincerely like to thank my supervisor, Dr. Usiskin, whose patience and guidance were instrumental to the completion of this thesis. I would also like to thank Dr. Scrimger for his critical comments during the course of my research, and for his suggestions concerning and corrections to the thesis itself.

I greatly appreciate the financial assistance from Dr. W. W. Cross Cancer Institute which enabled me to continue my research during the summer months.

With sincere gratitude, I would like to thank Dr. and Mrs. K. Scott for their encouragement and support throughout the course of this study. Thanks are also due to Dr. Scott and Dr. M. Leung for reading this thesis and for suggesting numerous improvements.

Special thanks are due to Mr. K. Liesner for letting me use his darkroom, for offering me technical assistance, and for sharing with me many stimulating ideas about photography. Thanks are also due to Mr. T. Drennan, Mr. S. Labahn and the technical staffs in Dr. W. W. Cross Cancer Institute. Without their generous help, this thesis would have been impossible to complete. Last but not least, I would like to thank Mrs. Shirley Fedorak for her attention and care in typing this difficult manuscript.

TABLE OF CONTENTS

CHAPTER	PAGE
I. INTRODUCTION	1
1.1 The Need for Photographic Dosimetry	1
1.2 Advantages and Disadvantages of the Photographic Method	3
1.3 Objectives of this Project	4
II. THEORETICAL BACKGROUND	6
2.1 Principles of Dose Distribution	6
2.1.1 The Concept of Absorbed Dose	6
2.1.2 Evaluation of Dose in a Phantom ...	7
2.2 Principles of Photographic Actions of X- and Gamma Rays	11
2.2.1 Introduction	11
2.2.2 Formation of Latent Image	12
2.2.3 Conversion of Latent Image	13
2.2.4 Action of X- and Gamma Rays on Emulsion	13
2.2.5 Relationship between Radiation Dose and Optical Density	15
2.3 Photographic Methods for Dose Measurement.	22
2.4 Energy Dependence of Photographic Emulsion	25
2.5 Angular Dependence of Film	29
III. EXPERIMENTAL SECTION	31
3.1 Photographic Gamma Ray Dosimetry	31

CHAPTER		PAGE
3.1.1	Measurement of Radiation Dose	31
3.1.2	Measurement of Depth Dose and Iso-dose Distribution	40
3.2	Processing Conditions	50
3.2.1	Modes of Film Processing	50
	(i) Automatic Processing	50
	(ii) Manual Processing	52
3.2.2	Parameters of Film Development	53
	(i) Developer	53
	(ii) Development Time	54
3.2.3	Monitoring of the Automatic Processor	57
	(i) Pattern of Variations in Processing	57
	(ii) Percentage Depth Dose Measurement	62
3.2.4	Uniformity of Film Development	65
	(i) Automatic Processing	65
	(ii) Manual Processing	67
3.3	Properties of Films	70
3.3.1	Introduction	70
3.3.2	Energy Dependence	71
	(i) Observation	71
	(ii) Comparison of Films	71
	(iii) Limited Phantom Method	80

(iv)	Effect on Penumbral Dose	
	Measurement	86
3.3.3	Angular Dependence	92
(i)	Introduction	92
(ii)	Observation	92
(iii)	Evaluation	93
(iv)	Explanation	94
(v)	Limited Phantom Method	96
(vi)	Factor Determining Angular De- pendence	97
(vii)	Low Energy Radiation	97
(viii)	Theoretical Comparison	99
(ix)	Effect on the Penumbral Dose Measurement	99
3.3.4	Effects of Development Conditions .	102
(i)	Different Developers	102
(ii)	Development Times	107
3.3.5	Stability of Latent Image	111
(i)	Introduction	111
(ii)	Experimental Conditions	111
(iii)	Observations	112
(iv)	Explanation	113
3.4	Thermoluminescent Dosimeter - Film Method	114
3.5	Plotting of Isodose Distributions	116
3.5.1	Densitometric Plotting	116

CHAPTER		PAGE
	3.5.2 Automatic (Isodensity) Plotter .	116
	(i) Introduction	116
	(ii) Basic Concepts of Plotter.	117
	(iii) Modification of Plotter ..	120
	(iv) Plotting Method and Time Consumption	124
	(v) Problem of Accuracy	125
IV.	RESULTS: APPLICATIONS	126
4.1	Uniform Beam, Homogenous Phantom	127
4.1.1	Single Radiation Field	127
4.1.2	Multiple Radiation Fields	134
4.2	Non-uniform Beam, Homogenous Phantom ..	141
4.2.1	Wedge Filter	141
4.2.2	Application of Wedge Filter	144
4.3	Uniform Beam, Inhomogenous Phantom	151
V.	CONCLUSIONS	156
5.1	Discussions and Observations	156
5.1.1	Energy Dependence.....	156
5.1.2	Techniques to reduce the Effect of Energy Dependence	158
5.1.3	Angular Dependence	162
5.1.4	Film as a Supplementary Detector	163
5.1.5	Comparisons among Films	164
5.2	Summary	168
	BIBLIOGRAPHY	170

	PAGE
APPENDIX I. PHOTOGRAPHIC EMULSIONS	175
APPENDIX II. STRUCTURE OF A DOUBLE EMUL- SION FILM	176
APPENDIX III. PATHS OF ELECTRONS THROUGH THE EMULSION	177
APPENDIX IV. TRAY METHOD OF PROCESSING FILMS	178

LIST OF TABLES

Table	Description	Page
I	Maximum Variances of Density for Different Films shown in Figure 4	41
II	Processing Times for the Automatic Processor	51
III	Monitoring of the Automatic Processor for the Period of 1 day	59
IV	Monitoring of the Automatic Processor for the Period of 1 week	60
V	Monitoring of the Automatic Processor for the Period of 6 months	61
VI	Experimental and Theoretical Estimations of Angular Dependence for both Kodak M and Ilfoline Film	95

LIST OF FIGURES

Figure		Page
1.	Dose Distribution in a Phantom	9
2.	Characteristic Curves of a film for Light and Radiation	17
3.	Methods used in the Measurement of Depth Dose and Isodose Distribution	23
4.	Characteristic Curves of Different Films	
	(i) Kodak M Film	35
	(ii) Ilfoline Film	36
	(iii) NDT 55, NDT 65 and NDT 75 Films	37
	(iv) GAF 400 and GAF 800 Films	38
	(v) Kodak AA and Fuji Medical Films	39
5.	The Structure of Full Phantom	46
6.	Automatic Processor	46
7.	Characteristic Curves of Kodak M Films in Different Developers	55
8.	Characteristic Curves of Kodak M Films at Different Development Times	56
9.	Consistency of Processing Conditions with Automatic Processor in the determination of Depth Doses	63
10.	Relative Sensitivity Graph for Kodak M and Ilfoline Films	72
11.	Depth Dose of Cobalt -60 Radiation as measured from Kodak M Films	
	(i) with Field 25 cm. ²	74
	(ii) with Field 100 cm. ²	75
	(iii) with Field 400 cm. ²	76

Figure		Page
12.	Depth Dose of Cobalt -60 Radiation as measured from Ilfoline Films	
(i)	with Field 25 cm. ²	77
(ii)	with Field 100 cm. ²	78
(iii)	with Field 400 cm. ²	79
13.	Depth Dose of Cobalt -60 Radiation as measured from Different Films in Full Phantom	
(i)	with Field 25 cm. ²	82
(ii)	with Field 100 cm. ²	83
14.	Depth Dose of Cobalt -60 Radiation as measured from Different Films in Limited Phantom	
(i)	with Field 25 cm. ²	84
(ii)	with Field 100 cm. ²	85
15.	Relative Profiles of 100 cm. ² Field Cobalt -60 Radiation as measured from Ilfoline and Kodak M Films	
(i)	at Depth 4.5 cm.	88
(ii)	at Depth 16 cm.	89
16.	Angular Dependence of Different Emulsion Thicknesses in Cobalt -60 Radiation	98
17.	Effect of Different Developers in the Determination of Depth Dose of Cobalt -60 radiation as measured from Kodak M Films	
(i)	with Field 25 cm. ²	104
(ii)	with Field 100 cm. ²	105
(iii)	with Field 400 cm. ²	106
18.	Effect of Different Development Times in the Determination of Depth Dose of Cobalt -60 Radiation as measured from Ilfoline and Kodak M Films	

Figure		Page
(i)	from Kodak M film with Field 400 cm. ²	109
(ii)	from Ilfoline film with Field 400 cm. ²	109
19.	Block Diagram of the Isodensity Plotter	118
20.	Calibration Graph for the Isodensity Plotter	123
21.	Isodose Distribution for a 6 x 6 cm. Field at 27 cm. SSD for Cesium -137 Beam as plotted from Kodak M Film	128
22.	Isodose Distribution for a 4 x 8 cm. Field at 15 cm. SSD for Cesium -137 Radiation as plotted from Kodak M Film	129
23.	Isodose Distribution for a 5 x 5 cm. Field at 35 cm. SSD for Cesium -137 Radiation as plotted from Kodak M Film	130
24.	Isodose Distribution for a 5 x 5 cm. Field at 80 cm. SSD for cobalt -60 Radiation as plotted from Kodak M Film	131
25.	Isodose Distribution for a 20 x 20 cm. Field at 80 cm. SSD for Cobalt -60 Radiation as measured from Ilfoline Film	132
26.	Isodose Distribution for a 10 x 20 (10) cm. Field at 80 cm. SSD for Cobalt -60 Radiation as measured from Ilfoline Film	133
27.	Resultant Isodose Distribution obtained by combining Two Cesium -137 Fields (10 x 10 cm., 27 cm. SSD) in Opposition 20 cm Apart	136
28.	Resultant Isodose Distribution obtained by combining Two Cobalt -60 Fields (10 x 20 (10) cm., 80 cm. SSD) in Opposition 20 cm Apart	137
29.	Resultant Isodose Distribution for three 6 x 6 cm Cobalt -60 Fields at SSD 80 cm.	139
30.	Resultant Isodose Distribution for four 8 x 15 cm. Cobalt -60 Fields at 80 cm. SSD arranged as Two Opposing Pairs	140
31.	Isodose Distribution for a 10 x 8 (w), 80 cm. SSD, Cobalt -60 Beam modified by a 45° wedge filter	142

Figure		Page
32.	Isodose Distribution for a 10 x 8 (w) cm., 80 cm SSD, Cobalt -60 Beam modified by a 60° wedge filter	143
33.	Isodose Distribution for a 10 x 8 (w) cm., 80 cm. SSD, Cobalt -60 Wedge Field with an Effective Angle of 30° obtained from a 45° wedge and an Open Field	145
34.	Isodose Distribution for a 10 x 8 (w) cm., 80 cm. SSD, Cobalt -60 Wedge Field with an Effective Angle of 30° as obtained from a 60° wedge and an Open Field	146
35.	Resultant Isodose Distribution for Two Opposing 8 x 8 (w) cm., 80 cm. SSD, Cobalt -60 Beams modified by a 45° wedge filter at the level of the tonsil area of the Rando Phantom	147
36.	Resultant Isodose Distribution for Two Opposing 8 x 8 (w) cm., 80 cm. SSD, Cobalt -60 30° Wedge Fields for the same contour and target volume as in Fig. 35	148
37.	Resultant Isodose Distribution for Two Opposing 8 x 8 (w) cm., 80 cm. SSD, Cobalt -60 Beams modified by a 45° Wedge Filter for same contour and target volume as in Fig. 35 (Redrawn from print-out of PC-12 computer).	150
38.	Calibration Graph for Lithium Fluoride (TLD) and Film (NDT55)	153
39.	Isodose Distribution for a 6 x 6 cm. Field at 80 cm. SSD for Cobalt -60 Radiation at the level of the tonsil area	154
40.	Comparisons of Depth Doses as measured from Kodak M Films by Different Investigators	165
41.	Comparisons of Depth Doses as measured from Different Single Emulsion Films	167

LIST OF PHOTOGRAPHIC PLATES

Plate	Description	Page
I.	Ilfoline Film Exposed by Parallel Method	43
II.	Ilfoline Film Exposed by Perpendicular Method	45
III.	Two Opposing Fields Exposed on Ilfoline Film	48
IV.	Kodak M Film Exposed by Parallel Method	66

CHAPTER I

INTRODUCTION

In planning radiotherapy treatment, to ensure that maximum dosage by radiation is given to the tumor while the adjacent normal tissue receives a minimal dosage, it is necessary to know the precise location and size and the possible extensions of the tumor. In addition, information concerning the radiation beam in use has to be ascertained in order to form reasonable estimates of the dosages that will be received by malignant and normal tissue respectively. One of the important representations of the radiation beam, as it penetrates the tissues, is the isodose chart, which quantitatively describes the relative distribution of radiation doses in the tissues.

1.1 The Need for Photographic Dosimetry

The usual procedure for obtaining such isodose charts involves the use of an ionization chamber for measuring the radiation dose in a tissue-equivalent material, such as water. As approximate point detection is desirable, an ionization chamber of small diameter is directly inserted into the material and points of equal dosage are measured. These points are connected together to give an isodose line; finally, these lines, each representing a different isodose level, are placed together in their appropriate locations on the basis of data obtained from the tissue-equivalent material to form the complete isodose chart for that

particular radiation field. This method is usually extremely time- and space-consuming, even with an automatic device to map the isodose lines.

It is apparent that this method of producing isodose charts may be too laborious and is only expedient for a few specially selected isodose distributions. Since a fairly large number of dose distributions in different situations are required for planning treatments, a simple and generally effective method of obtaining isodose charts becomes preferable. Alternative methods aimed both at reducing the time and labour involved and at giving satisfactory results have been developed; one of these is the photographic method. As film is generally easily accessible to most radiology departments, it would be convenient to employ films to extract information about isodose distributions. Granke et al. (1954) and Mauderli et al. (1960), among others, have shown that photographic dosimetry may furnish isodose charts very rapidly when the film is exposed to radiation in a tissue-equivalent material.

Photographic dosimetry has widespread applications in the field of health physics. Probably the best known is in the monitoring of radiation doses to personnel. If suitable methods are used, the developed film taken from the film badge can provide a permanent quantitative record of a person's exposure to radiation.

1.2 Advantages and Disadvantages of the Photographic Method

An extremely useful feature of film as a dosimeter, especially in the measurement of penetrating radiation such as x- and gamma rays, is its high spatial resolution. The reason for this high spatial resolution is that the basic unit for the detection of radiation, a silver halide crystal, usually does not exceed a few microns in size. The relatively compact dimensions of film also give it a great advantage over other detectors in that it can be directly inserted into the material under investigation or into the radiation field with a minimal perturbation of its spatial distribution. Because of the high spatial and virtually continuous resolution, information about dose distributions in various planes of the radiation field can be stored simultaneously in the film over relatively large areas. Thus all that is required is to extract the pertinent information from the film, whereas in other dosimeters, such as the ionization chamber, this kind of spatial storage of information is usually not available. Films are therefore ideal for mapping out the two-dimensional dose distributions of radiation fields.

Even though film can be a more advantageous medium for obtaining information about the radiation field, the silver halide crystal, the measuring device contained in the film, actually introduces a disadvantage, by being much more sensitive to low energy than to high energy radiation.

This phenomenon is usually referred to as the energy dependence of the dosimeter. Mainly because of this energy dependence, accurate dosimetry with photographic emulsions can be difficult, especially in a situation where a large amount of low energy radiation, such as scattered radiation, is present.

Although the compact size of the film causes little perturbation to the radiation field, its sheetlike structure introduces the element of angular dependence. This angular dependence occurs if the responses of the film are not identical when the plane of the film is oriented at different angles to the incident beam of radiation. The amount of angular dependence is also a function of the energy of the radiation used and of the nature of the individual film. Large angular dependence in a film can give rise to serious errors in the interpretation of information stored in the film.

It is well known in photography that the development conditions, such as the developers used and the development times involved, can alter the nature of the developed film. Changes in development conditions apparently change the sensitivity of the silver halide grains towards radiation of different energies. This implies that the stored information in the film may be similarly changed.

1.3 Objectives of this Project

In this project, the above problems and other related

topics have been studied so that films may be used in appropriate ways to map isodose distributions and thereby to produce satisfactory, quantitatively meaningful results.

CHAPTER II

THEORETICAL BACKGROUND

2.1 Principles of Dose Distribution

2.1.1 The Concept of Absorbed Dose

The potential for successful treatment of a tumor by radiation depends upon the differential between the dose received by the tumor and that delivered to the normal tissue. Therefore the radiation dose given to a mass of tissue is of paramount interest.

When x- or gamma rays traverse a thickness of tissue, they deliver their energy via a two-step sequence (Attix, 1968):

- 1) they transfer their energy to the atomic electrons
- 2) the electrons deposit their kinetic energy along their tracks by means of the multiple coulombic force interactions with electrons of the atoms in the tissue.

Energy deposition by ionizing radiation is the energy imparted to matter per unit mass of irradiated material at the point of interest and is defined as 'absorbed dose'.

The volume in question must be large enough to contain many interactions and to be traversed by many particles. At the same time, it should be small enough that further reduction in size would not appreciably change the measured values of absorbed dose (I.C.R.U., 1968).

Consequently,

$$(1) \quad D = \Delta E_d / \Delta m$$

where D is the absorbed dose and ΔE_d is the energy imparted to a mass Δm of this volume. The symbol Δ precedes the symbols for the quantities that may be involved in a statistical averaging procedure. What is really meant by energy imparted is simply that particular part of the energy which is removed from the radiation field as a whole, excluding that part given to the increase of rest mass of the atom, since the latter part has no known biological effects (Neufeld, 1971).

Historically, the unit of absorbed dose was known as the rad which was defined as 100 ergs per gram. Recently, the International Commission on Radiation Units and Measurements (I.C.R.U.) (Wyckoff et al., 1976) has recommended the adoption of the gray (Gy), i.e. the S.I. unit, joule per kilogram (J/Kg), when applied to absorbed dose unit. Thus,

$$(2) \quad 1 \text{ gray} = 100 \text{ rad} = 1 \text{ J/Kg}$$

2.1.2 Evaluation of Dose in a Phantom

In the determination of the distribution of absorbed doses in a medium, there are two useful, basic concepts: central axis depth dose and the off-axis dose evaluation.

The dose given to a tumor is usually evaluated from the data obtained from a semi-infinite, homogenous medium of unit density called a phantom, which can simulate the

absorption and scattering of radiation in normal tissue.

An important aspect of the description of the radiation beam as an integral part of treatment planning is the central axis depth dose. The depth dose, D_t , is the radiation dose delivered at a certain depth, t , within a phantom (Hendee, 1973). It is usually expressed as a percentage of the maximum dose, D_m , which may occur at the surface or at an equilibrium depth, depending upon the quality of the radiation used, so that

$$(3) \quad \text{percentage depth dose} = (D_t/D_m) \times 100$$

In general, the most frequently encountered form of depth dose is the central axis depth dose which is simply the depth dose measured along the central axis of the radiation field in the phantom (Fig. 1). British Journal of Radiology Supplement 11 (1972) is a catalogue of tabulations of central axis depth doses for different radiation qualities.

Mathematically, the dose at a certain depth on the central axis in the phantom can be considered as (Bagne, 1974):

$$(4) \quad D_t(t, W, f, E) = A \exp^{-\mu t} S_t(t, W, f, E)$$

where W is the field size at the depth t in the phantom and f the source-skin distance (radiation source to skin or phantom surface distance). A is the dose of the primary radiation given to the surface or at the equilibrium depth, t_m . μ is the linear attenuation coefficient of the phantom

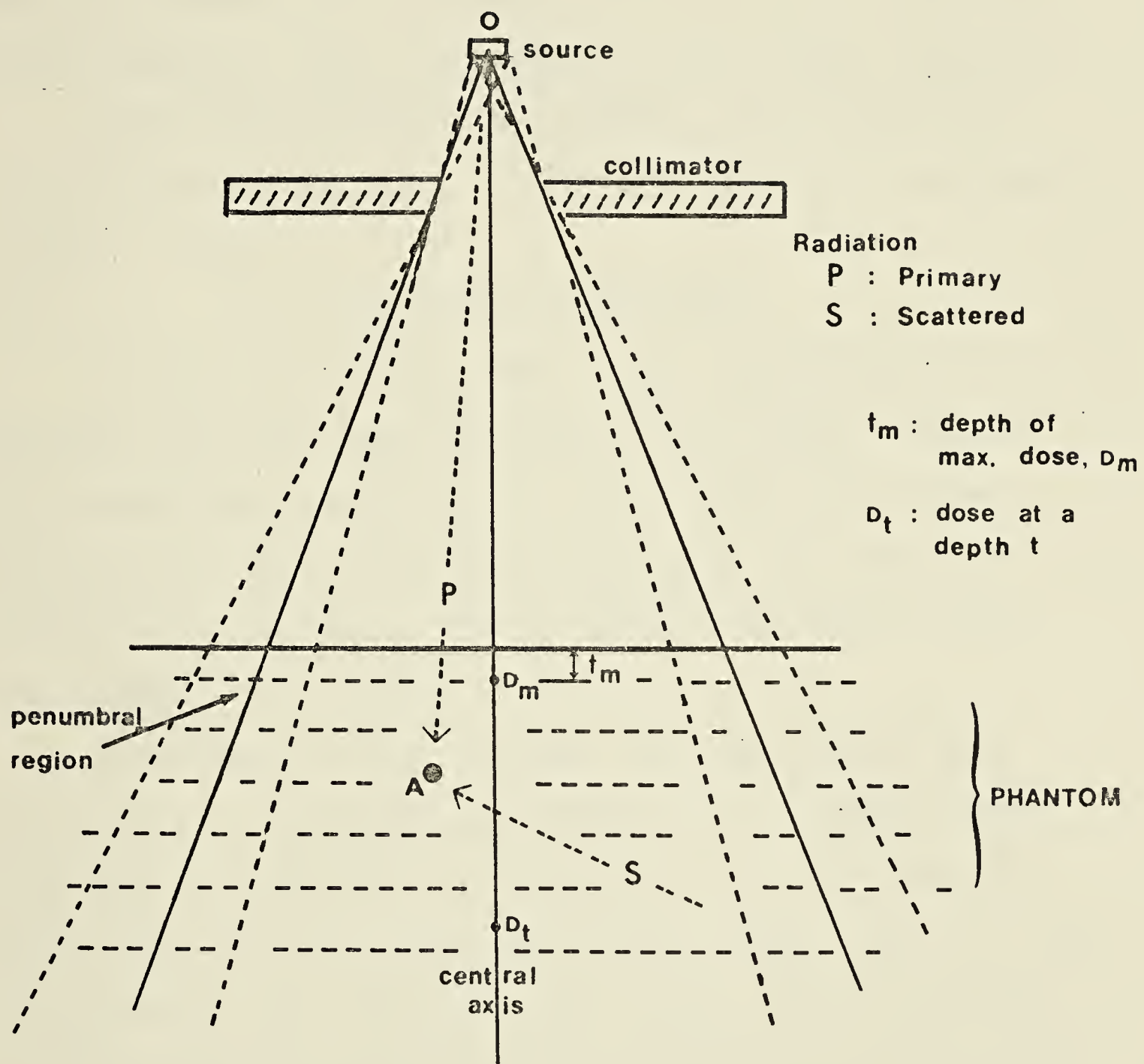


Fig. 1 Dose Distribution in a Phantom

and depends on the radiation quality as well as on the phantom material. S_t is a numerical scatter factor accounting for the radiation scattered to the point of interest in the phantom, and E the energy of the primary radiation.

A fair approximation to equation (4) has been discussed by Mauderli et al. (1960) and Johns and Cunningham (1974). It is

$$(5) \quad D_t = D_m \exp^{-\mu t} (t_m + f)^2 / (t + f)^2$$

In order to evaluate the isodose distribution in a phantom, off-axis doses also have to be known. Much of the fundamental background for calculating the isodose distribution from the central axis depth dose has been developed by Clarkson (1941), Meredith and Neary (1944) and Quimby et al. (1956).

According to their concept, the total dose, D , at any point, A , in a phantom exposed to x- or gamma radiation can be considered as being made up of two distinct parts (Fig. 1): (a) that due to the primary beam, P , coming directly from the radiation source, and (b) that due to the scattered radiation, S , contributed from the whole phantom, so that

$$(6) \quad D = P + S$$

The primary contribution may be considered as the radiation dose given to the zero area field anywhere within the geometrical beam, and can be readily obtained from the published standard data, such as British Journal of Radiology

Supplement 11 (1972). The scattered radiation dose can be deduced from the standard dose data, assuming a primary dose of 1 gray.

2.2 Principles of Photographic Actions of X- and Gamma Rays

2.2.1 Introduction

Commercially available films usually possess a single or double emulsion layer on a blue or transparent base made of cellulose or polyester. The element in the emulsion sensitive to the x- or gamma rays and to the secondary electrons is the microscopic silver halide crystals (grains) which are randomly suspended in the gelatin of the emulsion (Appendix II).

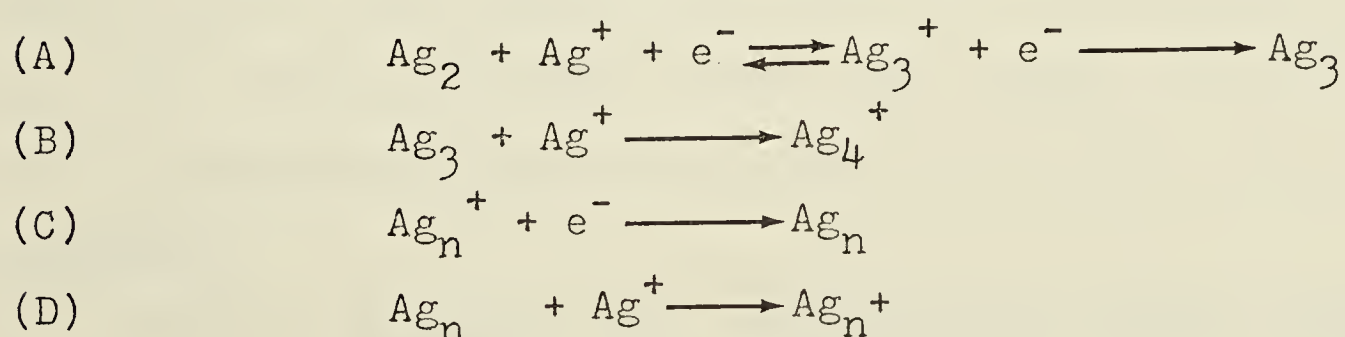
Radiation absorbed in an individual grain makes it alter in such a way that it reacts differently toward certain chemical reducing agents known as developers. These grains are reduced to metallic silver by the developer, while the grains unaffected by radiation are not reduced at all. The term 'latent image' is used to describe this developable state of the silver halide grains. Such an image is not susceptible to direct observation. Fixing and washing help to cleanse the excessive developer still present on the film emulsion, remove the undeveloped grains, and make the developed grains permanent for observation (Herz, 1969).

2.2.2 Formation of Latent Image

The theory of latent image was advanced by Gurney and Mott (1938) and Mitchell (1957). The essentials of their theory are that, if sufficient energy is imparted to the silver halide grains by radiation, one or more bound electrons are raised into the conduction band of the crystals and migrate until trapped at certain sensitivity centers, which are usually provided by dislocations and impurities present in the crystals. The positive silver ions are attracted to the electrons and subsequently neutralized (equation A). This process is repeated at suitable sites and if silver atoms are aggregated to a sufficient degree, the grains will be rendered developable (equations B, C, and D). If insufficient number of atoms of silver are trapped, this aggregate is referred to as the 'sub-latent image' state which can only be distinguished from the latent image state through precise development conditions. Upon receiving a further amount of energy from the radiation, this sub-latent image is then converted to the latent image.

Chemical Equations for the Formation

of the Latent Image (after Mitchell, 1957)



2.2.3 Conversion of Latent Image

The essential step in processing is development, i.e. the conversion of a latent image into a visible quantity of metallic silver in the shape of the image. The chemical process of development is one involving the oxidation-reduction reaction, wherein the silver halide grains in the film emulsion are reduced by the developer solution to black metallic silver.

The most common chemicals used to bring out the latent image are the combination of elon (N-methyl-p-aminophenol sulfate) and hydroquinone (p-dihydrobenzene). It is usually the composition of the solution that plays the dominant role in determining the photographic properties of the developer (Jacobson and Jacobson, 1972). The basic chemical reaction can be as (Jacobi and Paris, 1968):



2.2.4 Action of X- and Gamma Rays on Emulsion

When the indirectly ionizing particles, x- or gamma rays, pass through the emulsion layer of a film, some of the photons may be absorbed and some scattered, but a majority of them are actually transmitted. A high energy photon must first generate the directly ionizing particles, i.e. the recoil electrons, which then impart the majority of the exposing actions to the grains to render them developable.

With x- or gamma rays, especially the higher energy

ones, electrons originate predominantly from the medium surrounding the film emulsion, but some may come from the silver halide grains, gelatin and the film base. Therefore, it should be recognized that the major contribution to the formation of latent images is not caused directly by the x-rays absorbed, but indirectly by the electrons (Hine, 1950; Herz, 1969).

Rendering a grain developable depends upon the amount of energy imparted by radiation to it. The efficiency with which energy is imparted to the grains to render them developable is often referred to as the "quantum efficiency", which may be expressed as the number of silver halide grains rendered developable per absorbed quantum (Bromley and Herz, 1950).

It has been well established (Silberstein, 1922; Silberstein and Trivelli, 1930; Charlaby, 1940; Pelc, 1945) that one x- or gamma ray quantum absorbed leads to the developability of at least one grain. With higher energy x- or gamma rays, several grains may be rendered developable per quantum absorbed (Bromley and Herz, 1950; Greening, 1951). This may serve as an indication that the extra grains are made developable by the secondary electrons accompanying the primary photons.

However, for light photons, it was found (Webb, 1948; Okrent and Solomon, 1951) that the quantum efficiency is always less than one. The number of hits, i.e. the inter-

actions that may impart energy to the grain, which are required by light photons to render one single grain developable, are in the order of 10 to 40, depending upon the wavelength of light in question and the sensitivity of the individual grains. Therefore, it can be concluded that the transfer of energy by a light photon in a single hit is insufficient to render a grain developable.

Since electrons of sufficient energy can make several grains developable, the number of radiation particles required to produce a given optical blackness may be as much as 2 or 3 powers of ten less than the number of photons involved in an exposure to light (Hamilton, 1966). The electrons of high energy do not necessarily expend all their energy in the emulsion. Those with 1 MeV and higher energy travel in an almost straight path through the film (Hine, 1954) as shown in Appendix III. Electrons with energies as low as 3 to 4 keV have been observed to render a grain developable (Pniewski, 1952).

2.2.5 Relationship between Radiation Dose and Optical Density

With a given radiation dose, the degree of blackness of a developed film can be quantitatively measured by its optical density.

The optical density (or simply density) is defined as the logarithm to the base 10 of the ratio of the intensity, I_0 , of an incident light beam to the intensity, I_t ,

of the beam which is transmitted through the silver deposits in the emulsion, so that

$$(7) \quad D = \log (I_o/I_t)$$

where D is the optical density.

The density of a developed film depends upon the nature of the developer and of the film itself in addition to the development conditions.

The characteristic curve of a particular film is a representation of the relationship between the dose received by the film and its corresponding density.

One of the forms of characteristic curve frequently encountered is represented by plotting the density against the logarithm to the base 10 of the exposure, also known as the 'H & D' curve, after Hurter and Driffield (1890) who first suggested this quantitative description of the effect of light on photographic films (Fig. 2 i).

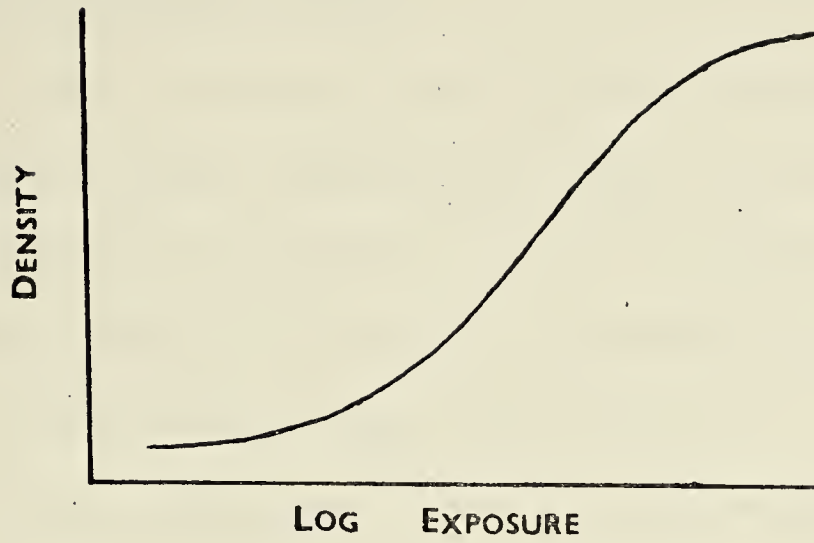
A widely used equation, equation (8), describes reasonably well the density of an emulsion given an exposure (E) by light (Barkas, 1963):

$$(8) \quad D = c(\log E) + D_o$$

where D_o is the density of the background fog which comes from the unexposed grains and the film base, and

c is defined as $dD/d(\log E)$, the instantaneous slope of the curve.

For x- and gamma rays, the above equations may not reveal the true nature of the action of the radiation on



i. 'H AND D' CURVE FOR LIGHT

REPRESENTATIONS OF RESPONSE
CURVE FOR RADIATION

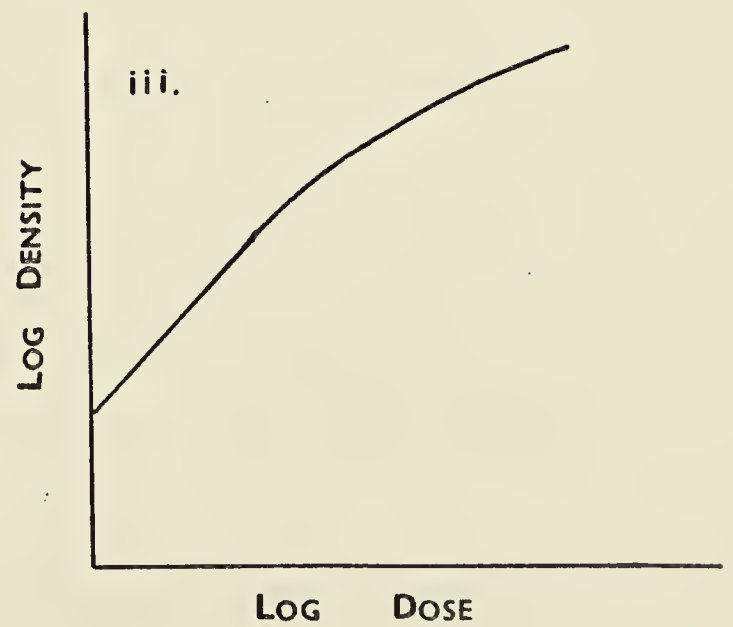
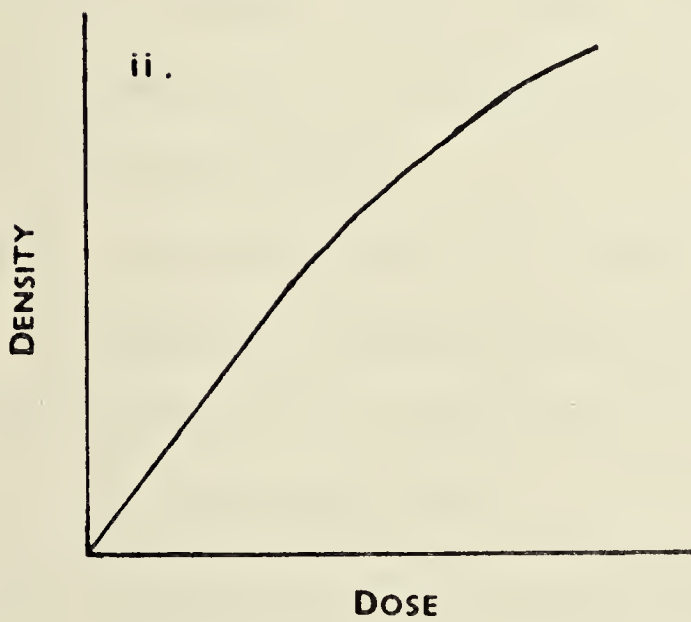


Fig. 2 Characteristic Curves of a film
for Light and Radiation

the silver halide grains.

The more frequent form of representation of the relationship between density and dose is simply the plot either of density against dose on a linear scale, or of log density against log dose, depending upon the purpose of the illustrations (Fig. 2 ii & iii). Both graphs reveal a linear function up to a certain given dose. In addition to the development conditions, the physical and chemical properties of the emulsion play a major role in defining the shape and the length of this linearity (Farnell, 1966).

In order to explain the linear function between the dose and the density of an emulsion in the case of x- and gamma rays, certain assumptions have to be made (Becker, 1966; Dudley, 1968; Herz, 1969):

- 1) Each grain is rendered developable by a single hit of radiation,
- 2) All grains have the same projectional area, a , which does not change during the course of development,
- 3) There is no absorption or scattering of the radiation in the emulsion,
- 4) Irradiation is in the direction normal to the plane of the film,
- 5) The film emulsion is considered as one elemental layer,
- 6) The sensitivity of all grains to high energy photons and ionizing particles is approximately the same.

(Sensitivity at a particular radiation energy is defined as the reciprocal value of the dose required to produce a certain density. The sensitivity of a grain varies with the energy of the incoming radiation.)

Using the above assumptions, the theoretical relationship between dose and density can be considered. Let X be the dose given to the emulsion. A fractional dose of X , x , is imparted to a grain. Let it be presumed that m , the least number of hits, is sufficient to render the grain developable and that, after developability has been attained, no excessive energy is wasted upon the grain.

After a hit of radiation to the grain, the probability of rendering it developable is proportional to the fractional dose, x , given to it. Then after m hits, the final probability of rendering it developable is proportional to the multiplication of the individual fractional doses or x^m , since all m hits are mutually independent (Farnell, 1966).

As x is a fractional dose of X , therefore the final probability is proportional to X^m . If, after these m hits, this probability can cause n grains per unit area to be developable, and if all these n grains are fully processed, the density is (Farnell and Solman, 1963)

$$(9) \quad D = 2.6(\log e)na$$

Since one hit is assumed to render one grain developable, i.e. $m=1$, therefore X ought to be proportional to n .

Then, according to equation (9), D is proportional to n . The final linear function can be obtained:

$$(10) \quad D = kX$$

where k is a proportionality constant.

Equation (10) has been derived experimentally by Dudley (1954) who used electrons and beta rays as a source of radiation. He also pointed out that the least number of hits, m , in his experiments, was about one.

He suggested further that the general function should be

$$(11) \quad D = kX^m$$

If logarithms are taken on both sides of the above equation,

$$(12) \quad \log D = \log k + m \log X$$

then this indicates that the slope of the line, in a $\log D$ vs $\log X$ plot, should reveal the approximate number of hits required to render a grain developable. In a comparative study between high energy x-rays and electrons, Tochilin and Golden (1961) have proved both types of radiation possess essentially identical characteristic curves for the same emulsion.

For high dose, X , given to the emulsion in which energy may be wasted on the developable grains, Silberstein (1922), Webb (1939), Tellez-Plasencia (1954) used a more comprehensive equation to describe the characteristic curve:

$$(13) \quad D = D_m (1 - \exp^{-aX})$$

with D_m as the maximum density of the emulsion for that

particular radiation energy so that $D_m = 2.6(\log_{10} e) aN$, where N is the number of grains per unit area in the emulsion. From equation (13), the linearity of the function between the dose and density for small doses in which no energy is wasted is self-evident.

To give some examples to show the validity of general equation (13): Price (1973) and Wrinkler and Levin (1966) found experimentally that, by using a sufficient number of terms of the series expansion of equation (13), they could effectively describe their characteristic curves of Kodak M films, even up to a density of 6.

It is apparent that no films can adhere strictly to the assumptions made; yet, they may provide a fairly good approximation to the physical situation if mono-energetic x- or gamma rays are considered.

The average grain size is usually about a micron; therefore, the average grain area is of the order of 10^{-12} m^2 , with the assumption that the grains are spherically shaped. The grains are considered to be randomly distributed in the emulsion. But when they are measured with a light beam which is normally incident to the plane of the film, they appear closely packed. The usual resolution in the measurement of the optical density is about 1 mm in diameter. The area resolved, then, is approximately 10^{-6} m^2 . The number of grains viewed is of the magnitude from 10^3 to 10^4 on the average. This suggests that, even

if individual grains do differ from one another in their properties, random measurements probably give consistent average data.

The linear function between the dose and the density, i.e. $D = kX$, of a film will be of primary concern throughout this study of photographic dosimetry. The representation of this function (either in linear scale or in log vs log scale) will henceforth be termed as the characteristic curve of that film. This characteristic curve as drawn in either mode therefore explicitly illustrates the property of linear response of the film.

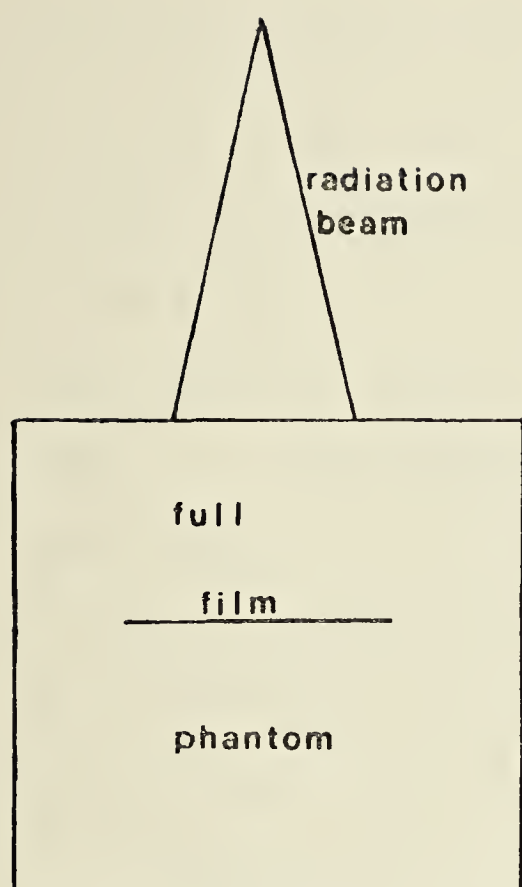
2.3 Photographic Methods for Dose Measurement

There are two basic methods of using films to measure the percentage depth dose of gamma rays in a phantom:

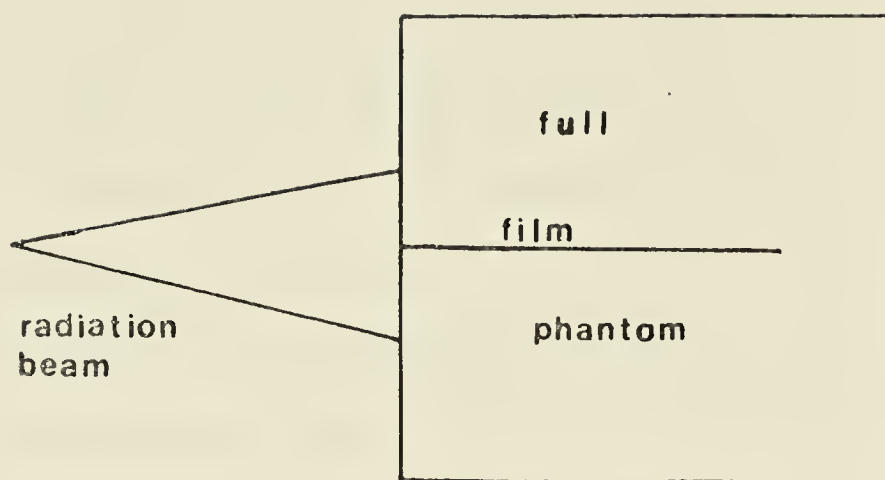
- 1) the perpendicular (Mauderli et al., 1960) (Fig. 3 i)
- and 2) the parallel methods (Granke et al., 1954) (Fig. 3 ii).

In the following discussion, all doses delivered to the film are assumed to be such that the densities recorded lie within the linear response of the characteristic curve.

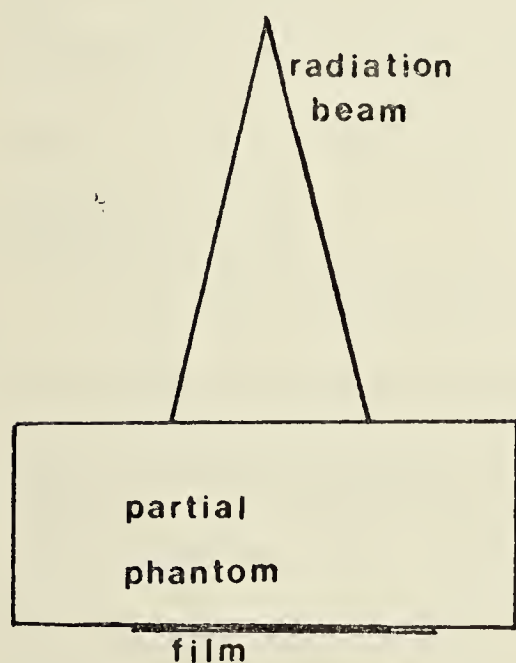
In the perpendicular method, the films are inserted into the phantom at various depths and placed perpendicularly to the direction of the incident primary beam. The density measured at the center of the radiation field which has been recorded by an individual film represents



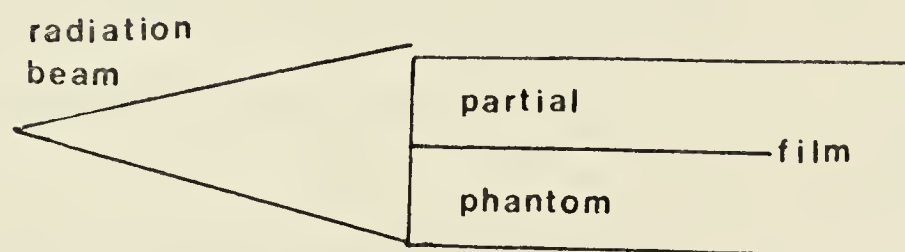
i. perpendicular method



ii. parallel method



iii. perpendicular method
without backing phantom



iv. limited phantom method

Fig. 3 Methods used in the Measurement of
Depth Dose and Isodose Distribution

the dose delivered on the axis at that particular depth. The percentage depth dose can then be evaluated by measuring the maximum density, D_m , at the depth where the maximum dose occurs, and the density, D , at the required depth and by using the following equation:

$$(14) \quad \text{percentage depth dose} = (D - D_o) / (D_m - D_o) \times 100$$

where D_o is the inherent background fog.

$D - D_o$ is usually referred to as the net density. Equation (14) holds true as long as the densities used lie within the linear portion of the characteristic curve.

Similarly, in the parallel method, one film can be inserted inside the phantom and the incident radiation is directed parallel to the plane of the film. The densities measured along the central axis of the radiation field are used to calculate the percentage depth dose by means of equation (14).

In both methods, the densities that are recorded in the entire plane of the film represent the doses received. However, the parallel method provides a two-dimensional depiction of the dose distribution which includes the depth dose along the entire central axis. This method is therefore far more desirable and useful than the perpendicular one.

In a semi-infinite phantom irradiated by gamma rays, a spectrum of radiations which include low energy scattered radiations in addition to the primary beam is generated

(Derbowka and Cormack, 1964; Bruce and Pearson, 1962).

Film is known to show energy dependent response, i.e. the sensitivities of the film vary according to the radiation energies. Hence, the percentage depth dose measured via optical density may not be the same as that measured by an ionization chamber whose sensitivity remains, for all practical purposes, constant for a wide range of radiation energies.

Techniques aimed at reducing errors of the photographic emulsion were sought. In the perpendicular method, the phantom materials behind the film were removed (Fig. 3 iii) so that no backscattered radiations could reach it (Mauderli et al., 1960). In the parallel method, however, the phantom materials were removed from both sides of the film (Fig. 3 iv) until an optimal amount of scattered radiation remained (Stanton, 1962). The depth doses obtained from the resulting optical density readings would then be consistent with the values obtained from an energy independent dosimeter. This reduction of materials in the parallel method is hence termed the 'limited phantom' method.

2.4 Energy Dependence of Photographic Emulsion

It has been mentioned in the previous section that films show an energy dependent response. In order to understand what the effect of energy dependence is on the percentage depth dose as measured by film, it is useful to formulate a model of the response of a film to the scattered

radiations in a semi-infinite phantom when it is irradiated by a primary beam.

It has also been noted that the linear function between dose and density of a film is valid if the incident dose given is small. This idea has been applied in personnel monitoring systems. In his discussion of such systems, Dudley(1968) suggested that if the energy spectrum of the radiation on a film is known, the resultant density can be converted to a dose in rad, using the appropriate values of relative sensitivity. Relative sensitivity is obtained by normalization of the sensitivities of all radiation energies to that of a given energy.

In mathematical terms, Watson (1959) and Kirchner and Ryan (1967) expressed the above ideas as:

$$(15) \quad D = \sum_{n=1}^k D_n$$

where D is the net density behind a filter of a film badge,

D_n the individual net density that results from each energy group of radiations, and

k the total number of energy groups involved.

If the dose given in each energy group is not large, linearity between dose and density is preserved. Thus,

$$(16) \quad D_n = m_n X_n$$

where m_n is the slope of the linear response, and

X_n the dose given by the n^{th} energy group.

Through the substitution of equations (16) in (15), the expression becomes

$$(17) \quad D = \sum_{n=1}^k m_n X_n$$

The above concepts can easily be extended into the present study of depth dose measurement via optical density readings. As the incident dose is usually small in an actual experimental procedure, so that density may remain in the linear portion of response, the scatter dose should be smaller still. Then, the linear response should hold true for all doses given by all energy groups.

Assuming that the film is isotropic in its response, the density at a certain depth inside the phantom can be given as:

$$(18) \quad D = m_p P + \sum_{n=1}^k m_n S_n$$

where P and m_p are the primary dose at that particular depth and the slope of the linear portion of the dose-density curve for the primary radiation respectively, and

S_n and m_n are the scatter dose from n^{th} energy group and the slope of the linear portion of density-dose curve for that energy group respectively.

Equation (18) can then serve as a basic model for the response of film emulsion to the radiations in the measurement of depth dose. Once the processing conditions are

specified, the slopes, m_p and m_n 's, may be determined and these are connected with each other via the relative sensitivity graph.

Utilizing the density-dose curve of the film for the primary radiation, the dose, X_f , as indicated by the density D of equation (18) is then

$$(19) \quad X_f = P + \sum_{n=1}^k (m_n/m_p) S_n$$

However, the actual dose, X , given to the point of interest is

$$(20) \quad X = P + \sum_{n=1}^k (S_n)$$

Since the relative sensitivity of the film, (m_n/m_p) , has been proved experimentally greater than or equal to 1, then assuming that all grains of the film are fully developed,

$$(21) \quad X_f \geq X$$

Hence, it can be expected that the depth doses detected by films should be higher than the values detected by an energy independent dosimeter.

The depth dose obtained by using an energy independent dosimeter is henceforth referred to as the accepted value. The central axis depth doses as published in British Journal of Radiology (1972) can serve as these accepted values.

It can easily be observed that unless the term S_n of equation (19) is very small as in the case of small field

size, the depth dose measured by photographic emulsion will be higher than the accepted values. Mauderli et al. (1960) reported that with a field size of only 6.7 cm.², where the scattered radiation is extremely small, the depth doses measured by film were almost identical to those of the accepted values. For larger field sizes, the depth doses were always higher than the accepted values.

2.5 Angular Dependence of Film

Because of the sheetlike configuration of film, in its response the film exhibits angular dependence to radiation, i.e. the density recorded is dependent upon the direction of the incident beam in relation to the plane of the film. The amount of angular dependence is defined as (D_θ / D_0) , where D_0 is the density obtained at normal incidence of radiation and D_θ the density measured with the same incident dose given at an angle of incidence, θ , from the normal for the plane of the film.

This dependence in films of the film badges has been extensively discussed by, among others, Ehrlich (1954), Wilsey et al. (1956), Heard et al. (1960), and Paic and Paic (1971). This problem may cause serious errors in the estimation of the radiation dose received by the wearer of the film badge.

The exhibition of angular dependence in the measurement of depth doses has been noted by Mathewson (1956), Hettinger and Svensson (1966) and Onai et al. (1970) in their studies of ionizing radiation, such as beta rays and electron beams.

The result of this dependence is that the films exposed by the parallel method failed to record the same doses as those exposed by the perpendicular method. Only a few articles (Onai et al., 1972) have pointed out the existence of angular dependence in gamma rays photographic dosimetry, but its cause is still uncertain. As both the parallel and the perpendicular methods are used in the present study, the effect of this dependence will be illustrated in section 3.3.3.

A simple, semi-quantitative elucidation of angular dependence has been advanced (Greening, 1951). Consider a parallel beam of x- or gamma rays of intensity, I , incident at an angle ϕ , from the normal for the plane of the film, directed onto an emulsion with a thickness of d , μ being the mass energy-absorption coefficient of the emulsion for the radiation energy in question. Then the energy absorbed in the emulsion is

$$I \cos \phi (1 - \exp^{-\mu d / \cos \phi})$$

if the exponent is very small, after its series expansion is evaluated, the expression becomes $I \mu d$, independent of ϕ , the angle of incidence.

However, if the exponent is not small, the percentage depression of optical density obtained at ϕ^0 , as compared to 0^0 incidence is

$$(22) \quad \frac{I(1 - \exp^{-\mu d}) - I \cos \phi (1 - \exp^{-\mu d / \cos \phi})}{I(1 - \exp^{-\mu d})} \times 100$$

$$= (1 - \cos \phi (1 - \exp^{-\mu d / \cos \phi}) / (1 - \exp^{-\mu d})) \times 100$$

The validity of expression (22) in estimating the angular dependence of a film will be pointed out in section 3.3.3.

CHAPTER III

EXPERIMENTAL SECTION

3.1 Photographic Gamma-ray Dosimetry

3.1.1 Measurement of Radiation Dose

To make use of a film as a measuring device for depth dose and dose distribution, the range of linearity between the dose given and the net density (the linear portion of the characteristic curve) for the film has to be known. In this way, the net density is linearly related to the dose.

The characteristic curves of films with respect to x- or gamma rays ought to be measured with a minimal presence of scattered radiation. To attain this objective, a small radiation field size was used. In addition, films should also be (and were) covered by a thickness of phantom material sufficient to establish the electronic equilibrium through the emulsion so as to respond to the maximum dose delivered (Greening, 1951). The maximum electron build-up for high energy radiation occurs at the equilibrium depth (Johns and Cunningham, 1974). The covering material for the films may also serve as a protection from exposure to light.

The majority of the experiments were carried out with the Picker '600' cesium-137 and AECL 'Theratron-80' cobalt-60 teletherapy units which served as the sources of gamma rays. Both Picker 'Superficial' and 'Deep' x-ray machines

provided x-rays of qualities ranging from 1.2 to 3.8 mm. Al HVL and 1.2 to 3.4 mm. Cu HVL respectively. The Half-Value Layer (HVL) of an x-ray beam is the thickness of a material which reduces the exposure rate of the beam to one-half (Hendee, 1973). The x-rays used here served primarily for the calibration of films.

To make uniform the description of the qualities of the radiation beams, the effective energies instead of the HVL's were used in the present study. The effective energy of a x-ray beam is the energy of a monoenergetic beam which is attenuated in a similar fashion to the spectrum of the x-ray radiations under consideration. British Journal of Radiology Supplement 11 (1972) provides a tabulation relating the effective energies of radiation to the HVL's of x-rays. For the x-rays used in the present study, the effective energies were obtained by interpolating on the graph of the HVL's and the effective energies as published in British Journal of Radiology Supplement 11.

In this project, several types of films were used which may be roughly grouped as follows:

I) Double emulsion

i) fast film: Kodak AA, Gevaert-Agfa (GAF) 800,
Dupont Cronex NDT 75 and 65, and Fuji
Medical film.

ii) slow film: Kodak M, NDT 55 and GAF 400.

II) Single emulsion

Ilfoline IN.3

The basic study on films was concentrated mainly on Ilfoline and Kodak M which, as pointed out in Appendix I, have been frequently used for measuring depth doses. All films mentioned above are available commercially.

To obtain the characteristic curves of a film at different radiation energies, the following calibration procedures were carried out:

- 1) For effective x-ray energies from 0.023 to 0.035 MeV of the 'Superficial' x-ray machine, the field size used was 1.5 cm. diameter at target-skin distance (TSD) of 20 cm.; for effective x-ray energies from 0.085 to 0.14 MeV of the 'Deep' x-ray machine, the field size was 9 cm.² at TSD of 50 cm. In this range of x-ray energies, the films were inserted inside a black paper cassette of thickness of about 0.1 mm.
- 2) For gamma ray energy of 0.66 MeV (cesium), with the field size of 4 cm. diameter at source-skin distance (SSD) of 27 cm., the films were inserted in a 1 mm. thick black cardboard cassette which had approximately unit specific gravity. For 1.25 MeV (cobalt) gamma ray, with the field size of 16 cm.² at SSD of 80 cm., they were set behind 0.5 cm. thick temex, a tissue-equivalent rubber (Johns and Cunningham, 1974). All radiation beams were directed perpendicularly to the

plane of the film.

In the experimental procedure, a film was cut into pieces of smaller dimensions. Individual doses were administered separately on these pieces of film so as to avoid scattered radiation resulting from the previous dose. In this method, all the exposed films originated from the same film, and thus the possibility of variation from film to film was avoided. These exposed films were taped to a leader-film and processed. The leader-film became necessary as the automatic processor (section 3.2.1) available was not able to accomodate the small sizes of the exposed films. Furthermore, all exposed films could be processed simultaneously when taped to the leader-film.

After the films were processed, their optical densities (and transmittances, if desirable) were measured using a Photovolt Corp. (New York), model 501A-52 densitometer. It gives density readings ranging from zero to three and from zero to four with a light beam resolution of diameter of 1.5 mm. and 4 mm. respectively. The majority of the optical readings were obtained with the 1.5 mm. light beam.

Fig. 4 i, ii, iii, iv, and v show the characteristic curves at different radiation energies of Kodak M, Ilfoline, NDT 55, 65 and 75, GAF 400 and 800, Kodak AA and Fuji Medical respectively on a log density against log dose scale as measured by using the above method. The results for

Fig. 4 1
Characteristic Curves
of Kodak M Films

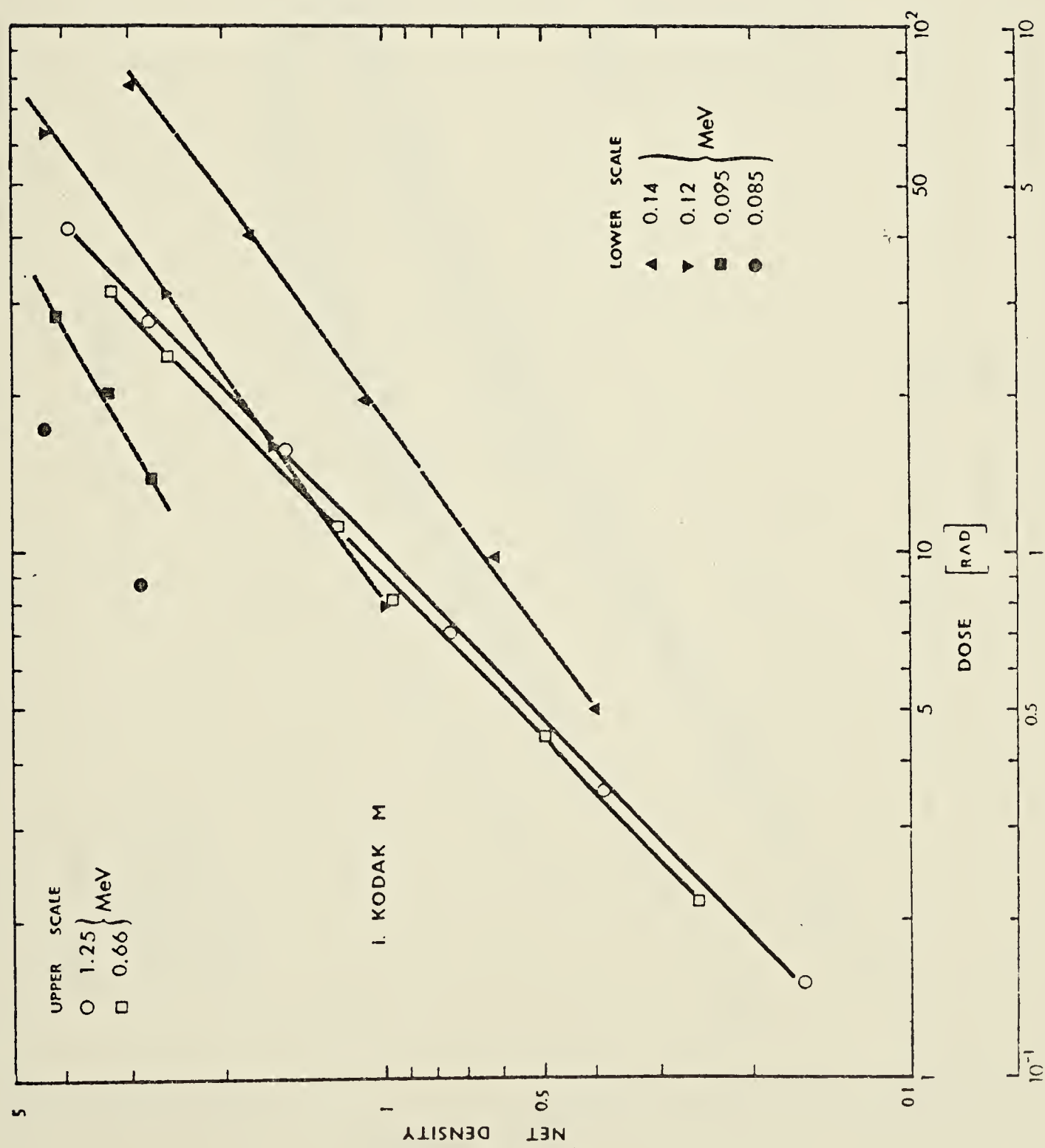


Fig. 4 ii Characteristic Curves of Ilfoline Film

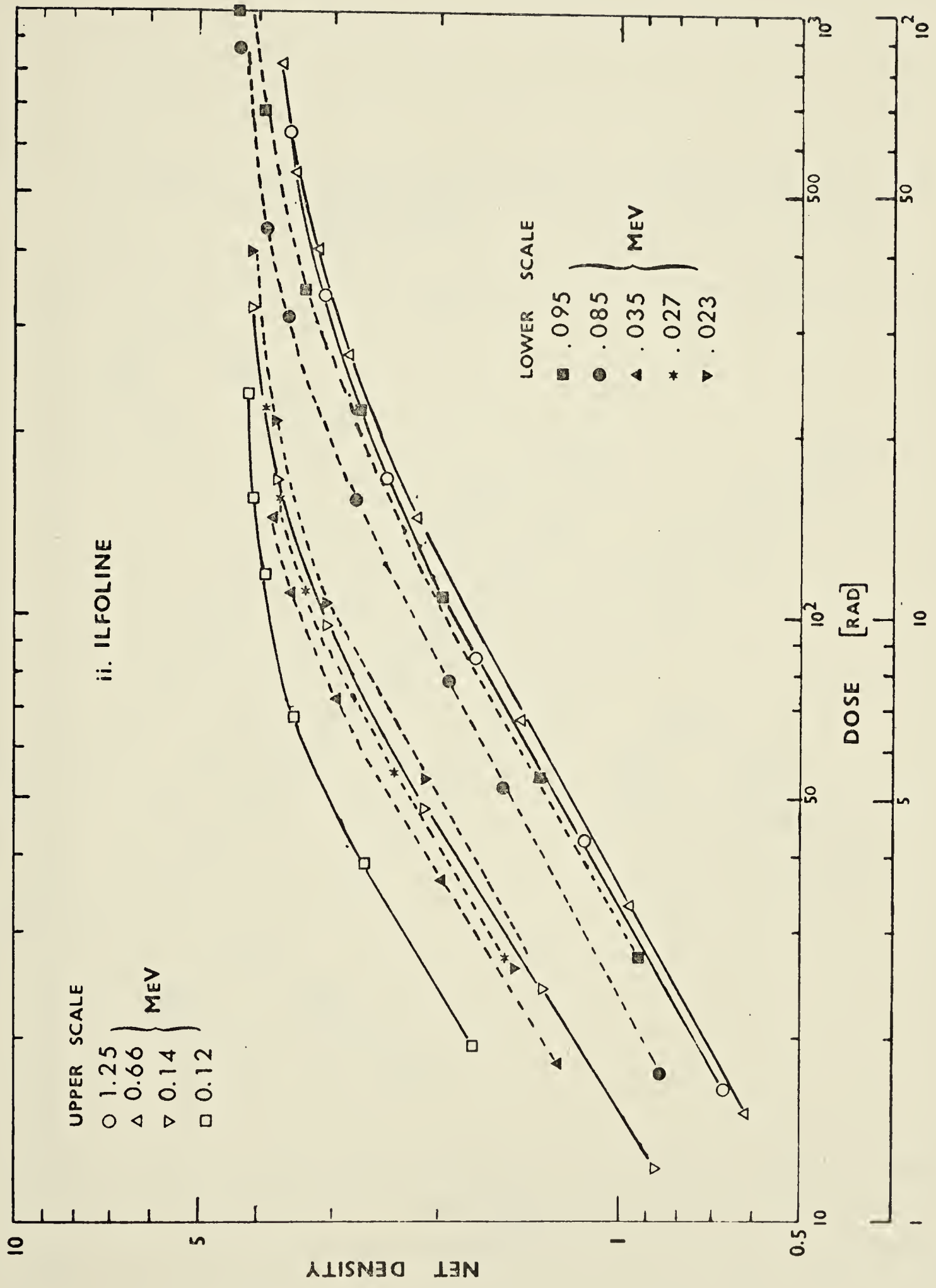


Fig. 4 111 Characteristic Curves of NDT 55, NDT 65 and NDT 75 Films

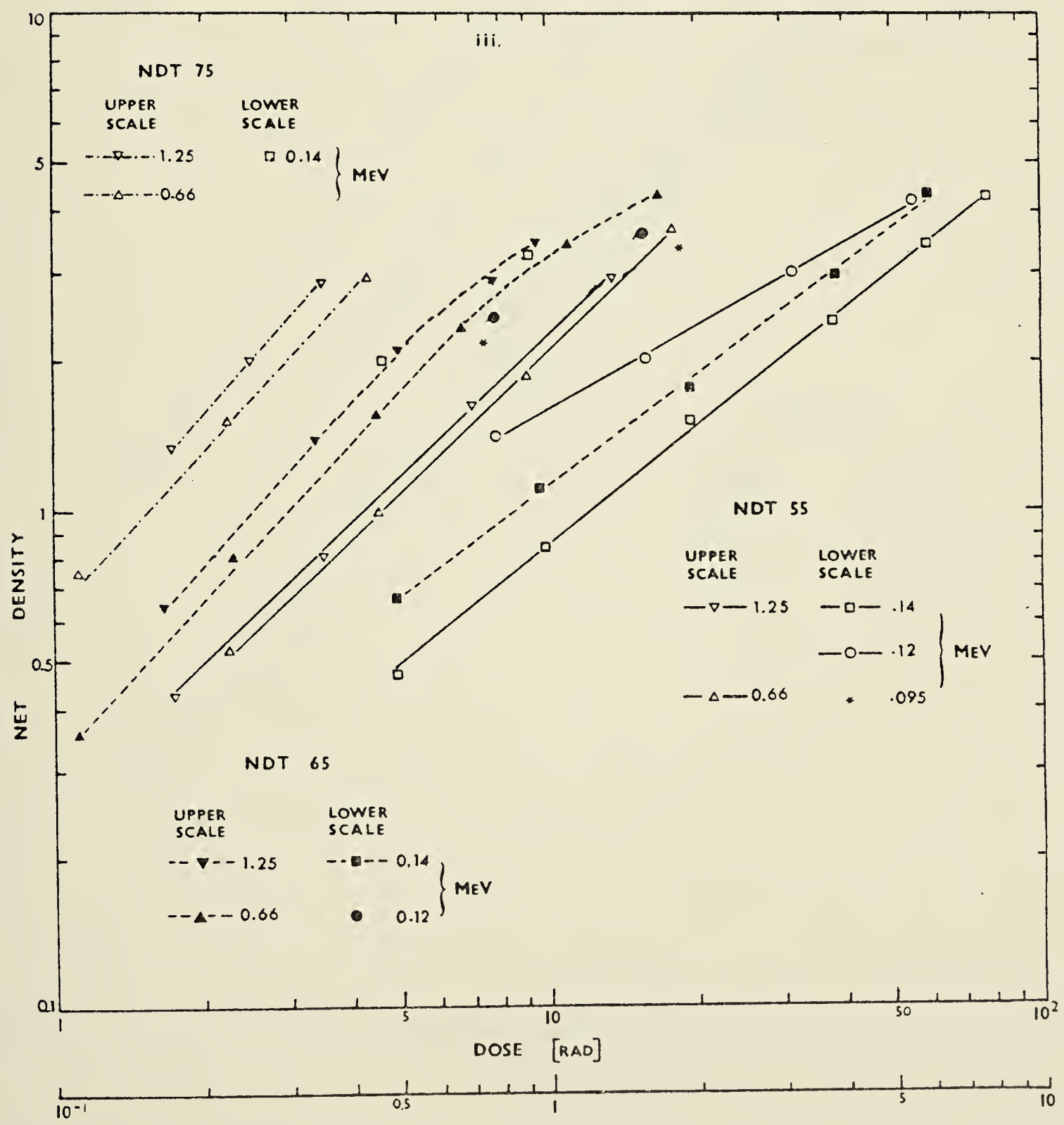


Fig. 4 iv Characteristic Curves of GAF 400 and
GAF 800 Films

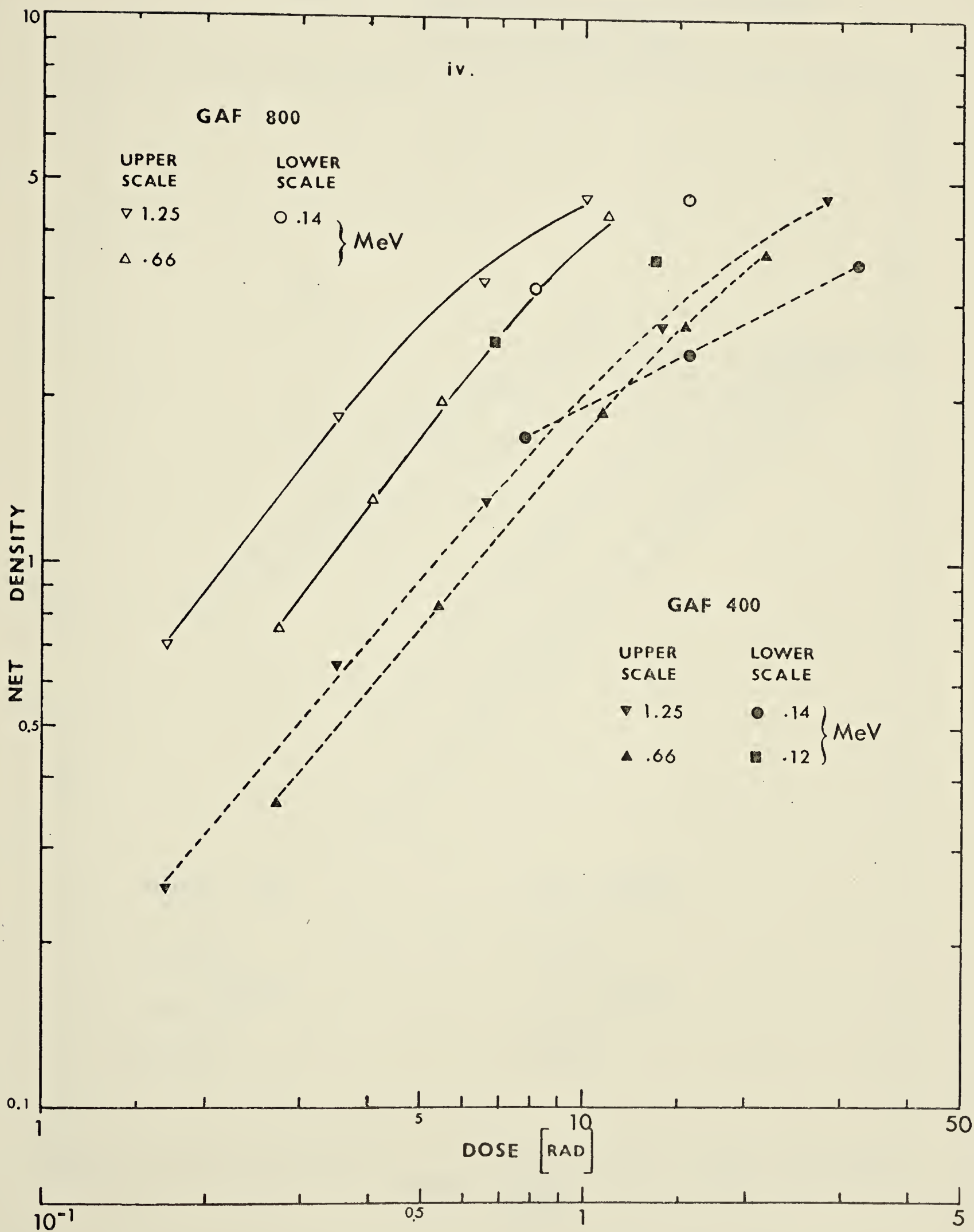
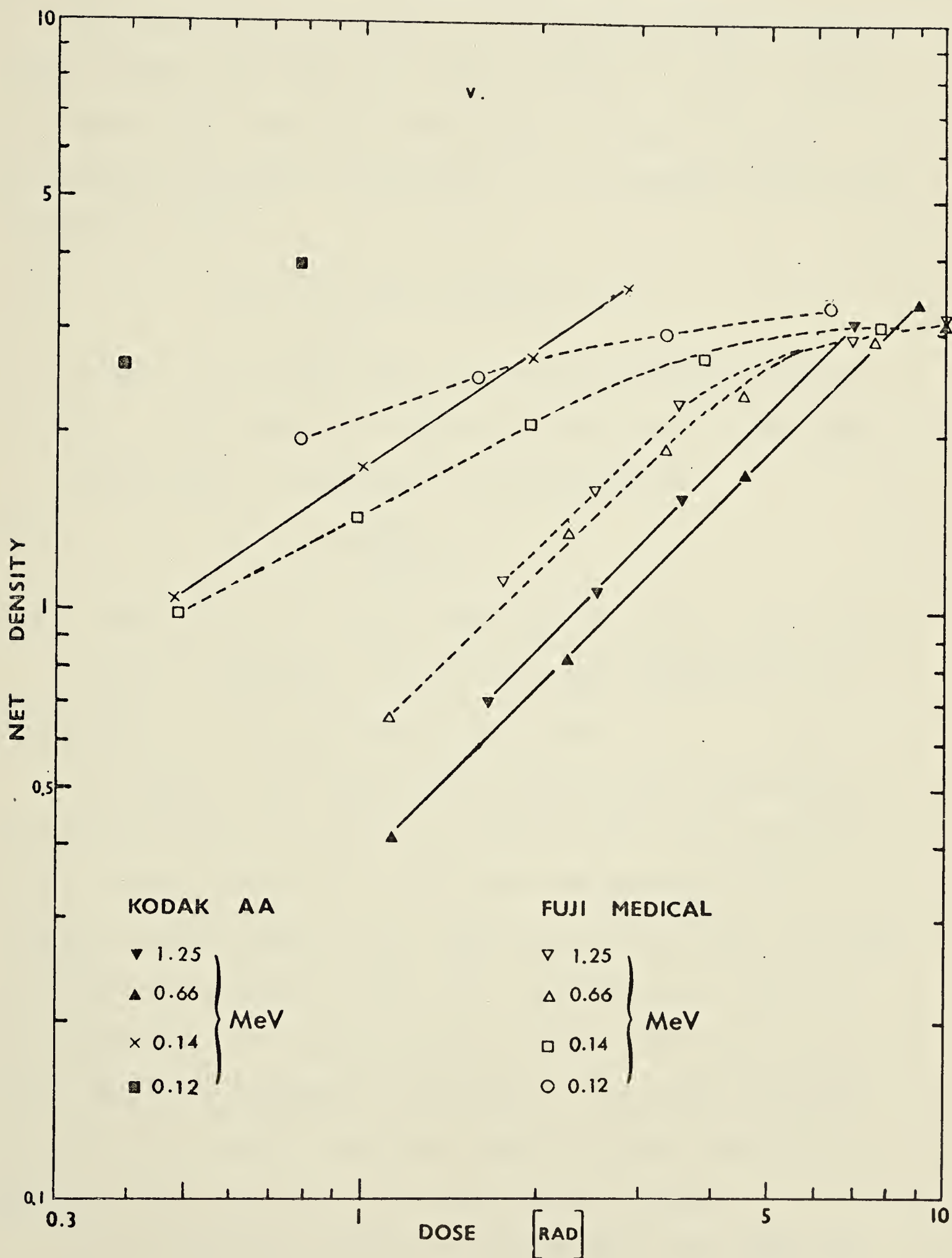


Fig. 4 v Characteristic Curves of Kodak AA
and Fuji Medical Films



each film were obtained within a period of one week.

The maximum variances of net densities shown in Fig. 4 are listed for different films in Table I. The number of sample films used for each point in Fig. 4 are 10. The sample estimate of variance, s , is defined as follows (Natrella, 1963):

$$(1) \quad s^2 = \sum_{i=1}^n (x_i - \bar{x})^2 / (n - 1)$$

where x_i , in this case, is the experimental density and n the number of densities obtained for the same given dose. The mean, \bar{x} , is defined as

$$(2) \quad \bar{x} = (1/n) \sum_{i=1}^n x_i$$

3.1.2 Measurement of Depth Dose and Isodose Distribution

Within a phantom, one of the first parameters to be determined is the percentage depth dose.

In some of the experimental procedures, films were inserted between two blocks of temex which could provide solid contact between the film and the phantom material, thereby eliminating any air space that could give misleading density readings on the film. In order to simulate the situation of a semi-infinite phantom (full phantom), which can give adequate scattering to the film, pressed-wood of unit density (another type of tissue-equivalent material) was added on both sides of the temex.

In the parallel method of measurement, the edge of the film was carefully lined up with that of the temex

Name of Manufacturer	Name of Film	Max. Variances of Density
Kodak	Industrial Type AA	0.13
	Industrial Type M	0.10
Ilford	Ilford Line film	0.12
Dupont	Cronex NDT Type 55	0.14
	Cronex NDT Type 65	0.16
	Cronex NDT Type 75	0.16
Gevaert-Agfa	Industrial Type 400	0.18
	Industrial Type 800	0.16
Fuji	Fuji Medical Film	0.08

Table I. Maximum variances of density for different films shown in Figure 4.

material, and the four corners of the film were taped tightly to the temex to secure the film in its correct position during the entire course of the experiment. Another piece of temex was placed on the film and the junction between the two blocks of temex was sealed off from exposure to light by means of black electrical tape. All of the above had to be done inside a darkroom.

The whole phantom was assembled on top of the treatment table in the radiation room in such a way that the matching edges of the film and temex could be aligned facing the source of radiation. It was then located so that the film contained within it could intercept the entire radiation field. The plane of the film was placed parallel to the direction of the radiation beam. The dose administered to the phantom was such that the maximum density produced on the film lay within the linear portion of the characteristic curve of the primary radiation. Measurements of densities were made on the developed film along the central axis of the radiation field at various depths. (Plate I shows an Ilfoline film exposed by the parallel method with a 100 cm.² field using cobalt radiation.)

These densities, D , represented the depth doses. After normalization to the maximum density, D_m , at the equilibrium depth, the percentage depth dose was obtained by the following expression:



PLATE I. ILFOLINE FILM EXPOSED BY
PARALLEL METHOD

$$(3) \quad \% \text{ depth dose} = (D - D_o) / (D_m - D_o) \times 100$$

where D_o is the background fog.

In the perpendicular method, the film was inserted at the center of the temex, rather than lined up with the edge of the temex, as in the parallel method. Six to eight films were placed at various depths in the phantom with the plane of the film made perpendicular to the direction of the beam of radiation. The rest of the experimental procedures were similar to those of the parallel method. The evaluation of the percentage depth doses was as follows. Point measurements of densities at the center of the radiation field as recorded by the films were made. (Plate II shows an Ilfoline film exposed by the perpendicular method with a 100 cm.² field using cobalt radiation.) These densities at various depths represented the depth doses and the percentage depth doses were then calculated by using the same expression as in the parallel method.

Fig. 5 shows the dimensions and the structure of the semi-infinite phantom employed. The dimensions for the limited phantom method to reduce the scattered radiations reaching the film depend upon the film in use, and will be discussed later.

The Rando Phantom Man (manufactured by Alderson Research Lab., Connecticut, U.S.A.), a tissue-equivalent material shaped according to the size of a 'standard' man



PLATE II. ILFOLINE FILM EXPOSED BY
PERPENDICULAR METHOD

Fig. 5 The Structure of Full Phantom

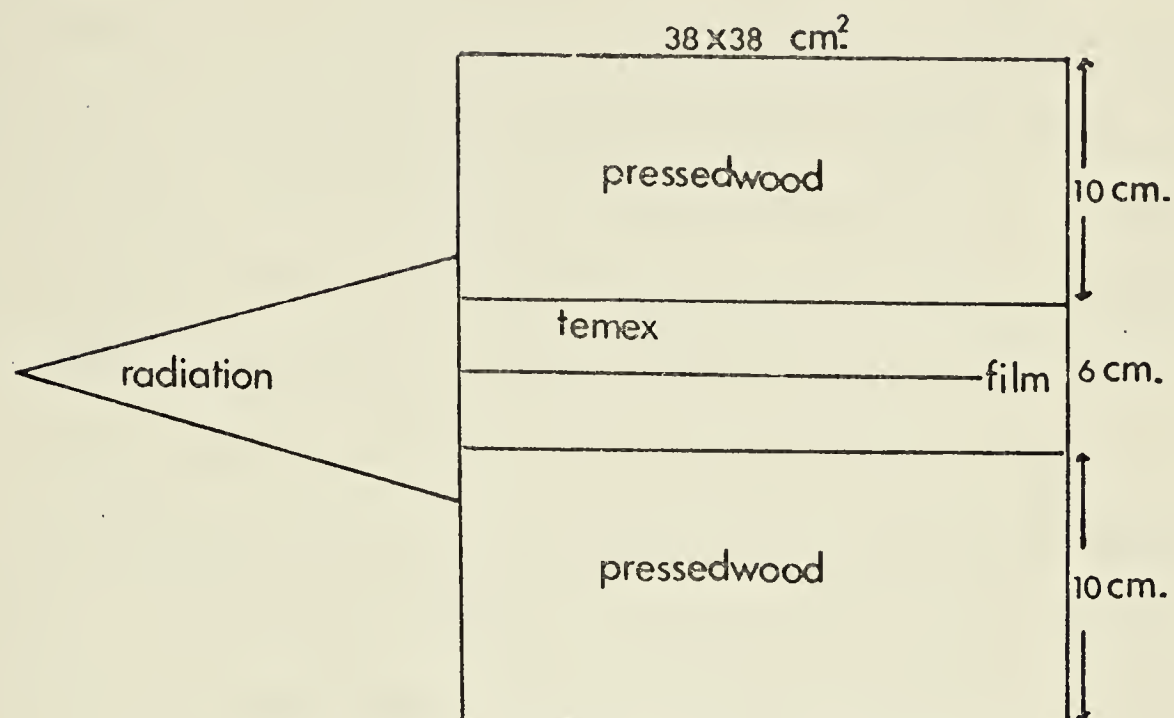
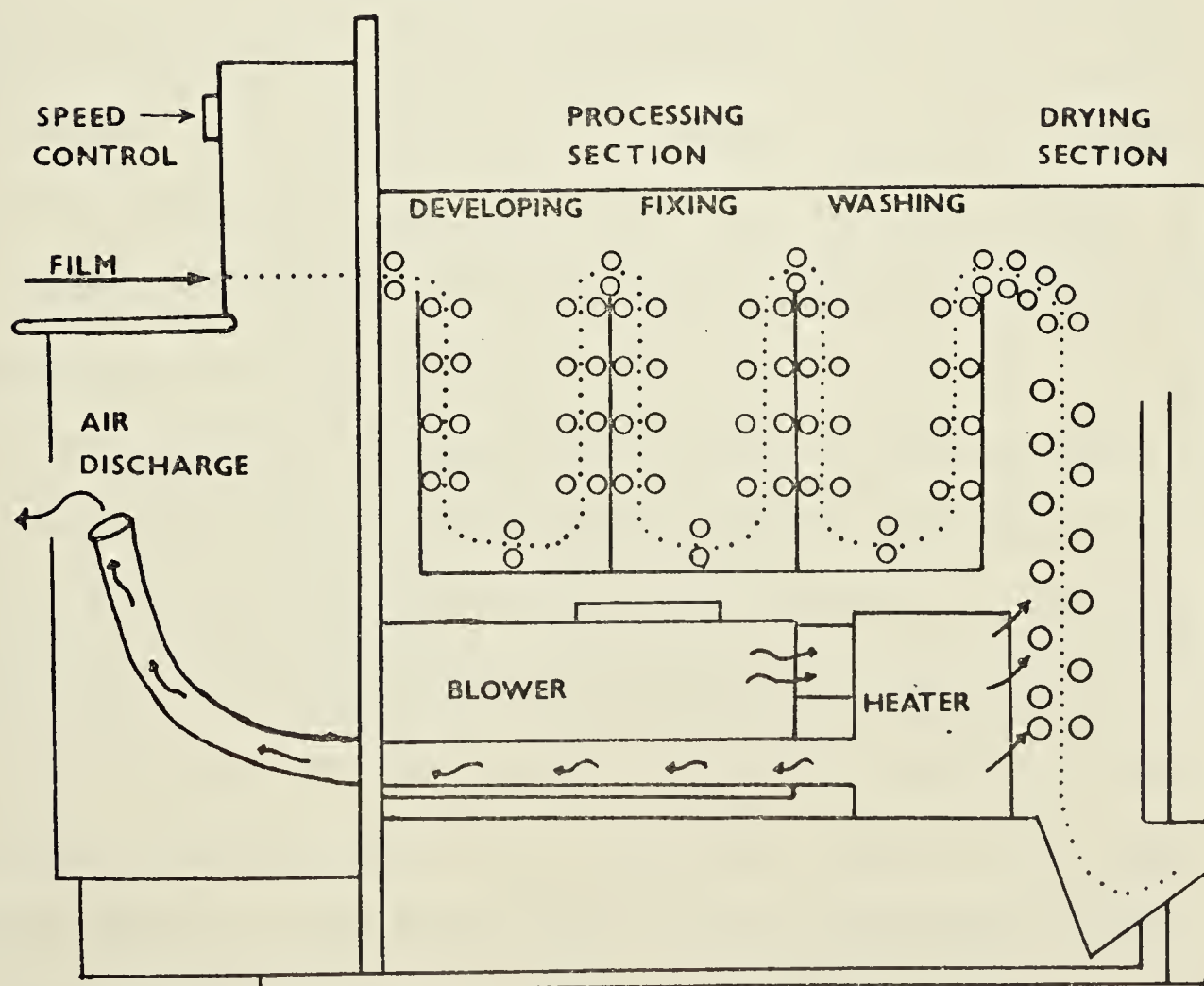


Fig. 6 Automatic Processor



with some simulated internal organs, was also used to obtain the dose distributions of multiple fields. This Phantom Man has been subdivided by the manufacturer into many sections. Each section has the contour of a particular level of the 'standard' man and is about 2.5 cm. thick. The sections also have small holes bored in them. These holes are suitable for the insertion of small thermoluminescent dosimeters or ionization chambers.

When the limited phantom method was used to reduce the scattered radiations, only several sections of Phantom Man were required. The film, in this situation, was placed inside a black paper cassette which was then sandwiched between the two pre-selected sections of phantom material designated for the experiment. The black paper cassette was used to fill any air space that might exist between the material and the film. The sections were taped tightly together to ensure good contact between the material and the film.

To obtain the isodose distribution of two or more fields by using the limited phantom method, the following procedure was adopted. (Plate III shows two opposing fields (25 cm.² field) exposed on an Ilfoline film) First, in the case of two simple opposite fields, the single fields obtained from the films were checked with the standard isodose charts available in the Radiation Oncology Department. Second, in the case of more complex



PLATE III. TWO OPPOSING FIELDS EXPOSED
ON ILFOLINE FILM

fields, the percentage depth dose of a single field utilized for the multiple fields was obtained through a PC-12 Console Computer (manufactured by Artronix Instrumentation, St. Louis, Mo., U.S.A.). This computer contains information about the radiation fields that have been measured by ionization chambers or other energy independent detectors. The necessary thickness of Rando Phantom Man material on both sides of the film was established so that the percentage depth dose obtained from the film would approximate that provided by the computer.

With this thickness of material, the field distribution pattern was tested by exposing the film to the designated fields to check the experimental alignments of these fields. If the alignments were correct, then the experiments were repeated to guarantee that the results could be reproduced. The doses in this case were administered in such a way that the maximum density resulting from any combination of doses did not go beyond the linear response of the film to the primary radiation.

3.2 Processing Conditions

3.2.1 Modes of Film Processing

(i) Automatic Processing

Unless stated otherwise, all films were processed in the roller-type automatic processor, model X-U Pako/Pakarad, Type Med. (manufactured by Pako Corp., Minnesota, U.S.A.). Fig. 6 shows the internal structure of this automatic processor. It is equipped with a development time control feature by means of which the development times can be easily altered simply by switching the 'speed control' to suit different types of film. Once the 'speed control' is set, the total processing time is fixed, the development time being a constant fraction of it. Table II gives the processing and the development times for some of the more frequently used speeds available in the 'speed control'.

For all industrial films (such as some of the double emulsion films shown in section 3.1.1), the speed normally used was '30', while the single emulsion and the non-industrial films with thinner emulsion may be processed at the speed '50'.

The water temperature of the processor, throughout the whole period of the project, was set at $78 \pm 2^{\circ}\text{F}$ with the corresponding developer temperature at $83 \pm 2^{\circ}\text{F}$. The drying temperature was set at $138 \pm 2^{\circ}\text{F}$.

The developers used, unless stated otherwise, were

'Speed' Setting	Total Processing Time (+5 sec)		Development Time (+5 sec)
	Minutes	Seconds	
20	8	45	123
25	6	35	92
30	4	45	67
40	3	10	45
50	2	30	35
60	2	5	27

Table II. Processing Times for the Automatic Processor.

#3790 developer and replenisher concentrate (manufactured by Picker Corp., U.S.A.) which contained caustic alkali and acetic acid, in addition to the developer agents. The fixer and the replenisher were also #3790 fixer and replenisher concentrate which contained acetic acid, sulfuric acid and other chemicals.

Automatic film processing was used because it could bring a degree of precision and reproducibility to the film development which was not easily achieved with manual processing. Utilizing mechanized processing equipment has two important advantages:

- 1) Overall quality of thorough development usually is improved; the thoroughness of development becomes particularly important in the case of a large film area. Incomplete development or fixing will cause drastic fluctuations in the optical density obtained.
- 2) Automatic processing usually provides savings in time, material, space and skilled manpower (Kodak, 1968).

(ii) Manual Processing

In one part of the project, the manual method of processing was used. This method consisted of using separate trays containing the developer and the fixer in a constant temperature water bath (the tray method, the steps of which are depicted schematically in Appendix IV).

The tray method of processing can be reliable in giving

consistent density readings if the processing conditions are carefully controlled. In order to minimize the variables in the tray method, the following procedure was employed. The developer and the fixer were freshly prepared and immersed in a constant temperature water bath for a period of time prior to the actual experiment, the temperature of the bath being the same as that used in the development of the film. Films were processed one at a time to avoid possible local exhaustion of the developer. Once the optimal development and fixing times were determined, they had to be strictly adhered to, so that consistency could be maintained. The addition of fresh developer after each film development was vital to the thoroughness of development. Constant agitation of both developer and fixer solutions during the developing and fixing processes were essential for uniformity in the processing of the film.

3.2.2 Parameters of Film Development

(i) Developer

The shape of the characteristic curves is known to be dependent upon the developers used (Ehrlich, 1954).

To investigate the effect of different developers, the tray method of processing was used for developers other than Picker #3790. Films (Kodak M) were processed in different developers manufactured by Kodak: x-ray, D-19, D-72, and D-76 with the development times of 9, 16, 16, and 15 minutes respectively, so that all character-

istic curves appeared within the same range of optical density. The fixing solution was Picker 3790 fixer, in which all films were fixed for 3 minutes. The water temperature was held at 69-70°F, with the strength of the solutions prepared according to the instructions supplied by the manufacturer.

Fig. 7 depicts the characteristic curves of Kodak M films in different developers for 0.66 MeV (cesium) gamma ray. Obtained from 4 runs within the period of one day, the maximum differences in density for the points in the figure are listed as follows: for D-19, 0.17; for D-72, 0.21; for D-76, 0.20; and for x-ray, 0.15. The curves for 1.25 MeV (cobalt) gamma ray were almost identical to those presented in Fig. 7 and therefore not shown. Fig. 7 also includes the characteristic curve produced with Picker #3790 developer and with the automatic processor, as a reference.

The procedure for producing the characteristic curves is described in section 3.1.1.

(ii) Development Time

The shape of the characteristic curve of a film at a particular radiation energy also depends upon the development times (Ehrlich, 1954; Golden and Tochilin, 1959).

Fig. 8 shows the characteristic curves, for 1.25 MeV (cobalt) gamma ray, of Kodak M films processed at different speeds and hence for different development times, in the automatic processor. The speeds were set at '20',

Fig. 7 Characteristic Curves of Kodak M Films in Different Developers

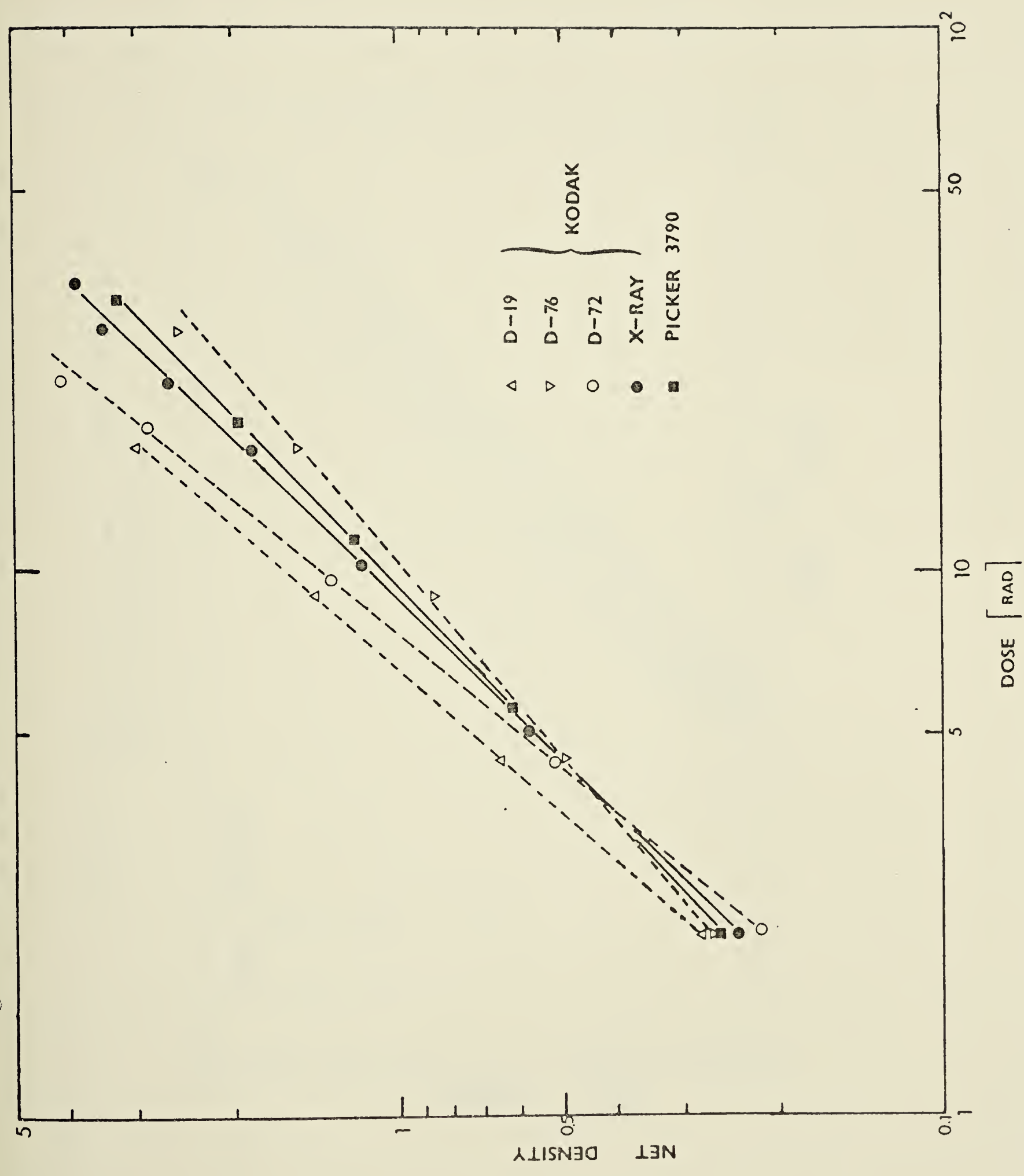
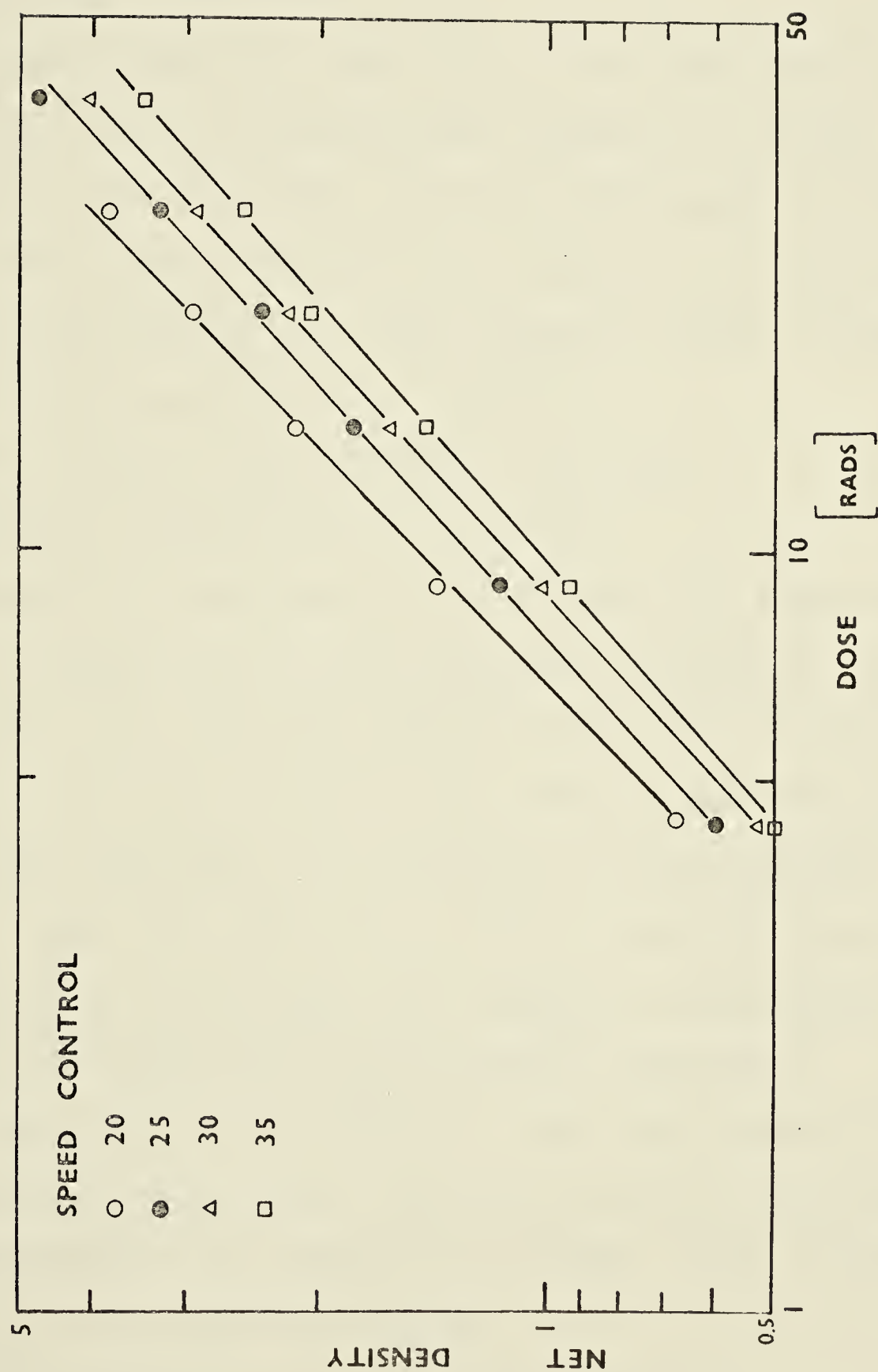


Fig. 8 Characteristic Curves of Kodak M Films at
Different Development Times



'25', '30', and '35'. The maximum difference in density obtained from 4 runs within the period of 1 week for the results of Fig. 8 was 0.09.

It can be observed, from Fig. 8, that the sensitivity of the film at the particular energy of 1.25 MeV gamma ray is enhanced with increasing development times. The increased sensitivity of film response is in agreement with Golden and Tochilin's (1959) general results using beta particles as a source of radiation.

3.2.3 Monitoring of the Automatic Processor

(i) Pattern of Variations in Processing

The optical densities of a developed film vary according to the variations in the processing conditions. If the densities are used as a means of comparing the doses received by different films of the same brand, the variances of the densities as a function of the processing conditions over time have to be known. Once these variances have been established, the degree of uncertainty involved in the comparison can be clearly perceived.

The detection of the effect of the variations in the processing conditions over a period of time on the densities thus produced was carried as follows, using 0.66 MeV gamma ray as the radiation source:

1) Over a period of one day, Fuji Medical

films were stacked inside a black cardboard cassette of thickness 0.1 cm., so that doses were re-

ceived at the same time. The total thickness of the films did not exceed 3 mm.; therefore, attenuation of radiation, for all practical purposes, should not have a major effect on the doses given. The films were prepared and exposed according to the technique presented in section 3.1.1. The densities recorded during this period came from a total of 6 films.

- 2) Over the periods of one week and of six months, films of the types of Fuji Medical and of Kodak M respectively were used. The number of films employed for the experiments were 14 and 12 for Fuji Medical and Kodak M respectively. All doses were given to the same film with the individual doses well separated spatially from one another on the film to minimize the stray radiations coming from the doses given later. The film was then processed immediately after it had been exposed.

Tables III, IV, and V illustrate the mean and the variances of the densities obtained by means of the above methods over the periods of one day, of one week and of six months respectively.

Lawrence (1973) described a different processor-monitoring method which employed a processor control sensitometer. However, for the purposes of this experiment, the method described above was simple and convenient and required a less expensive instrument.

The variances of the densities over a certain period

Dose (rad)	Mean Density	Variance
1.12	0.78	0.03
2.24	1.51	0.05
4.48	2.47	0.06
8.96	3.09	0.04
17.9	3.35	0.02

Time Period: 1 day
Film Used: Fuji Medical Film

Table III. Monitoring of the Automatic Processor for the period of 1 day.

Dose (rad)	Mean Density	Variance
1.12	0.81	0.16
2.24	1.49	0.08
4.48	2.44	0.08
8.96	3.01	0.06

Time Period: 1 week

Film Used: Fuji Medical Film

Table IV. Monitoring of the Automatic Processor for the period of 1 week.

Dose (rad)	Mean Density	Variance
2.2	0.41	0.22
6.7	0.94	0.18
12.3	1.54	0.17
16.8	1.99	0.21
22.0	2.48	0.14
26.9	2.90	0.18

Time Period: 6 months

Film Used: Kodak M

Table V. Monitoring of the Automatic Processor for the period of 6 months.

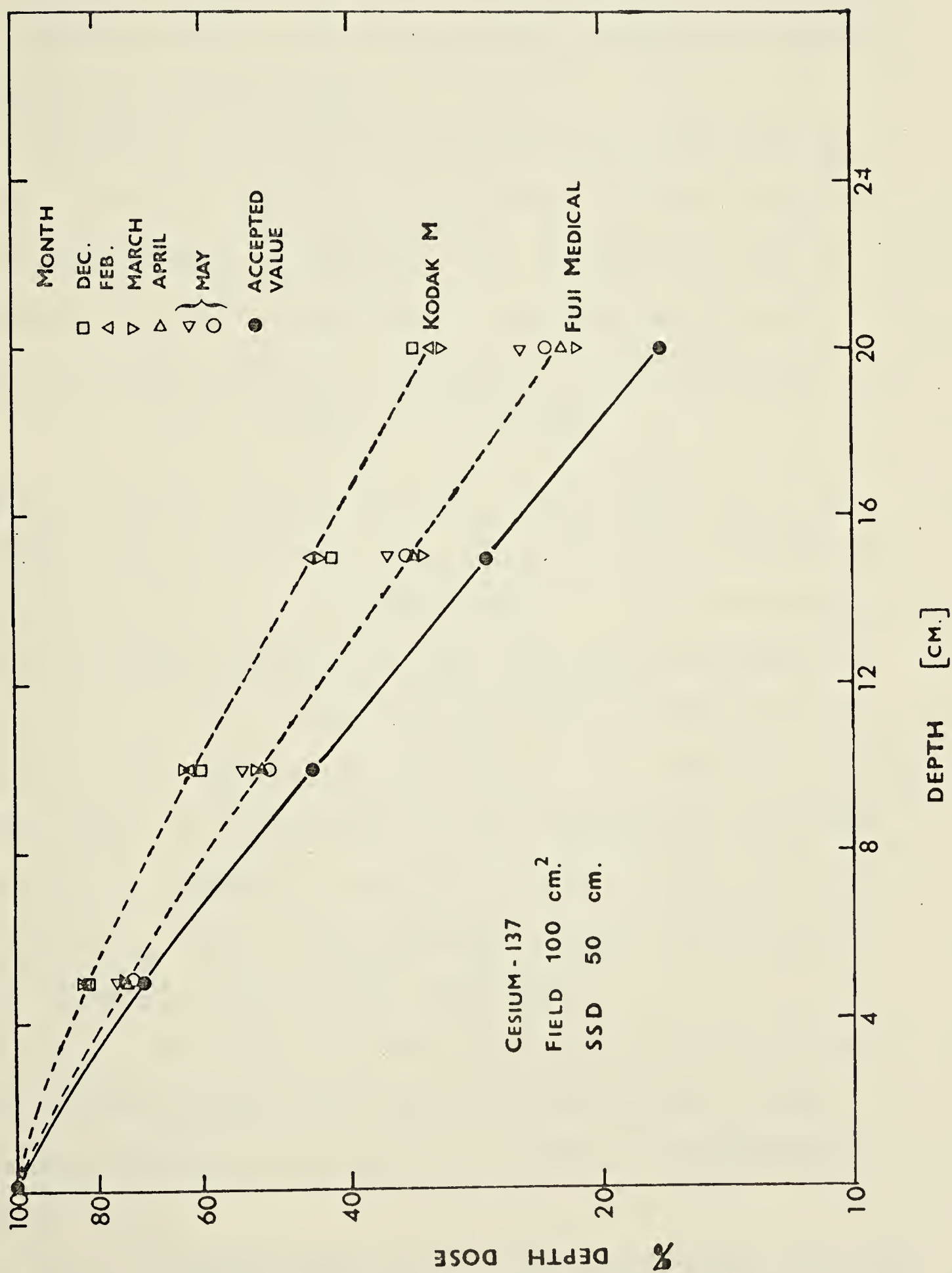
of time indicate the variations in the processing conditions over the same period of time. The variance of ± 0.16 shown in the first dose of Table IV is probably due to the shutter error of the radiation machine, as the actual exposure time is in the order of one second. This machine is normally manufactured for use in long exposure times rather than those of one second. In general, the variances increase over a period from one week to six months. Lawrence (1973) suggested that variances of ± 0.15 to ± 0.20 may be satisfactory for most purposes in department of radiology.

The variance is least if the films are processed on the same day. This can be expected since many of the parameters, such as temperature, developer conditions, etc. involved in the process remain fairly constant throughout the course of a single day. The implication of the least variance in one day is crucial; if the densities are to be used for comparisons of the doses given, the films ought to be processed within the same day or, better yet, simultaneously or one after another to reduce the uncertainties of the processing conditions.

(ii) Percentage Depth Dose Measurement

Since there are variations in the processing conditions, it is necessary to know if the automatic processor, which has been adjusted to the standard conditions as described in section 3.2.1, can indeed produce consistent results of percentage depth dose. Fig. 9 shows percentage

Fig. 9 Consistency of Processing Conditions with Automatic Processor
in the Determination of Depth Doses



depth doses for a field size of 100 cm.², SSD of 50 cm., of radiation energy 0.66 MeV as measured by Fuji Medical and Kodak M films in the full phantom, using the parallel method at different times.

From Fig. 9, it can be observed that the percentage depth doses are relatively insensitive to minor changes in the processing conditions. This consistency can be explained in the following way. The percentage depth dose is determined by the expression (3) of section 3.1.2

$$(D - D_o)/(D_m - D_o) \times 100\%$$

where D , D_m and D_o have the same definitions as in that section. The densities D , D_m and D_o are crucially dependent upon the processing conditions. If the processing conditions vary slightly so that the expected densities decrease or increase, the actual densities obtained from the film will change by approximately the same percentage with respect to one another if the processing conditions are altered slightly. Therefore, after taking the ratio $(D - D_o)/(D_m - D_o)$, the percentage changes in D , D_m and D_o will roughly cancel each other out.

Hence the values of percentage depth dose should remain fairly constant as long as the variations in processing conditions are kept to a minimum as suggested in section 3.2.1.

The discrepancy between the percentage depth dose as measured by the film and that of the accepted values is

mainly due to the energy dependence of the individual films. It can also be observed that some types of films, such as Fuji Medical, are less energy dependent than other types of films, such as Kodak M. This point will be elaborated later in sections 3.3.2 and 5.1.

3.2.4 Uniformity of Film Development

(i) Automatic Processing

In the parallel method of measuring the percentage depth dose, the developed film shows a decreasing degree of optical densities over its length (as illustrated in Plates I and IV, the latter showing a Kodak M film exposed by the parallel method with a 100 cm.² field using cobalt radiation). The maximum density occurs at the equilibrium depth where the maximum dose is given. The remainder of the densities recorded decrease as the radiation beam penetrates the phantom, thereby forming the basis for the measurement of depth doses.

With the dimensions of the film usually more than 20 x 15 cm.², non-uniform development of this large area of film surface could seriously affect the resulting optical density by virtue of the lack of total uniformity in the development of the exposed grains. This can lead to a discrepancy in the percentage depth doses obtained.

From the automatic processor, continuous and vigorous agitation in the development process can be expected. When a film is being processed, fresh developer is pumped



PLATE IV. KODAK M FILM EXPOSED BY
PARALLEL METHOD

into the development tank; hence, local exhaustion of the developer may not be a serious factor affecting the development process. As the film is continuously carried through the rollers, local concentration of reaction products derived from the film surface is very unlikely.

Nevertheless, films (Kodak M) were put through the automatic processor in different manners to check if any variations of optical density occurred. Firstly, those edges of the films that had received the greatest and the least doses were successively put through as the leading edges into the processor. Secondly, the lateral position was entered as the leading edge so that both the areas of film which had received the greatest and the least doses could be developed simultaneously.

The percentage depth doses from these three different manners of processing were essentially identical. The maximum discrepancy in the net density at various depths was about 3%. However, for consistency in processing films through the automatic processor, all films were subsequently processed with the edge of the film that had been exposed to the greatest dose entering the processor first.

(ii) Manual Processing

With the manual method of processing, unless great care is taken, artefacts due to non-uniform development of film can appear, thus affecting the resulting density readings. In the development of photographic films, Wilsey (1934) observed that continuous and vigorous agitation of

film was essential to secure the uniformity needed. He also pointed out that, if inadequate agitation took place, in the case of a film hanging in the developer solution in a tank, the lower areas of the film received a lesser degree of development than the upper ones even though all areas of the film had received the same initial exposure. This artefact was not detected under vigorous agitation.

With only intermittent paddle-stirring of the developer solution while using a hanger-type manual processing method inside a tank, Stanton (1962) noted that a discrepancy in the percentage depth dose occurred between two films exposed by the parallel method. One of these films was suspended with the edge that had received the greatest dose near the surface of the solution, the other one being hung with the opposite orientation. The difference in density obtained from these two orientations was about 6% at the depth of 5 cm. The percentage depth dose detected from the latter orientation was higher than that from the former. The films were separated from one another by about $1\frac{1}{2}$ inches. With greater separation, the discrepancy was reduced.

Stanton's observation can be explained by the fact that his intermittent agitation of the solution may not have been sufficient to disperse the reaction products resulting from the development process. These products

which usually have a higher specific gravity than the developer itself can inhibit the on-going development process of the film. As they emerge from the emulsion layer, in the absence of vigorous agitation to disperse them throughout the solution, they flow downward over the film surface. This leads to a local concentration of products and further development of the film is retarded in those areas where such concentration occurs, thus causing a lesser density to be recorded.

The percentage depth dose is defined by the expression $(D - D_o)/(D_m - D_o) \times 100$. Therefore, when a film is oriented with the area that has received the greatest dose submerged at great depth in the solution, the reaction products decrease the development of that particular area, implying that D_m will be less. A decrease in D_m will increase the values of the percentage depth dose, in agreement with Stanton's observation. With greater separation between films, the chance of concentration of reaction products in one particular area diminishes and hence the error involved could be reduced, also in accordance with Stanton's finding.

3.3 Properties of Films

3.3.1 Introduction

As Wilsey (1934) pointed out in his paper concerning the difficulties encountered in photographic photometry of roentgen rays, "it is important to understand clearly the limitation of this photographic method of radiation measurement and to know what procedures should be followed in order to secure the most satisfactory results."

Even though he did not explicitly discuss the difficulties involved, they may be roughly divided into two categories:

1. the inherent structure and attributes of the film itself,
2. the external factors which help bring about the final developed state of the film.

Most of the experiments in the present study were carried out with cobalt-60 (1.25 MeV) radiation. Payne et al. (1974) have published Theratron-80 cobalt unit percentage depth doses which are about 2% higher than the values contained in British Journal of Radiology Supplement 11 (1972). Payne et al.'s values have been compared with the depth doses from the isodose charts provided by AECL, the manufacturer, and good agreements were found. Hence all comparisons for cobalt radiation were made with the values from Payne et al. and the AECL isodose charts.

3.3.2 Energy Dependence

(i) Observation

Probably the most serious drawback of film emulsion as a dosimeter is the problem of energy dependence. This dependence can be illustrated by the relative sensitivity graph of films as shown in Fig. 10 which includes both Kodak M and Ilfoline films.

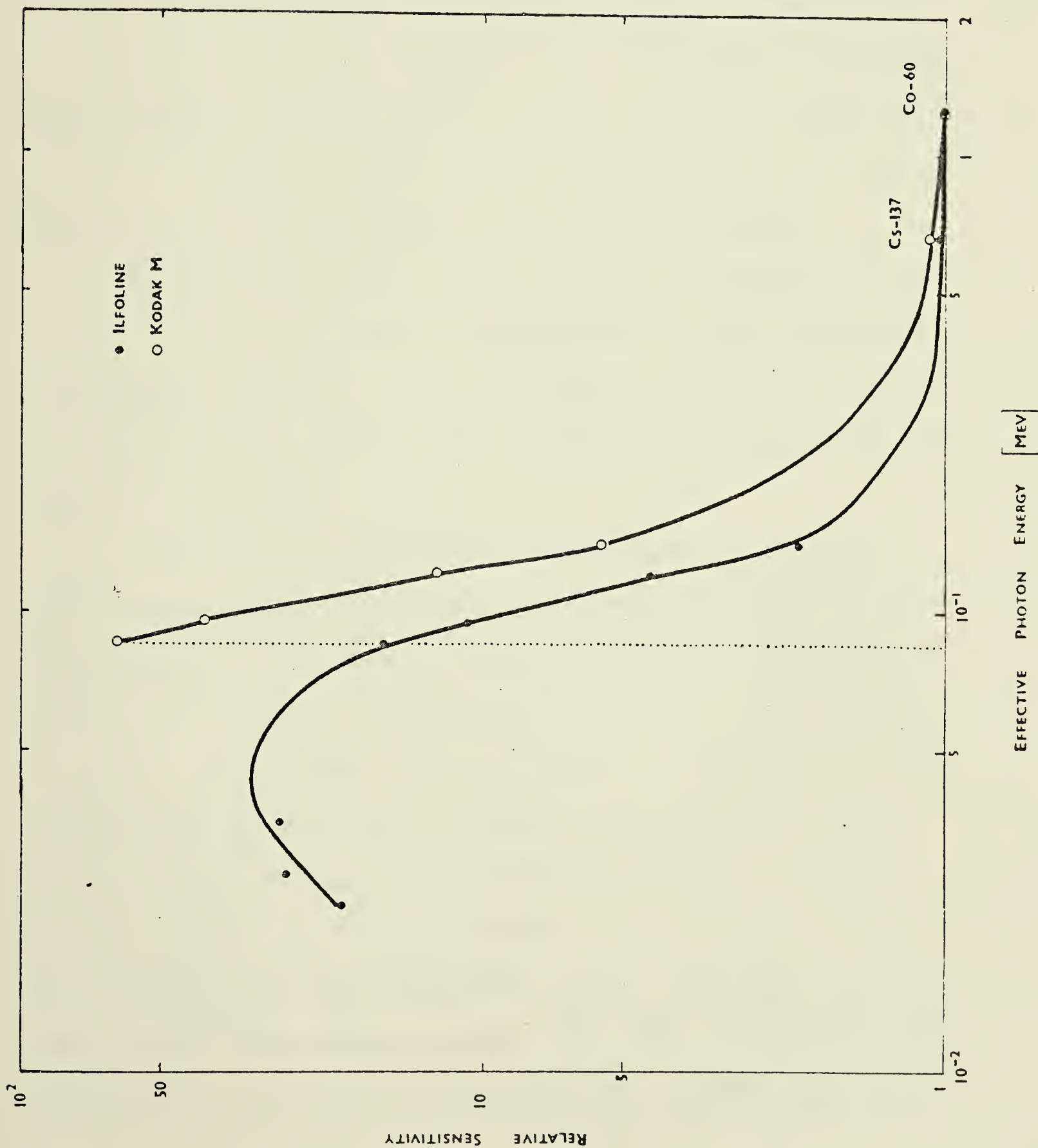
The points on the graph were obtained by using the reciprocal of the dose required to produce a net density of 1 at that radiation energy in question. The dose was read from the characteristic curve as shown in section 3.1.1. However, for points in the lower x-ray energy range, the doses were read from the curves by extrapolation to the net density of 1. The reciprocal values of doses so obtained were normalized to that of gamma rays of energy of 1.25 MeV (relative sensitivity).

(ii) Comparison of Films

Even though Ehrlich (1954) pointed out that the nature of energy dependence of films is quantitative rather than qualitative, from Fig. 10, it can be observed that Ilfoline shows less energy dependence than Kodak M. At the effective radiation energy of 0.085 MeV, Ilfoline demonstrates approximately 16 times greater sensitivity than at 1.25 MeV, whereas Kodak M indicates a ratio of 60:1 for these two energies.

From the film response model (section 2.4), since

Fig. 10
Relative Sensitivity
Graph for Kodak M
and Ilfoline Films



(m_n/m_p) of Kodak M is greater than that of Ilfoline, the terms

$$(4) \left[P + \sum_{n=1}^k (m_n/m_p) S_n \right] \text{Kodak M} > \left[P + \sum_{n=1}^k (m_n/m_p) S_n \right] \text{Ilfoline}$$

Therefore, the depth dose predicted by Kodak M should be higher than in the case of Ilfoline. In the lower parts of Figs. 11 i, ii, iii, and 12 i, ii, iii, the percentage depth doses as measured with Kodak M and with Ilfoline films by the perpendicular method are depicted for the field sizes of 25, 100 and 400 cm.² respectively.

All films for Figs. 11 and 12 were processed one after another to minimize the variations in the processing conditions. Out of 4 runs, the maximum difference in net density for the results was 0.06 for Kodak M and 0.05 for Ilfoline at a depth of 10 cm.

In the field sizes under investigation, Ilfoline gives better percentage doses than Kodak M when the results from both films are compared with the accepted values. For example, at the depth of 20 cm., the discrepancy for these three fields is about 5-7% higher for Kodak M than for Ilfoline. However, no percentage depth doses from the films agree perfectly with the accepted values. When the results measured from Ilfoline films are compared with the accepted values, the error for the small field sizes is no greater than 10%, whereas for the large sizes, it could be as high as or greater than 40%.

Fig. 11 i Depth Dose of Cobalt Radiation with Field 25 cm² as measured

from Kodak M Films

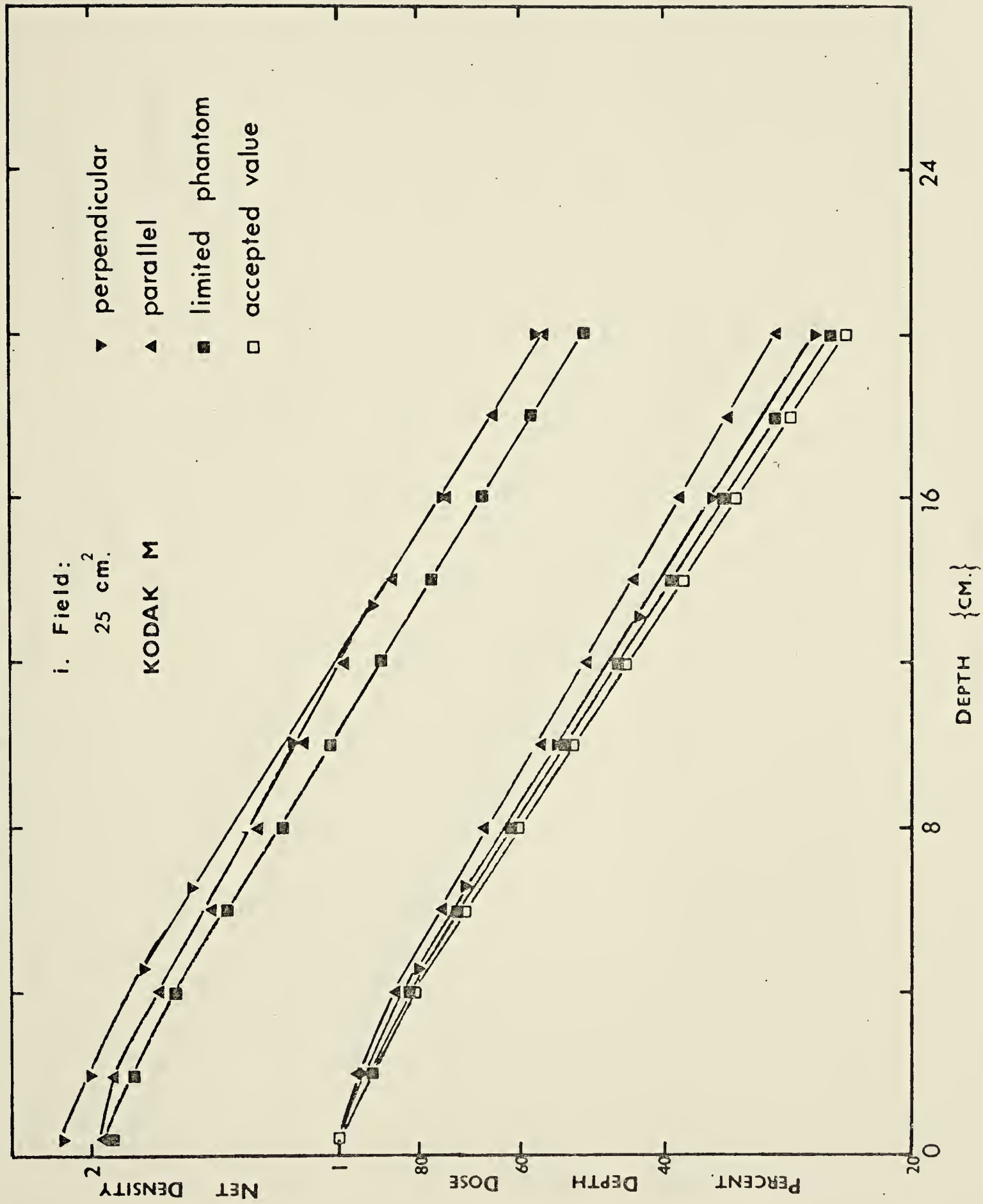


Fig. 11 11 Depth Dose of Cobalt Radiation with Field 100 cm^2 as measured from Kodak M Films

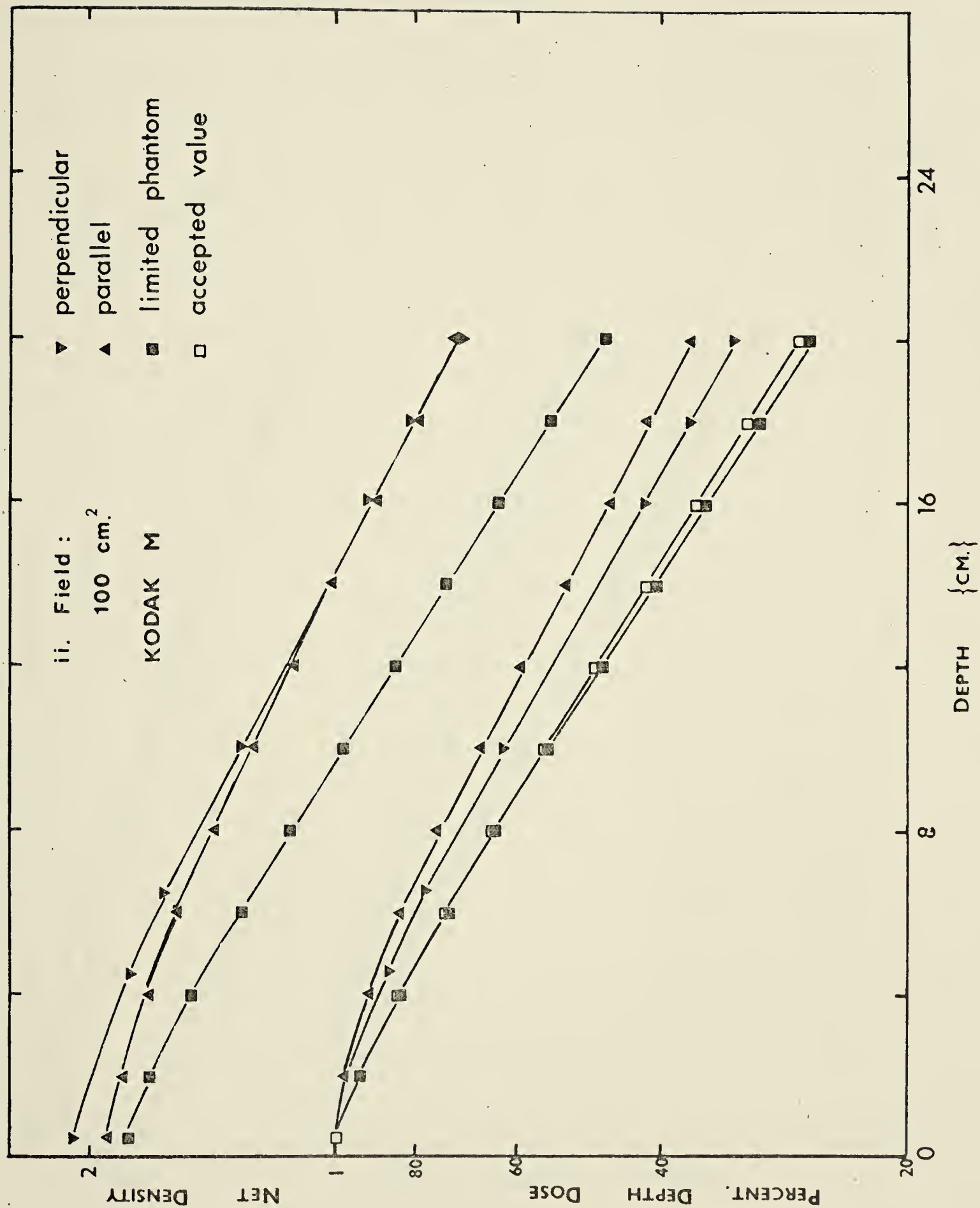


Fig. 11 i11 Depth Dose of Cobalt Radiation with Field 400 cm^2 as measured from Kodak M Films

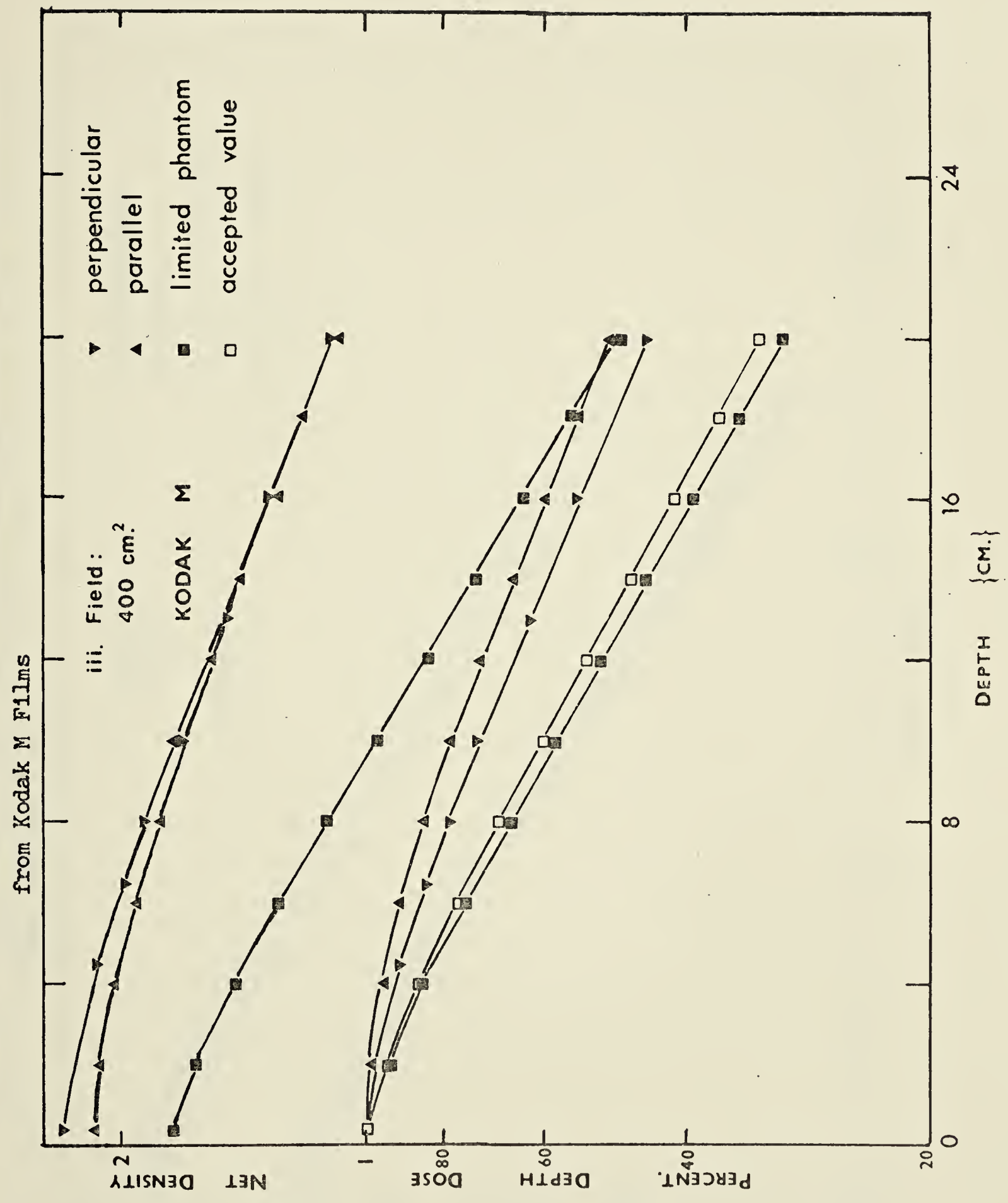


Fig. 12 i Depth Dose of Cobalt Radiation with Field 25 cm^2 as measured from Ilfoline Films

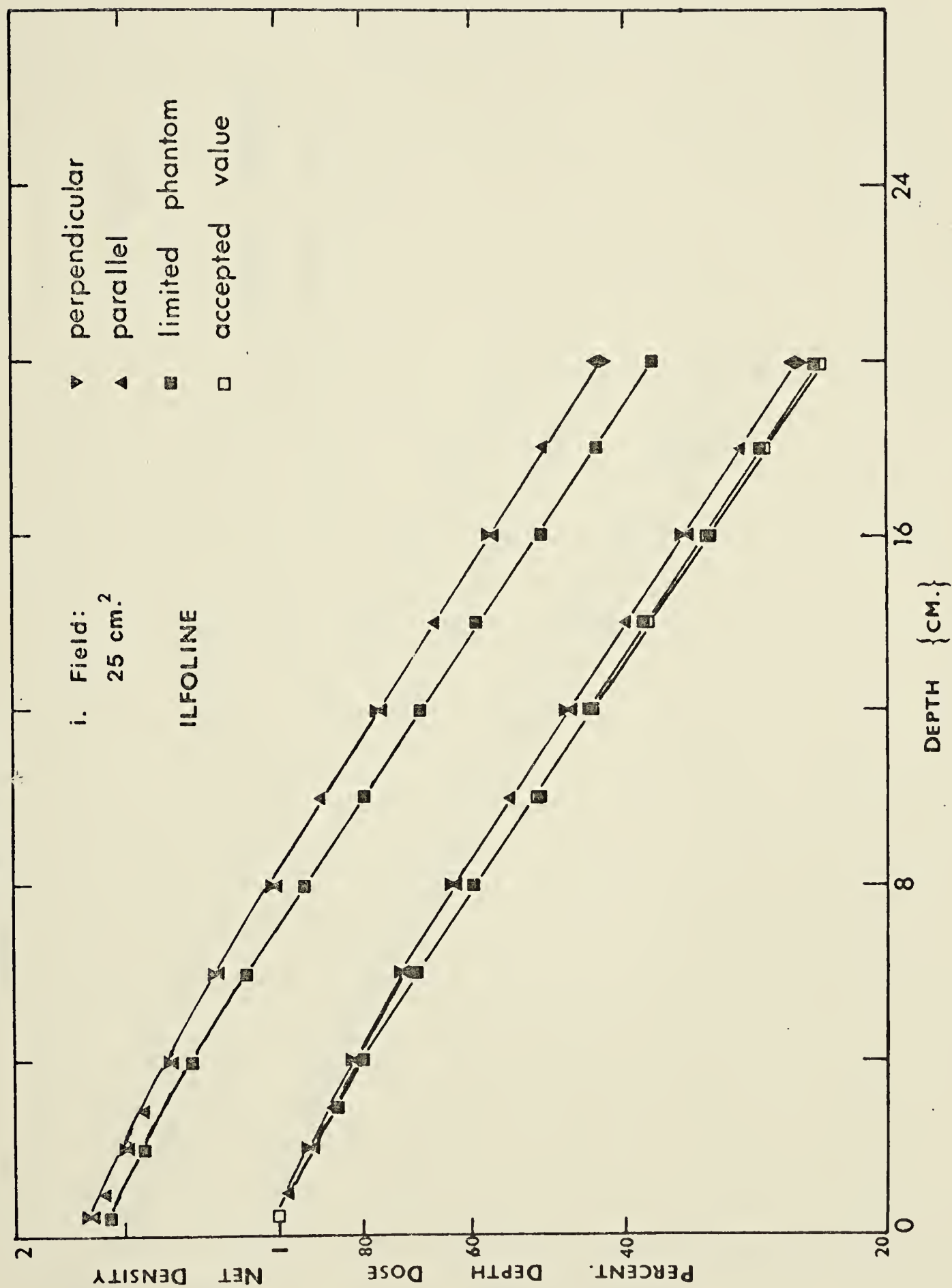


Fig. 12 ii Depth Dose of Cobalt Radiation with Field 100 cm² as measured from Ilfoline Films

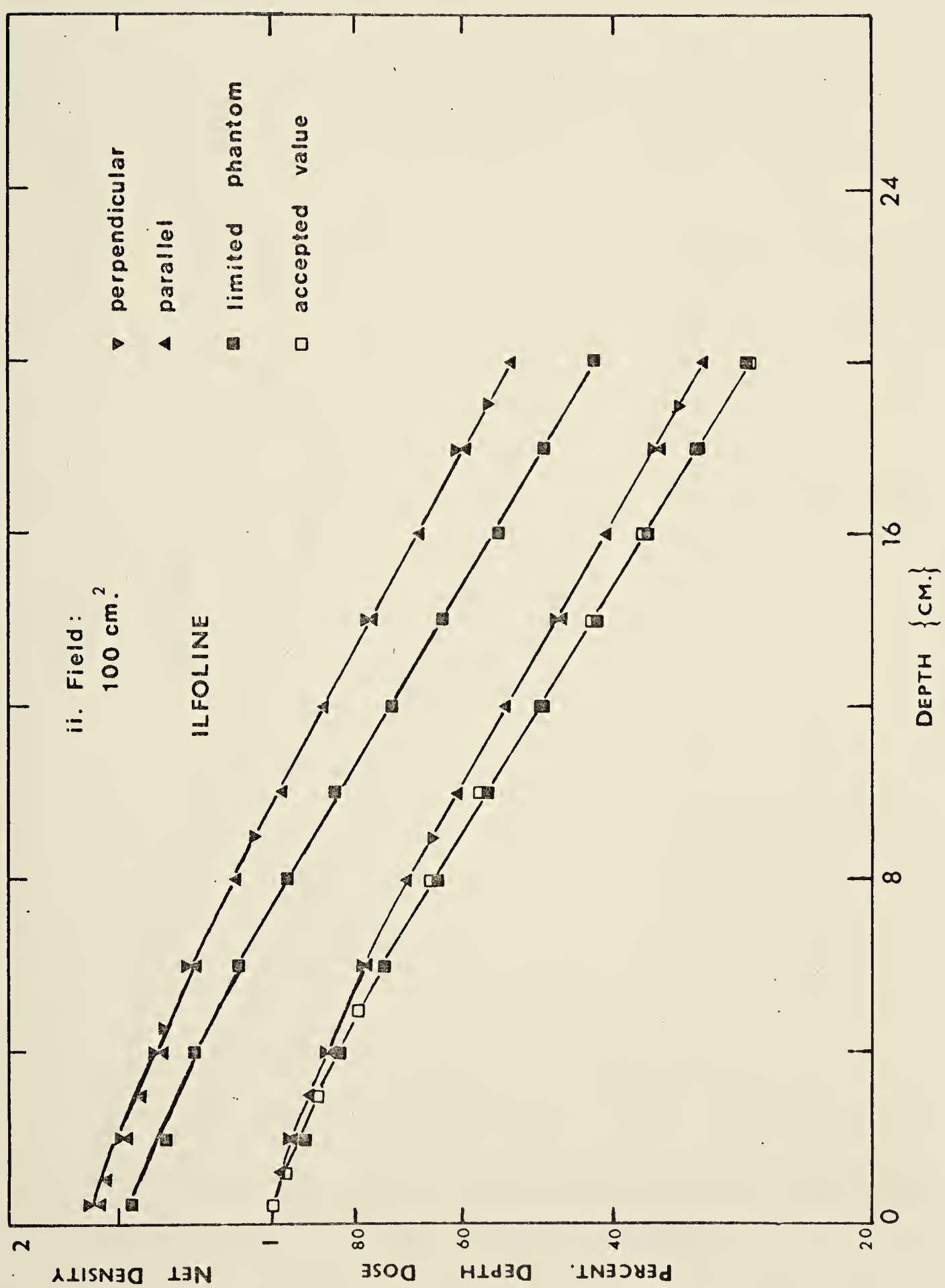
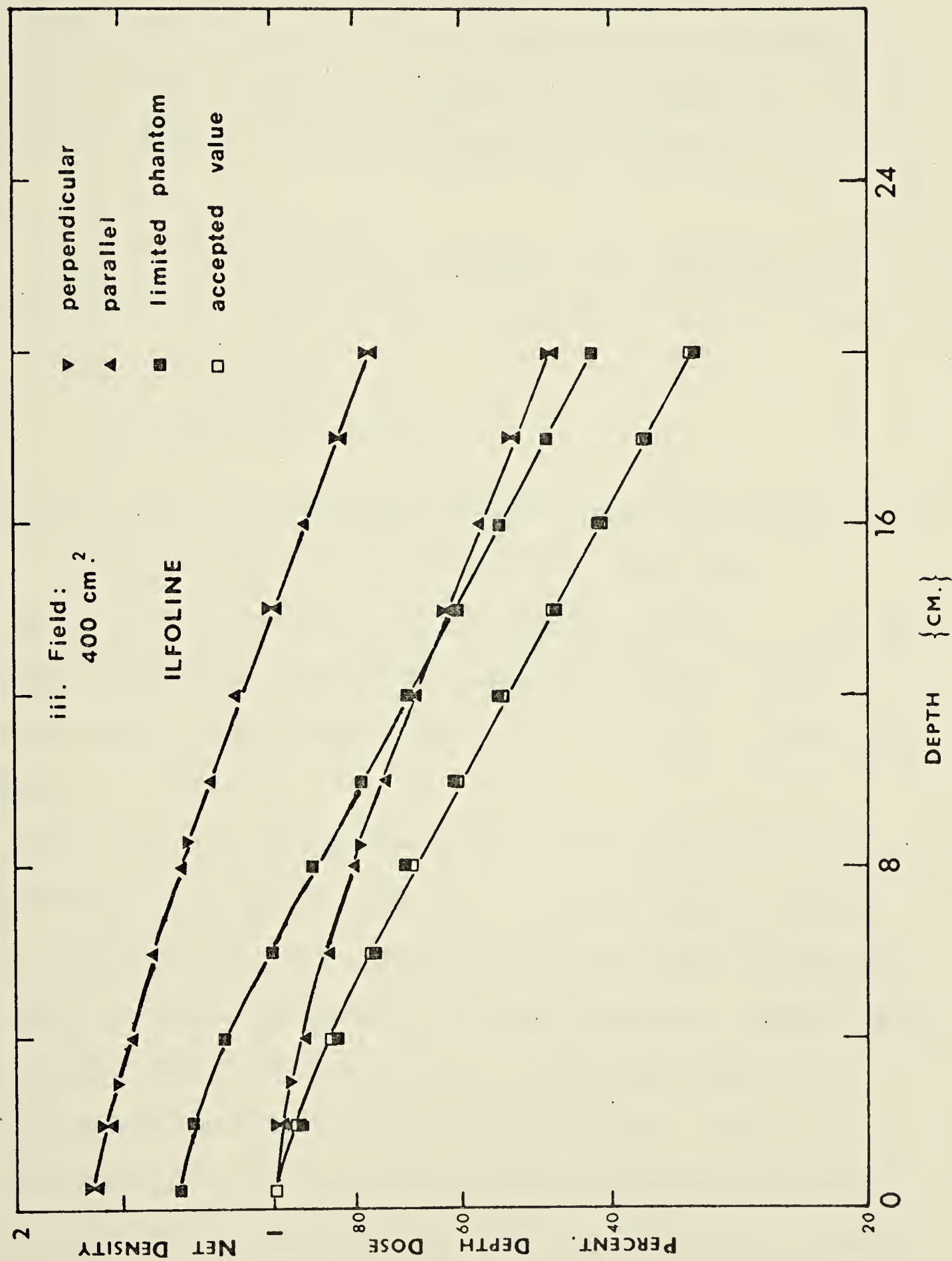


Fig. 12 iii Depth Dose of Cobalt Radiation with Field 400 cm^2 as measured from Ilfoline Films



(iii) Limited Phantom Method

Attempting to decrease the error introduced by the excessive dependence of films to low energy radiation, Mauderli et al. (1960) and Stanton (1962) proposed to reduce the amount of phantom material surrounding the film.

From the model of film response, the reduction of phantom materials is a method for manipulating the scattered dose term so that

$$(5) \quad \sum_{i=1}^k (m_i/m_p) S_i \approx \sum_{n=1}^k S_n$$

where S_i is the scattered dose from a limited phantom, and

S_n the scattered dose from a full phantom.

The S_i term in expression (5) is smaller than the S_n term because the amount of phantom material present in the limited phantom are smaller than those present in the full phantom.

The results obtained with the limited phantom are also plotted in Figs. 11 and 12 for Kodak M and Ilfoline films respectively. For Kodak M, the thickness of phantom necessary to approximate the accepted values is about 2.5 cm. of the material on each side of the film for small and medium fields, and 2.0 cm. for large fields. This phantom thickness of 2 or 2.5 cm. can be compared with Stanton's reported value of 1.1 cm. This difference in thickness may be due to the processing conditions and to the phantom materials used. For Ilfoline, the thickness of

phantom materials required on each side of the film to give a good approximation for a majority of fields is about 2.5 cm.

This limited phantom method is, at very best, an approximation. For Ilfoline films, the best possible results that can be obtained by using this limited method give errors of about 10% or less for a majority of field sizes.

As no films can suit all purposes in photographic dosimetric problems, it is necessary to know if this limited phantom method can be extended to other films. Figs. 13 i, ii, and 14 i, ii, show the percentage depth doses of Fuji Medical, GAF 400 and 800, NDT 55 and 65, and Kodak AA for the field sizes of 25 and 100 cm.² with the full and the limited phantoms. The size of the limited phantom used was 2 cm. on one side and 2.5 cm. on the other side of the film. For each type of film, the experiment was repeated three times. The films were processed on the same day. The maximum difference in density among the films was observed in Kodak AA to be 0.12. The maximum differences in density for the other types of films were less than that for Kodak AA.

From Figs. 13 and 14, it can be observed that the removal of phantom material can indeed reduce the scattered radiation and thus alter the percentage depth doses as measured by films. However, the thickness of this

Fig. 13 i Depth Doses of Cobalt Radiation with Field 25 cm^2 as measured from Different Films in Full Phantom

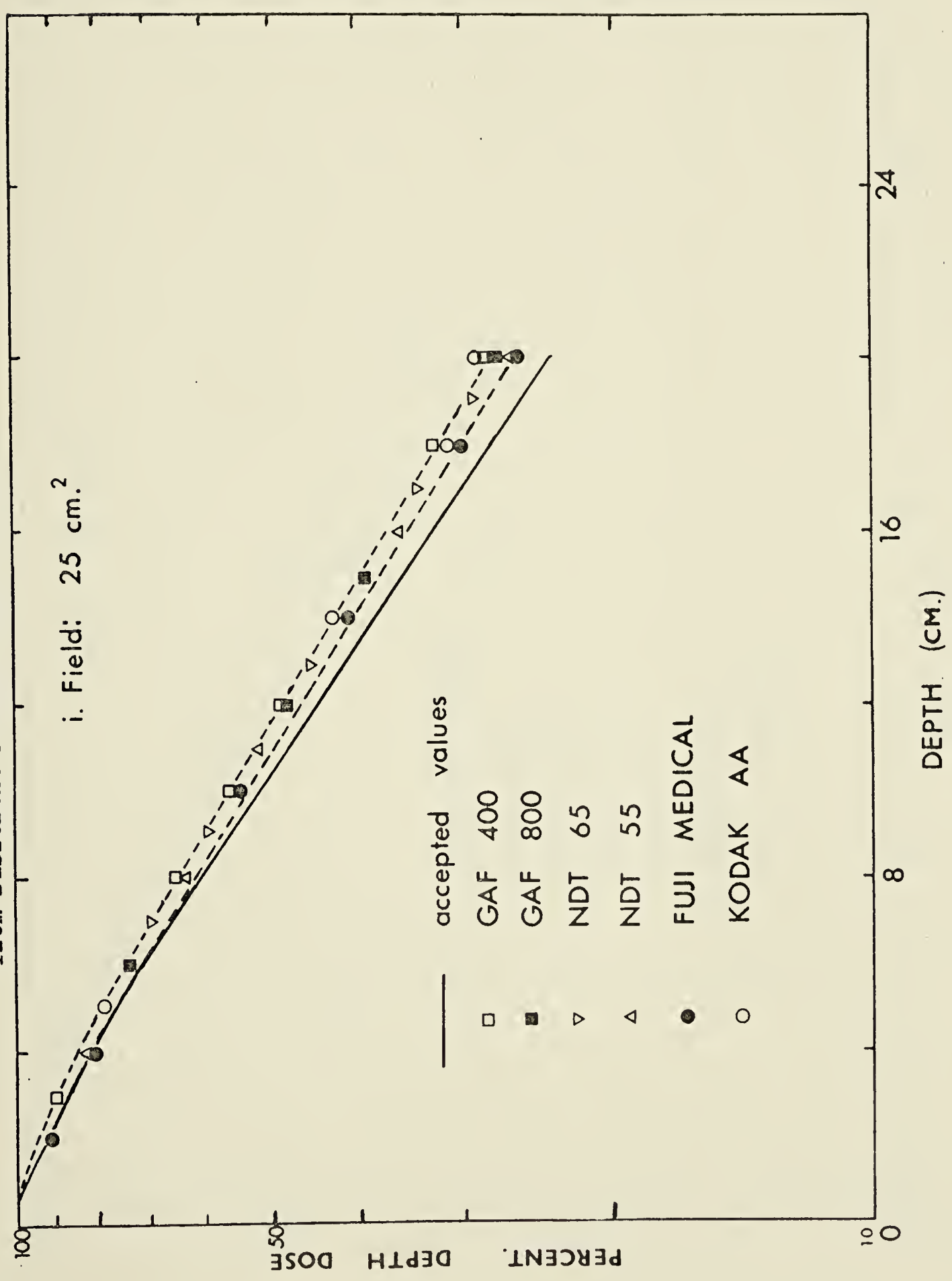


Fig. 13 ii Depth Doses of Cobalt Radiation with Field 100 cm^2 as measured from Different Films in Full Phantom

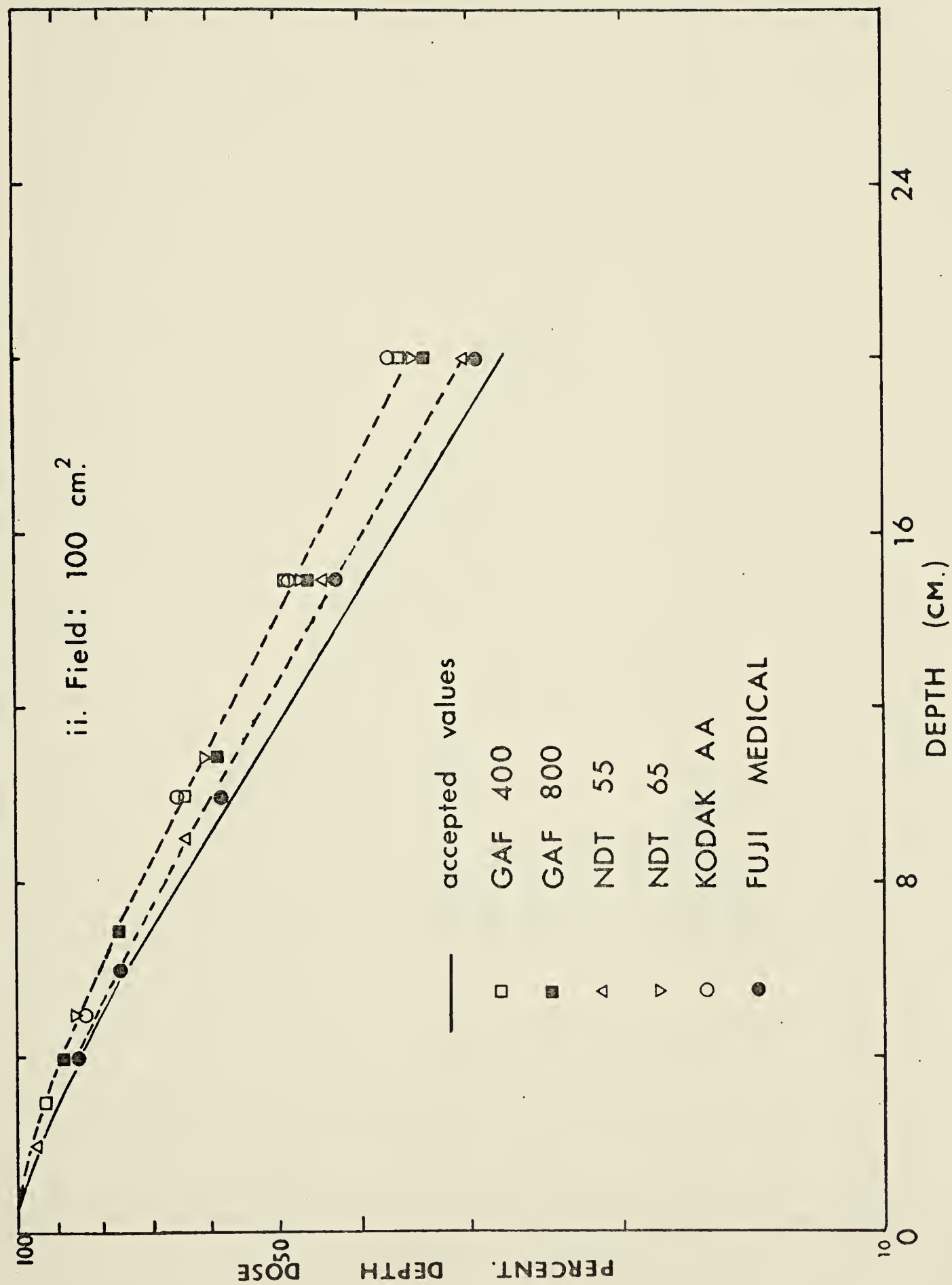


Fig. 14 1 Depth Doses of Cobalt Radiation with Field 25 cm^2 as measured from Different Films in Limited Phantom

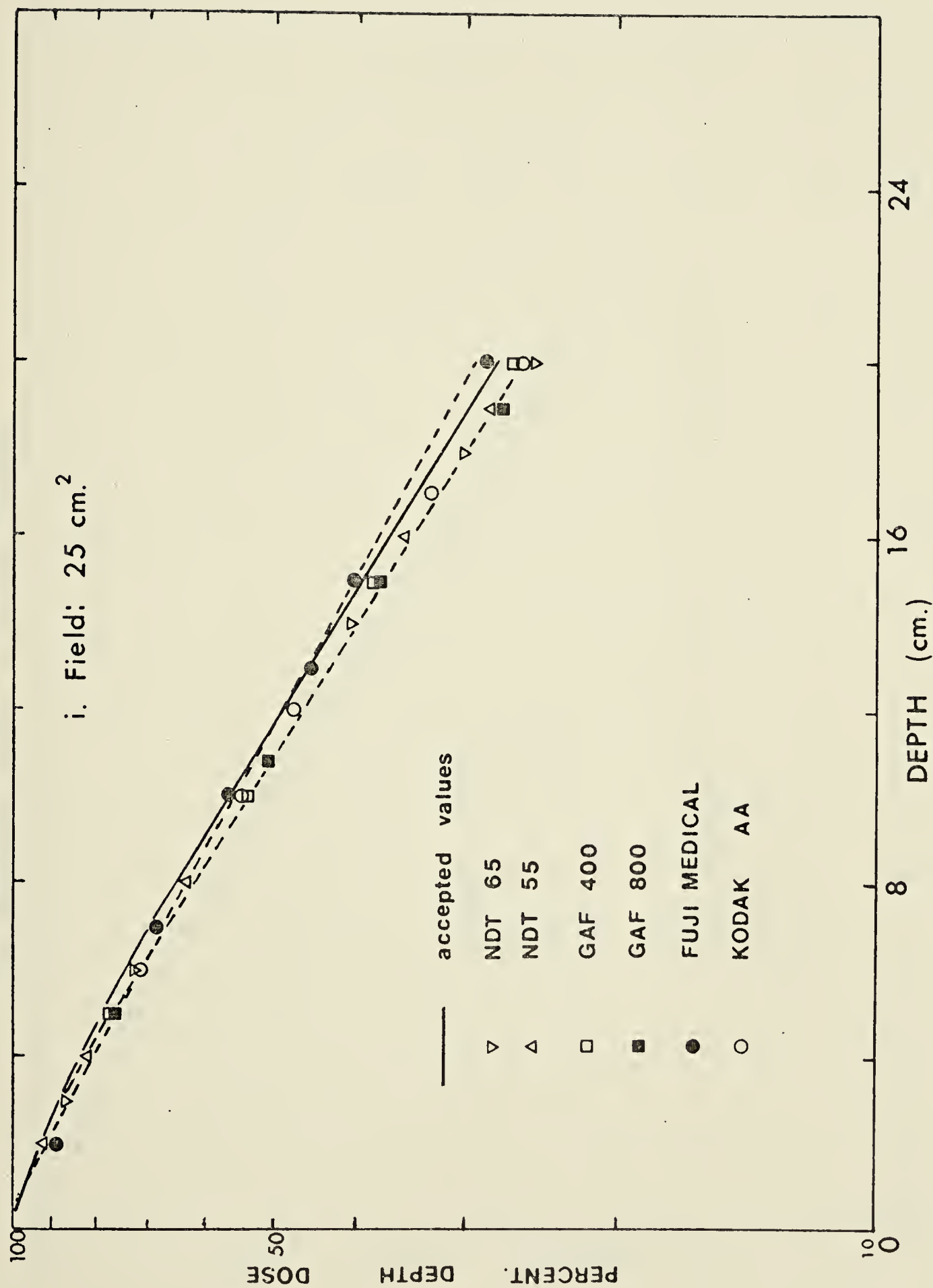
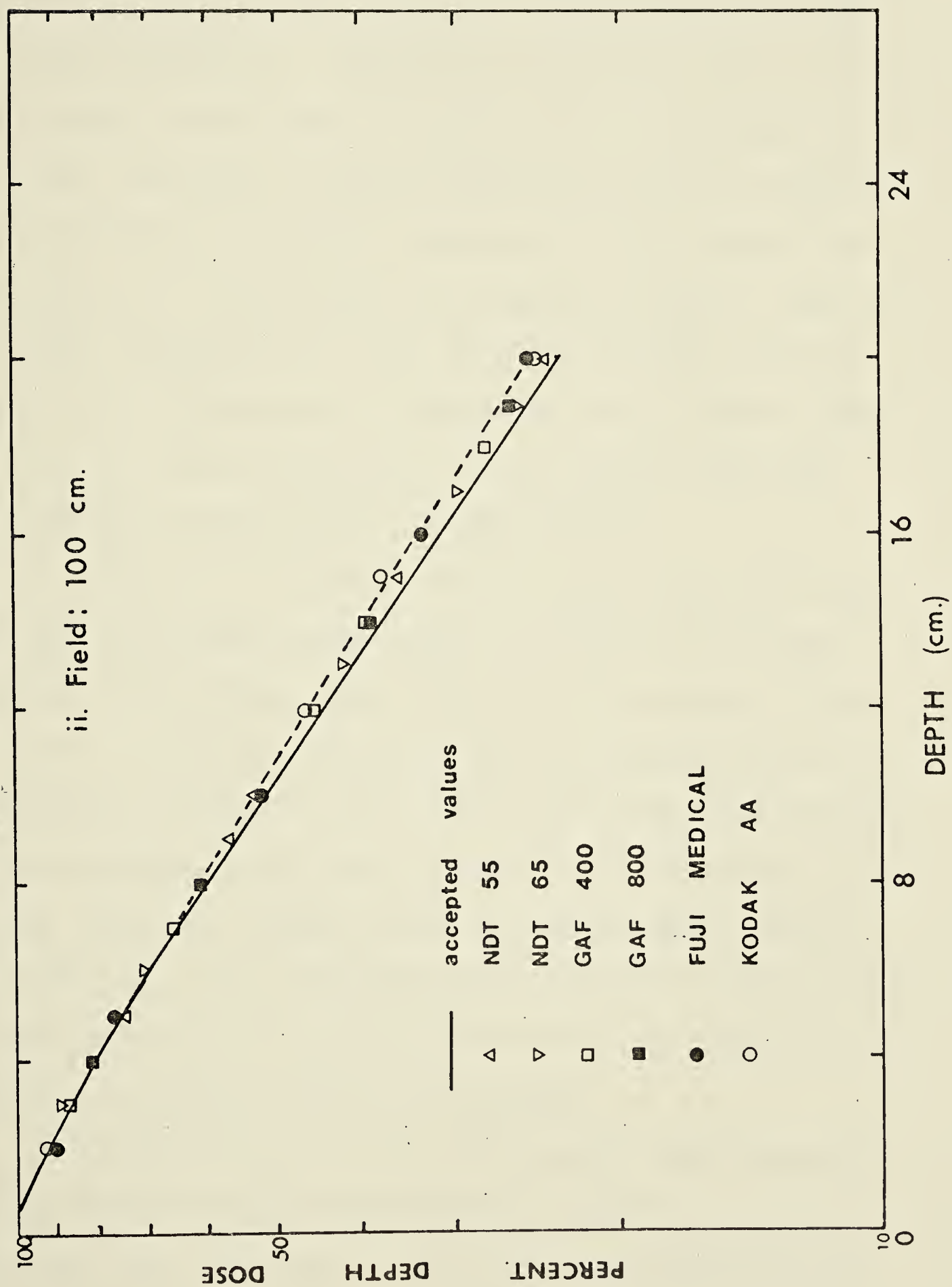


Fig. 14 ii Depth Doses of Cobalt Radiation with Field 100 cm^2 as measured from Different Films in Limited Phantom



limited phantom is not generally applicable to all films, as different films show different sensitivities to the low energy radiation. Therefore, for every film to be used in the limited phantom method, it is necessary to check the thickness of phantom that will give the appropriate amount of scattered radiation. This agrees with other reported thicknesses for different films: Onai et al. (1972) required 6 cm. for Fujilith Contact with radiation of 4.3 MeV x-rays; Tsunemoto et al. (1966) used 2.5 cm. for Sakura Industrial R with cobalt radiation.

(iv) Effect on Penumbra Dose Measurement

In addition to the fact that energy dependence can cause the percentage depth doses of films to be interpreted as being higher than those of the accepted values in the full phantom, Stanton (1962) pointed out that, at the penumbral region of the field, the major contribution to the penumbral dose comes primarily from scattered radiation, which is usually lower in energy than the primary radiation. The resulting high density caused by this scattered radiation can be interpreted as an apparent increase in the field size at all depths.

The densities in the penumbral region were measured from the films (Kodak M and Ilfoline) which were used to obtain the data for Figs. 11 and 12. Measurements were also made from AECL isodose charts and served as references.

Fig. 15 i and ii illustrate the relative profiles of an incident field size of 100 cm.^2 as obtained from Kodak M and Ilfoline films in both the full and the limited phantom at the depths of 4.5 cm. and of 16 cm. respectively. The points in Fig. 15 have been obtained by normalizing the densities in the penumbral region to the density on the central axis. To clarify the presentation of Fig. 15, the points from the limited phantom have been normalized to 200% and those from the full phantom to 100%.

In order to facilitate the comparisons between different types of films, the width of the distance from the central axis up to and including 0.4 of the relative profile was measured from Fig. 15, and is henceforth termed the 'width' of the relative profile. The following observations can be made:

1. Measurement of Penumbral Densities

For Ilfoline films, the penumbral densities obtained at all depths were nearly identical for both the parallel and the perpendicular methods.

With similar methods, Kodak M films did not produce nearly identical penumbral densities at all depths. Only the penumbral densities obtained at the depths greater than 10 cm. are nearly identical for both methods of exposing the film. At the depths less than 10 cm., penumbral densities as obtained by the parallel and by the per-

Fig. 15 i Relative Profiles of 100 cm² Field Cobalt Radiation at Depth 4.5 cm as measured from Ilfoline and Kodak M Films

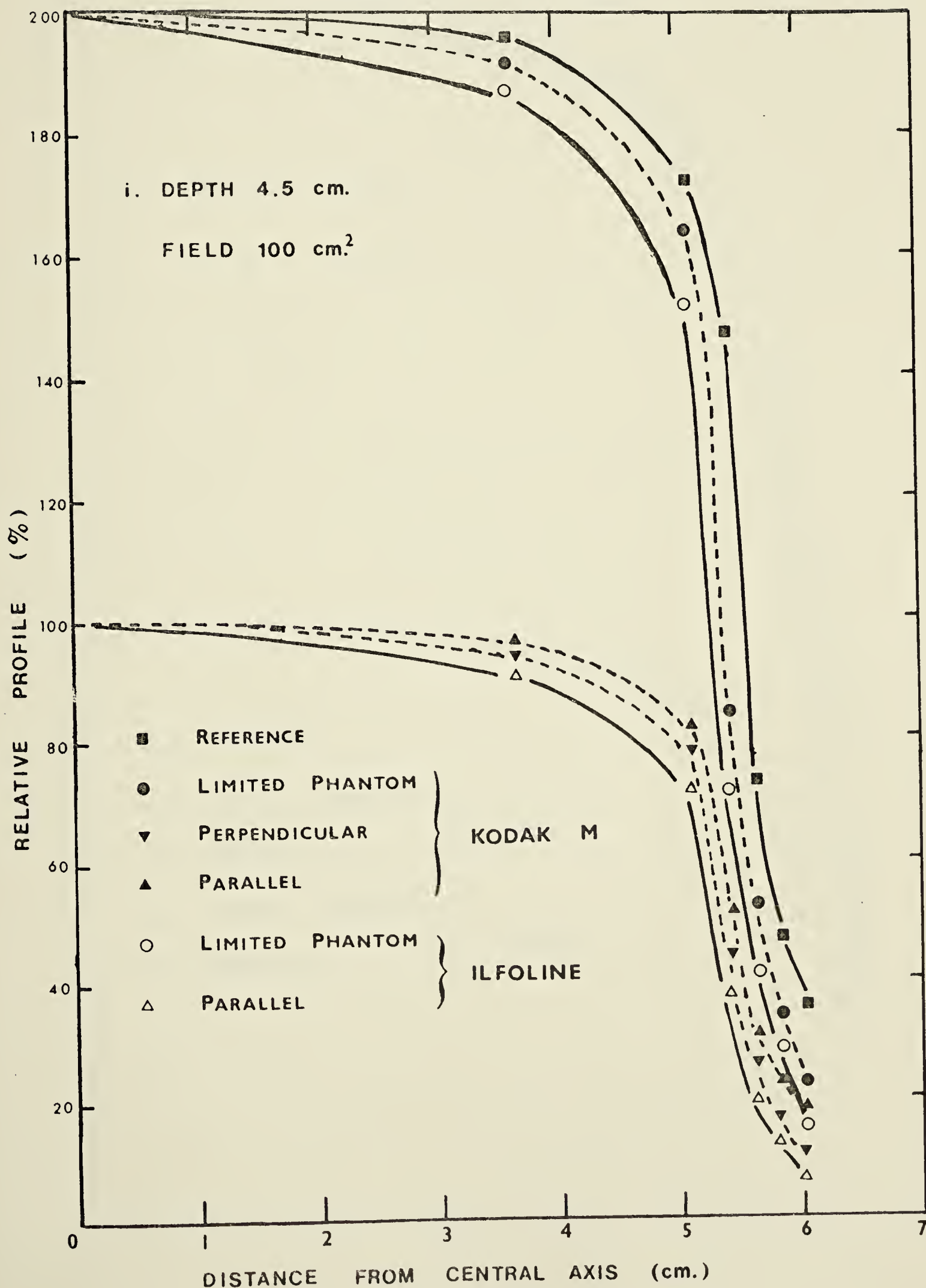
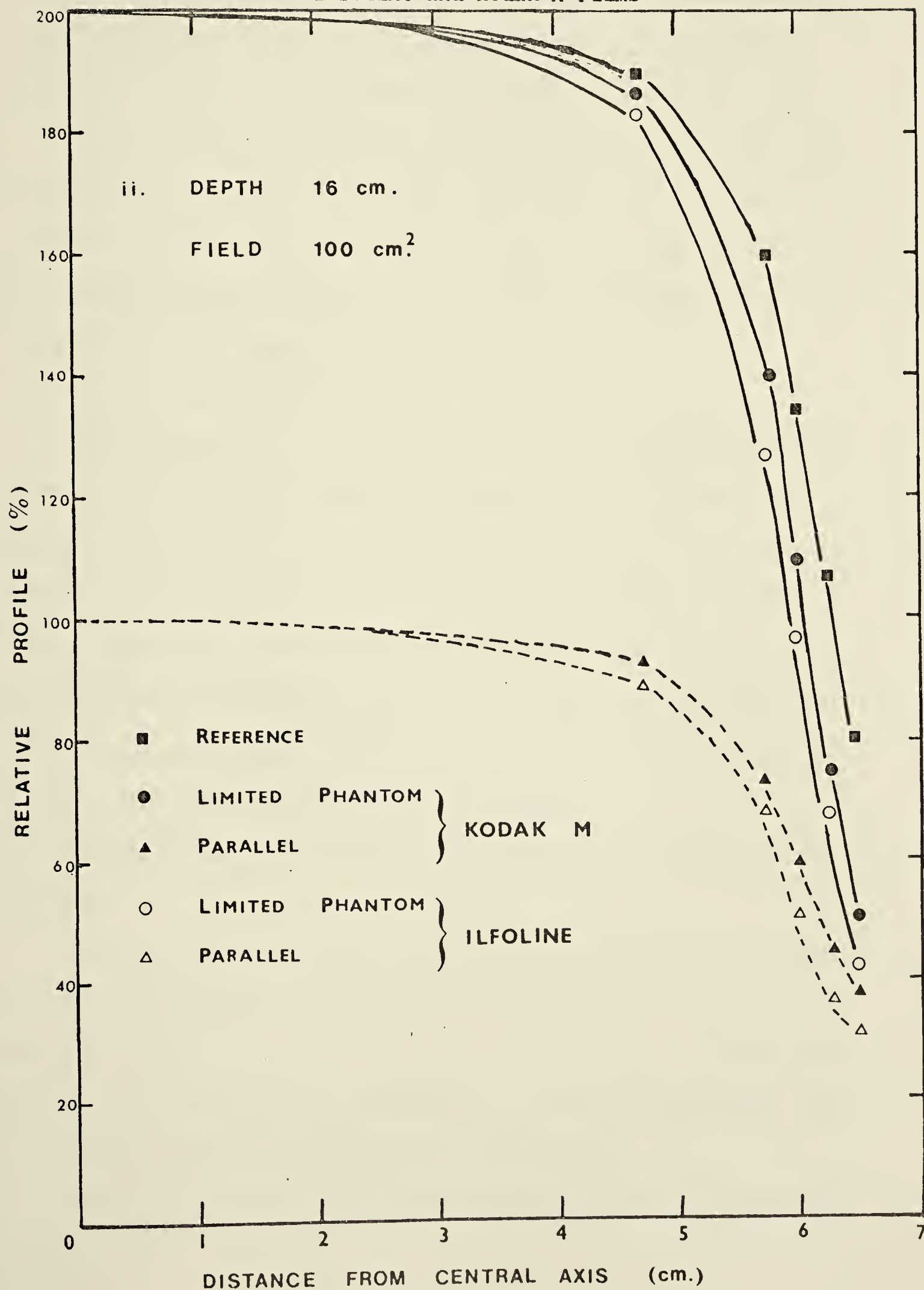


Fig. 15 ii Relative Profiles of 100 cm^2 Field Cobalt Radiation at Depth 16 cm as measured from Ilfoline and Kodak M Films



pendicular methods are observed to be different. However, the amount of difference in density depends upon where the point measurement is located. This difference is further elaborated below and in section 3.3.3.

In the case of nearly identical densities for both methods of exposing the films, only the results for the parallel method are presented in Fig. 15, and those for the perpendicular method can easily be deduced from the results for the parallel method.

2. Comparisons between Films

The 'widths' of the relative profile as demonstrated in Fig. 15 ii in the full phantom by Ilfoline and by Kodak M are 6.2 cm. and 6.5 cm. respectively. The larger value of the 'width' of the relative profile of Kodak M films than that of Ilfoline films indicates that Kodak M films are more energy dependent. This observation is consistent with the results obtained for the percentage depth dose measurement for both films.

3. Comparisons between the full and the limited phantom methods

The 'widths' of the relative profile as demonstrated in Fig. 15 ii in the limited phantom by Ilfoline and by Kodak M are 6.0 cm. and 6.2 cm. respectively. When compared with the results obtained in the full phantom, the present results are smaller for both films.

This observation can be attributed to the reduction

of scattered radiation reaching the film in the penumbral region. Conversely, these data indicating smaller 'width' prove the statement that the apparent increase in the penumbral profile as obtained by films is caused by the scattered radiation.

4. Comparisons between the parallel and the perpendicular methods

It can be observed from Fig. 15 i (at a depth of 4.5 cm.) that the 'width' of relative profile shown by Kodak M films as obtained from the parallel method is larger than that obtained from the perpendicular method. The 'widths' of relative profiles for the perpendicular and the parallel methods are 5.3 and 5.6 cm. respectively. This difference in relative profile will be explained in terms of angular dependence in section 3.3.3.

5. From Fig. 15 i and ii, it can be observed that the 'width' of the relative profile as demonstrated by the AECL chart is still larger than that obtained from the films in the full phantom. The cause of this discrepancy is uncertain, but could be attributed to the difference in the spatial resolution of the dosimeters used by AECL and those used in the present work.

6. For field sizes of 25 cm.^2 and 400 cm.^2 , which are not depicted here, similar observations concerning the 'penumbral width' and the relative profile can be made, thus further supporting the results as presented in the above observations.

3.3.3 Angular Dependence

(i) Introduction

It has been noted earlier in section 2.5 that the angular dependence of films in photographic beta ray dosimetry causes the film exposed by the parallel method to respond differently than when exposed by the perpendicular method, both films having received the same initial dose. Dudley (1954) in a critical study of angular dependence for beta particles suggested that the angular dependence of films is a strong function of the angle of incidence, especially for low energies and at large angle of incidence.

With gamma rays, much of the exposing action of the silver halide grains is brought about by the secondary electrons. Therefore, in photographic gamma ray dosimetry, the film, when exposed by the parallel method, receives the radiation at a larger angle of incidence than in the case of the perpendicular method. In this situation, angular dependence as demonstrated by the film can conceivably give misleading optical density, effectively limiting the usefulness of the film for giving accurate two-dimensional representations of isodose distributions.

(ii) Observation

The upper portions of Fig. 11 i, ii, iii, and 12 i, ii, iii depict the density-depth values by the parallel and the perpendicular methods with Kodak M and Ilfoline films for the fields of 25, 100 and 400 cm.²; the lower

portions show the percentage depth doses.

The angular dependence can be observed in Kodak M films, i.e. the parallel method did not measure the same density as the perpendicular method, up to a range of depth of 10 to 12 cm. The depth of 12 cm. occurs in a field size of 25 cm.² and that of 10 cm. in a field size of 400 cm.². Having been exposed by the parallel method, the film thus introduces a discrepancy by giving higher percentage depth doses than those obtained from the one exposed by the perpendicular method, as shown in the lower portions of the graphs.

The average difference in density between these two methods as measured by Kodak M films at the depth of 0.5 cm. is about 10%. This observation is in essential agreement with that obtained by Onai et al. (1972). In the case of Ilfoline, the difference is less than 2%. The percentage depth doses, at depths greater than 10 cm., determined by the parallel method with Kodak M are consistently 7-12% higher than those determined by the perpendicular method. On the other hand, Ilfoline does not reflect such deviation, as it is able to measure nearly identical depth doses at all depths by both methods.

(iii) Evaluations

In order to give an indication of the magnitude of angular dependence at various radiation energies, the following procedures were carried out. For 1.25 MeV

(cobalt), films were sandwiched between two small sheets of lucite, each of thickness of 0.5 cm.,; for 0.66 MeV (cesium), they were inserted between two pieces of 0.1 cm. thick cardboard; and for low energy x-rays, they were wrapped in a paper cassette. All irradiations were made with the smallest field sizes available. The films were then exposed to radiation by means of the perpendicular and the parallel methods.

The estimations of angular dependence of films are presented in Table VI. The percentage shown in this table is the difference in density between 0° and 90° incidence divided by the density at 0° incidence and the variances of the results are about 2-5%.

The observation of about 12% for 1.25 MeV gamma rays with Kodak M films is in basic agreement with the value of higher than 10% reported by Tochilin (1955).

(iv) Explanation

If the data presented in Table VI are utilized, the depth doses for cobalt radiation as determined by both photographic methods of exposing Kodak M and Ilfoline films can be interpreted.

Near the surface of the phantom, the primary radiation contributes a greater proportion than the scattered radiation to the total dose given to the film. This primary dose is delivered by the parallel method at approximately glancing angles of incidence to the film. As shown

Radiation Energy (MeV)	KODAK M		ILFOLINE	
	Experimental Results	Theoretical Evaluations	Experimental Results	Theoretical Evaluations
1.25	~12%	0.9%	~2%	0.26%
0.66	~10%	1.5%	~2%	0.28%
0.14	~18%	6.8%	~4%	0.31%
0.035	--	--	~15%	50.5%

Table VI. Experimental and Theoretical estimations of Angular Dependence for both Kodak M and Ilfoline Film.

in Table VI, Kodak M films show about 12% dependence with cobalt radiation. Therefore, this accounts for the depression of about 10% in the optical density as compared with the same type of film exposed by the perpendicular method.

However, with the increase of phantom depth traversed, the relative dose contribution from the scattered radiations increases (Derbowka and Cormack, 1965). These scattered radiations reach the film more isotropically than the primary. As the film shows an enhanced response to the low energy scattered radiations, the relative importance of angular dependence for the primary radiation diminishes as compared to energy dependence.

At the depths greater than 10 cm., energy dependence completely dominates the response of the film. Under this condition, a film, regardless of its orientation inside the phantom, measures approximately the same density, i.e. dose. In the case of Ilfoline films, because of their lack of angular dependence for the primary radiation, both the parallel and the perpendicular methods give nearly identical depth dose results.

(v) Limited Phantom Method

For Kodak M films in a limited phantom, the percentage depth doses obtained can approximate those of the accepted values as shown in Fig. 11. With the removal of scattered radiation, the effect of angular dependence of the primary radiation remains more dominant at all depths.

However, after reference to the maximum density, the angular dependent effect is cancelled out for all depths in the phantom. Hence, the percentage depth doses measured by the parallel method in the limited phantom are not seriously affected by this dependence.

(vi) Factor Determining Angular Dependence

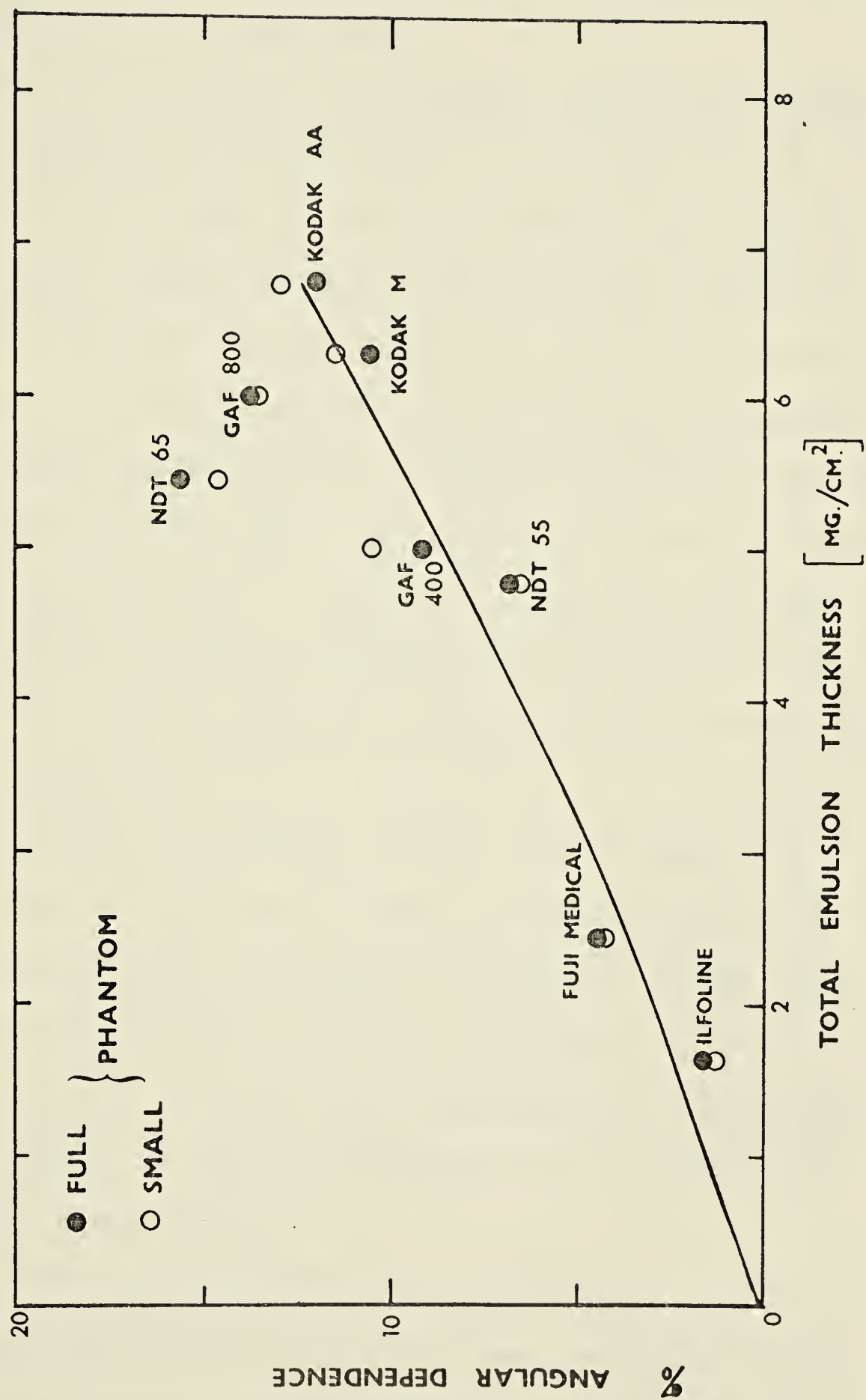
It is apparent that Ilfoline film is less angular dependent than Kodak M. Fig. 16 illustrates the percentage angular dependence of different emulsions as measured for cobalt radiation by the parallel and the perpendicular methods, at the depth of 0.5 cm. with the field size of 25 cm.² in the semi-infinite and the 0.5 cm thick phantoms.

The angular dependence increases with increasing emulsion thickness, from observation in Fig. 16. All emulsions having thickness of more than 5 mg./cm.² show an angular dependence of at least 10%. The result appears to support Dudley's (1954) general claim for beta particles. All values of emulsion thickness of films were obtained by stripping the emulsion layer from the film base with warm water. The difference in weight per unit area between a film and its film base determined the emulsion thickness for that particular film. These results are within 10% of the manufacturers' supplied data.

(vii) Low energy radiation

Preliminary results of depth-density measurements for effective x-rays energy of 0.14 MeV also indicate a similar angular dependent effect to that for cobalt .

Fig. 16 Angular Dependence of Different Emulsion Thicknesses in Cobalt Radiation



radiation with Kodak M and with Ilfoline films.

(viii) Theoretical Comparison

A possible expression for angular dependence of density has been given in section 2.5. In order to give an estimate of the accuracy of that expression, the value of μ , mass energy-absorption coefficient, for an emulsion at a radiation energy has to be assessed. Let it be presumed, for purposes of simplification, that a film is primarily a layer of emulsion elementally composed of silver bromide grains. Dudley (1968) gave the values of the mass energy-absorption coefficient for AgBr as a function of photon energy. Then the values of coefficient at different radiation energies were read from his graph and used to evaluate the expression.

At the angle of incidence of 89° (to simulate the parallel method of incidence), the computed values of % angular dependence are presented in Table VI. When compared to the experimental results, the values computed by using the expression are not too satisfactory, especially for predicting the angular dependence at low energy radiation and for Kodak M films.

(ix) Effect on the Penumbra Dose Measurement

As noted in section 3.3.2 (iv), measurements of the penumbral densities at any depth, for Ilfoline films exposed by both the parallel and the perpendicular methods, give nearly identical data. Therefore, the 'widths' of

the relative profiles of the fields as obtained by both methods were essentially identical.

In the case of Kodak M films, at the depths greater than 10 cm., nearly identical penumbral densities were also measured for both methods of exposing the film. Hence, nearly identical 'widths' of relative profiles were also obtained.

However, at the depths less than 10 cm., the 'widths' of the relative profiles determined by the parallel method are larger than those determined by the perpendicular method, as illustrated by Fig. 15 i. The penumbral densities measured by using the parallel method were less than those for the perpendicular one, depending upon the location of measurement. As the distance from the central axis increased, the discrepancy in densities decreased until nearly identical densities appeared, in essential agreement with Onai et al.'s (1972) observations.

With the above observation, the difference in the 'widths' of the relative profiles as obtained by the perpendicular and by the parallel methods may be explained.

Because of angular dependence in the central axis, the densities obtained from the parallel method are less than those obtained from the perpendicular one. However, in the penumbral region, the response of the film is dominated by the scattered radiations which are isotropically incident on the film regardless of its orientation

with respect to the primary beam. Therefore, this leads to the eventual identical densities for both methods of exposing films as the distance from the central axis increases.

Hence, after normalization to the density at the central axis, the 'widths' of the relative profiles measured by the perpendicular method are smaller than those measured by the parallel one, since the film exposed by the perpendicular method recorded higher density in the central axis than the film exposed by the parallel method. This difference in the 'widths' of the relative profiles can be observed in Fig. 15 i and, from 100% to 40% of the relative profile, is about 0.3 cm., as pointed out in section 3.3.2 (iv).

3.3.4 Effects of Development Conditions

(i) Different Developers

The percentage depth dose as determined by films can be evaluated from expression (3) of section 3.1.2, i.e. $(D - D_o)/(D_m - D_o) \times 100$. These densities, D , D_m and D_o , are dependent upon the developers and development times. To test if the percentage depth dose depends upon the developer in which the film was developed, films (Kodak M) exposed by the parallel method in the phantom were processed manually with the procedure already described in section 3.2.2. The developers were all manufactured by Kodak company.

Two main difficulties encountered in using the non-x-ray developers (D-19 and D-72) were:

- 1) the thoroughness and the uniformity of the processing of films in these developers were not easily achieved;
- 2) in addition, the linear response of the film is dependent upon a combination of development conditions and film type.

The optimal results of the characteristic curves have been presented in Fig. 7 of section 3.2.2, in agreement with Frey's (1954) observation that the shapes of the characteristic curves of a film depend upon the developers used. Reduction of development time with the non-x-ray developers caused non-uniformity in the processing of films. However, prolongation also caused a loss in the linear response of the film. Except under extreme deve-

lopment times, these difficulties were not encountered when films were processed in x-ray developers.

Fig. 17 i, ii, iii show the percentage depth dose with Kodak developers: D-19, D-72 and x-ray, (also the depth dose with Picker #3790 developer used in the automatic processor included as a comparison), for the field sizes of 25, 100 and 400 cm.² of cobalt radiation. For the points in this graph, the maximum difference in density among 4 runs was about 0.19 within the period of one day.

An important point emerges from these observations: that the depth dose obtained from the film is unique if and only if every parameter involved in the processing conditions is uniquely defined. If any parameter for the procedure is altered, the percentage depth as measured by film may be changed.

Another important observation can also be made. The percentage depth doses as obtained by using various developers for the field sizes employed still show the effect of energy dependence of emulsion, i.e. with the increase of the field size, hence the increase of scattered radiations, the percentage depth doses as measured by films increase in discrepancy from the accepted values.

The reasons for the difference in results among the developers are not clear. Further efforts are required to explain the differences noted in the experimental data.

Fig. 17 i Effect of Different Developers in the Determination of
Depth Dose of Cobalt Radiation with Field 25 cm^2 as measured
from Kodak M Films

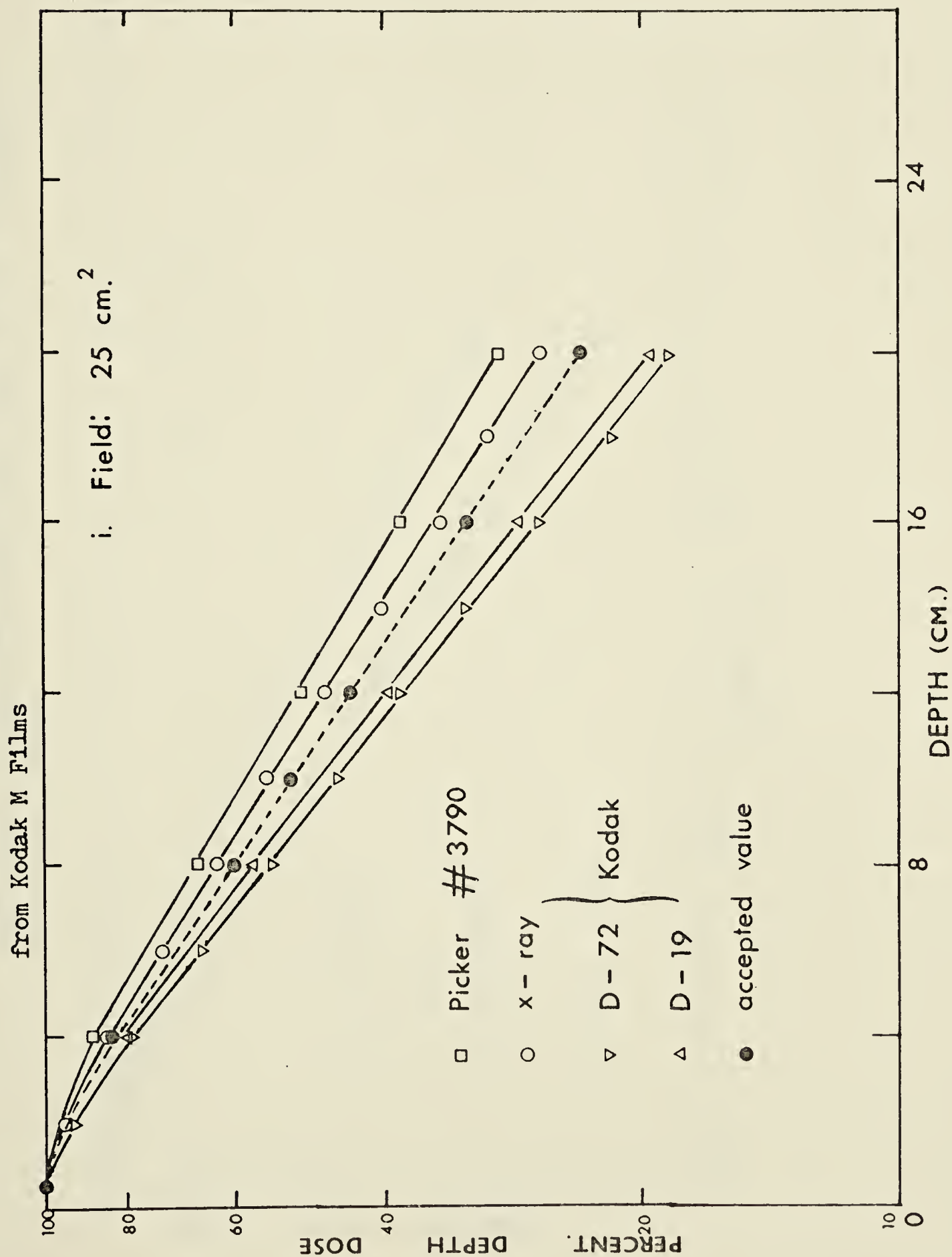


Fig. 17 11 Effect of Different Developers in the Determination of
Depth Dose of Cobalt Radiation with Field 100 cm^2 as measured
from Kodak M Films

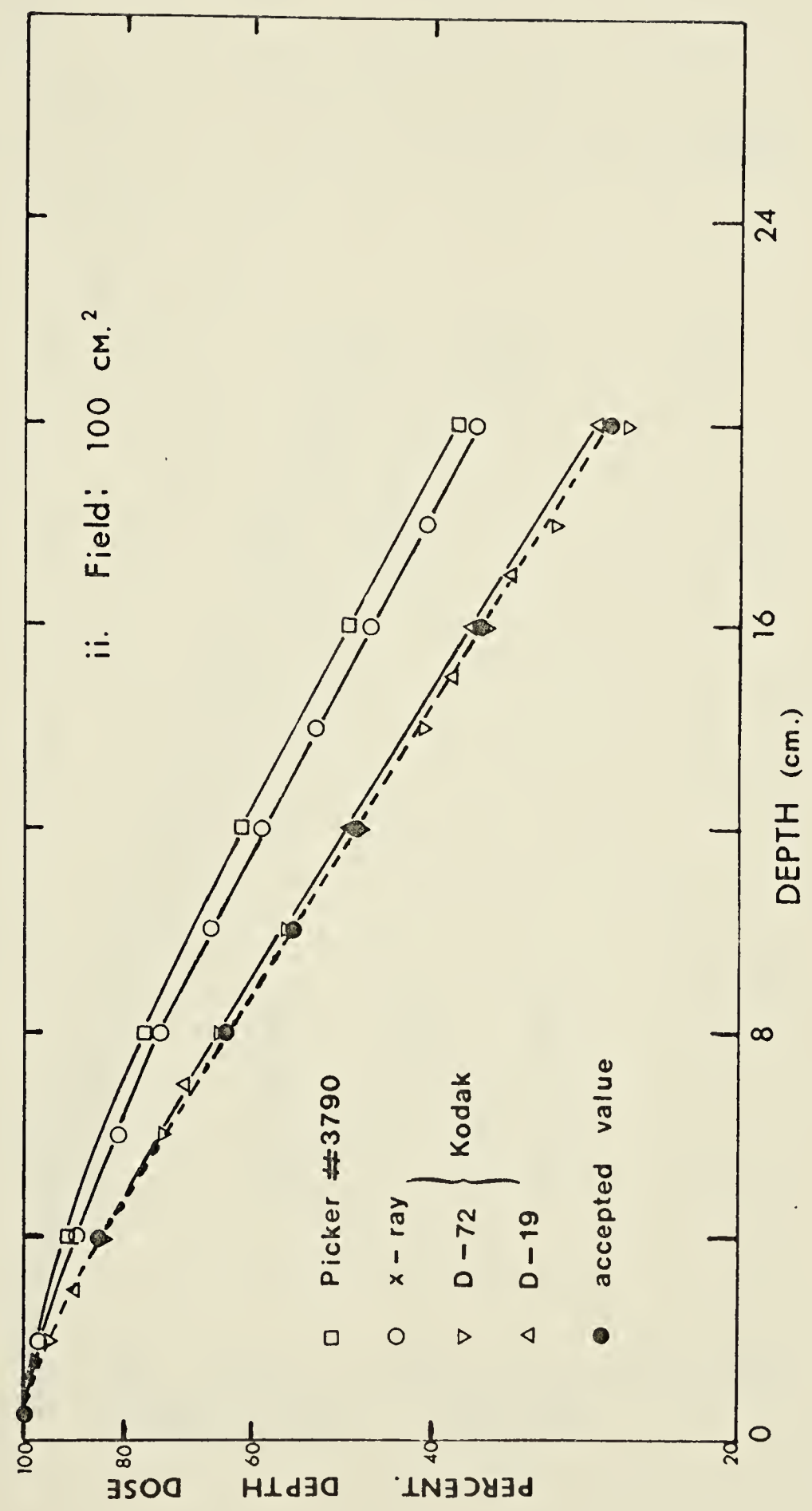
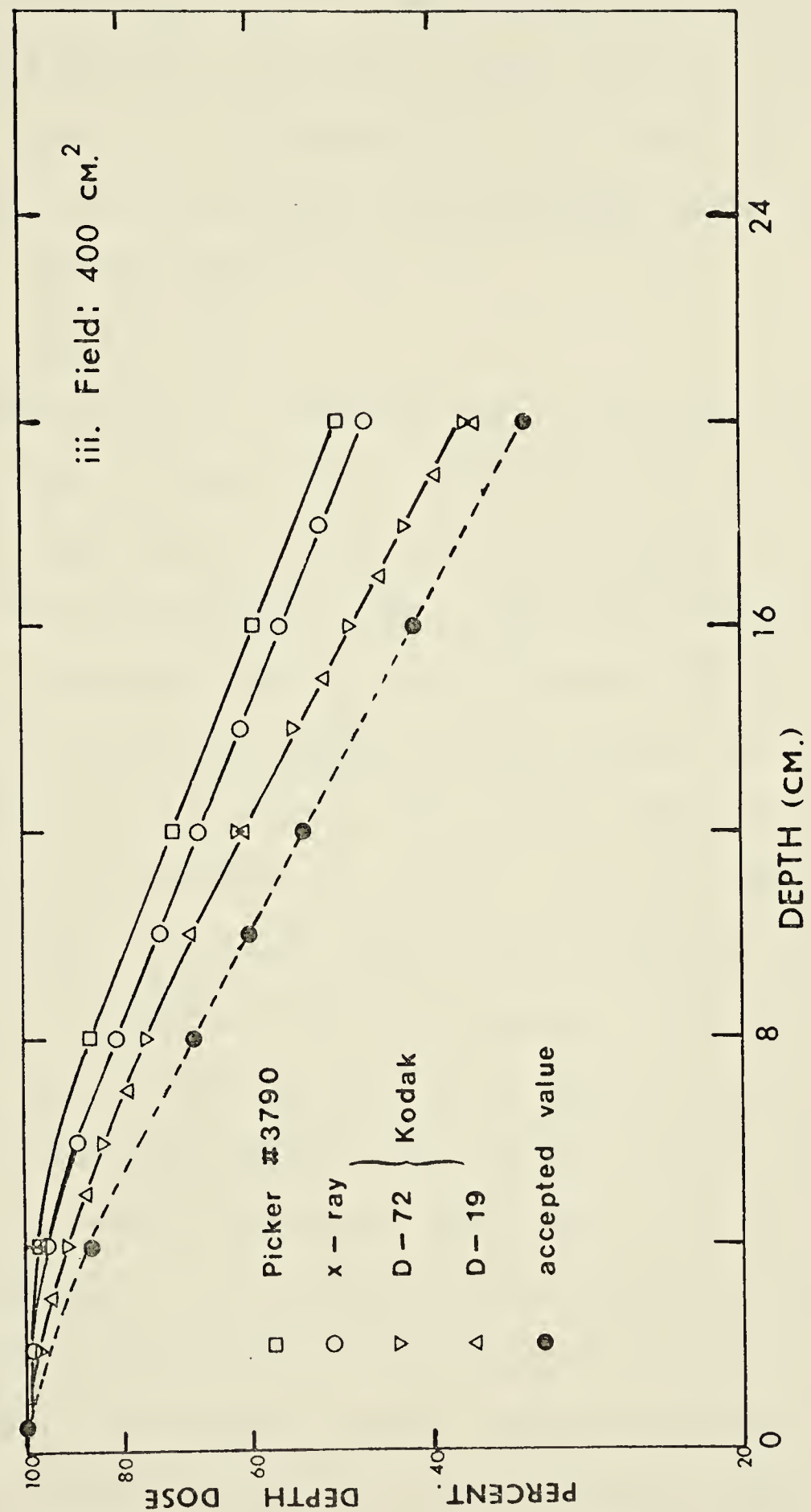


Fig. 17 iii Effect of Different Developers in the Determination of
Depth Dose of Cobalt Radiation with Field 400 cm^2 as measured
from Kodak M Films



It is uncertain if any method is available to readjust the lower percentage depth doses measured by using the non-x-ray developers, as shown in Fig. 17 i, to the accepted values. One alternative is to avoid the use of developer that can lower the percentage depth doses below the accepted values.

(ii) Development Times

The densities of a developed film are also a function of the development time. The Picker #3790 developer was used to process the films in the automatic processor for different development times. With this developer, the linear response could be still retained after the development times were changed. The results have been already presented in section 3.2.2 where Kodak M films were processed at different speeds, hence different development times. Similar results were obtained for the other films, including Ilfoline, but they were not shown.

Both Kodak M and Ilfoline films exposed by the parallel method were processed at two other speeds, one higher and one lower, than the normal speed available in the automatic processor. For Kodak M films, speed settings used were 35, 30 (normal) and 20, and for Ilfoline films, they were 60, 50 (normal) and 30. Speed settings higher than 35 for Kodak M films or 60 for Ilfoline films did not provide adequate processing time; therefore, they were not attempted.

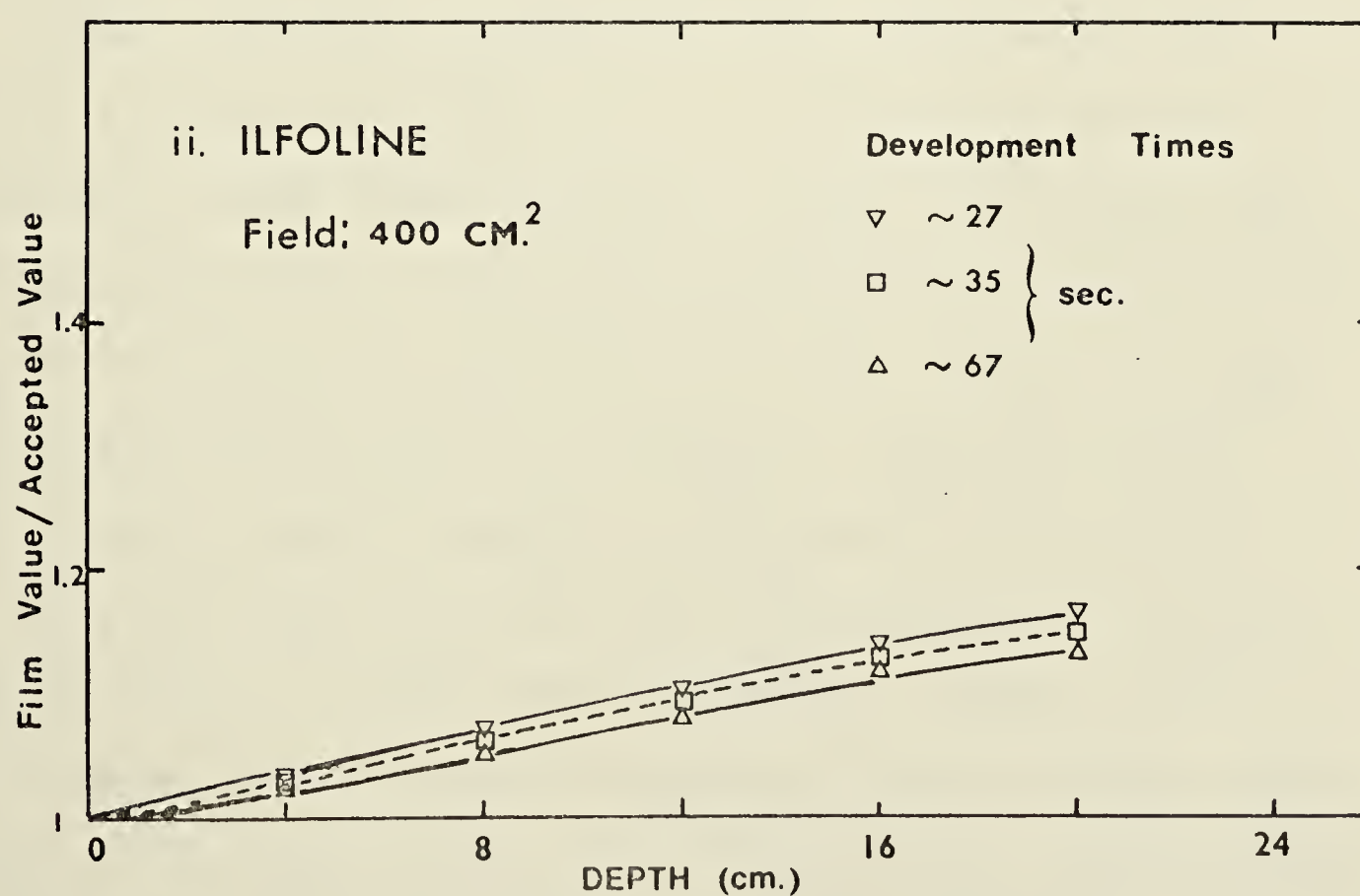
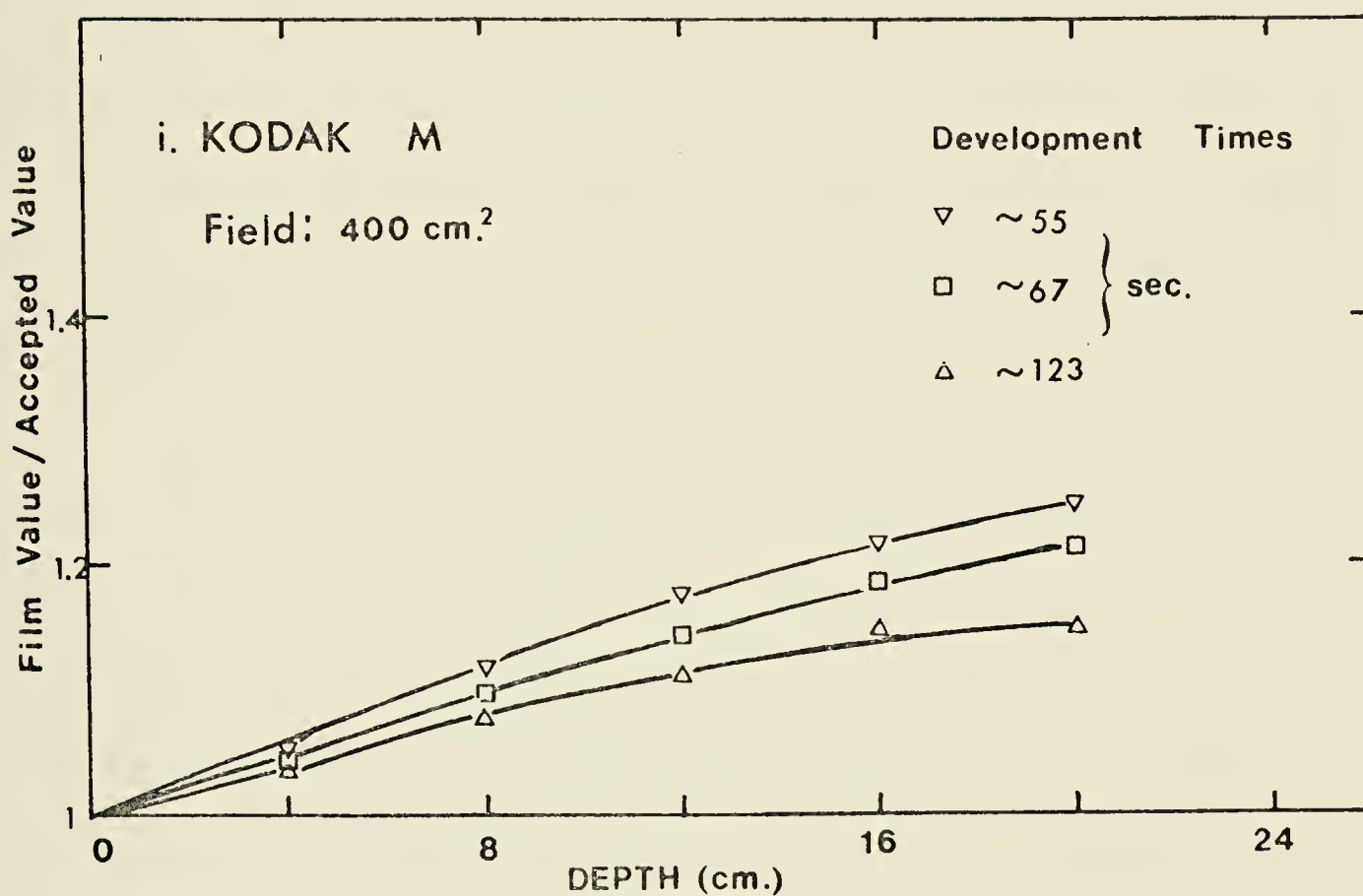
Fig. 18 i, ii give the ratio of the percentage depth doses measured by films to the accepted values for the field size of 400 cm.^2 of both Kodak M and Ilfoline films respectively, for the different development times described above. Between three runs, the maximum difference in density measured for Fig. 18 was about 0.08 for Kodak M and 0.06 for Ilfoline.

For field sizes of 25 and 100 cm.^2 , the difference between the results for both films in different development times is only 2-4% at the depths of 10 and 20 cm., and is therefore not shown. With the field size of 400 cm.^2 (Fig. 18 i & ii), the difference between Kodak M and Ilfoline films is apparent. At a depth of 20 cm., the difference in the data points in Fig. 18 between the shorter or the longer development times and the normal development time is 6-10% for Kodak M, but is only 2-3% for Ilfoline.

Dudley (1954) reported that, with Eastman no-screen films, the sensitivity at different energies of electrons increased monotonically with development times, but the increase was less rapid for low than for high energy electrons. Since the exposing actions are attained mostly by secondary electrons with x- or gamma rays, Dudley's results indicate that prolonged development will reduce the relative sensitivity of film to the low energy radiations.

From the model of film response (section 2.4), any prolongation of development that tends to decrease the

Fig. 18 Effect of Different Development Times in the Determination of Depth Dose of Cobalt Radiation as measured from Ilfoline and Kodak M Films



relative sensitivity of the low energy radiation, also reduces the ratio of (m_n/m_p) . In the case of small and medium field sizes, the contribution of the term, $\sum_{n=1}^k (m_n/m_p) S_n$, to the total dose is relatively not too dominant, and a slight change in the development times does not alter the percentage depth dose very much. This is in accordance with the observations for both Kodak M and Ilfoline films.

In the case of large field sizes such as 400 cm.^2 , the term $\sum_{n=1}^k (m_n/m_p) S_n$ becomes the dominant factor affecting the response of a film. For films which are extremely sensitive to low energy radiations, a decrease in the ratio of (m_n/m_p) will definitely give better percentage depth doses, in accordance with the present results for Kodak M.

Under identical conditions, this observation with Ilfoline films also points out a distinctive inherent feature of Kodak M and Ilfoline, in that the latter film is less sensitive to low energy radiations. Slightly prolonged development should not alter the ratio of (m_n/m_p) drastically in the case of Ilfoline. Even with large field sizes, slight changes in development time should not vary the effect of the term, $\sum_{n=1}^k (m_n/m_p) S_n$, for Ilfoline as much as in the case of Kodak M. Hence, if the development time is varied slightly, the percentage depth doses of all field sizes with Ilfoline films remain fairly constant, in agreement with the present findings.

3.3.5 Stability of Latent Image

(i) Introduction

In this study, all films were processed within 24 hours after the initial exposures had been made. Whether the silver halide grain has the ability to retain the latent image for such a period of time is a problem to be answered.

It has been pointed out by McLaughlin and Ehrlich (1954) that whether formed by the action of visible light, x- or gamma rays or ionizing particles, the latent image is unstable if the film is kept for a period of time before processing. Buchignani and Howlett (1973) reported that Dupont Cronex 4 showed a decrease in densities resulting from various exposures by light if the films were processed at different times after initial exposures were made. No such observation was made with two other different films.

(ii) Experimental Conditions

To check the stability of the latent image, three different films were chosen in the present experiment: Kodak M, Fuji Medical and Ilfoline. They were selected to represent three different emulsion types: Kodak M and Fuji Medical being double emulsion, the emulsion thickness of the former being about triple that of the latter, and Ilfoline being a single emulsion film. Films were prepared by exposing to radiation using methods similar to those described in section 3.2.3, Table III, where they

were stacked under an electron equilibrium material and exposed simultaneously. They were stored in their respective boxes inside the storage bin of the darkroom.

No attempts were made to influence either the humidity or the room temperature of the darkroom. The relative humidity and the room temperature over the course of 4 weeks were monitored by a wet and dry bulb thermometer. Readings were taken three times daily: morning, afternoon and evening, except Sundays, since the room temperature and the humidity could be expected to remain constant during the weekends as there was no operation of any machinery. The room temperature varied between $73 \pm 2^{\circ}\text{F}$ and the relative humidity remained at $20 \pm 4\%$ throughout this period.

(iii) Observations

Overall results indicated that the fading of the latent image was not too serious a problem in the above environment for all emulsion types under consideration. The largest drop in density was observed in Ilfoline films with a maximum difference of no more than 5% over the monitoring period. But taking into account the variations in the processing conditions occurring during the same period, this drop in density was not too significant. This is in accordance with the findings of Heard et al. (1960) that, under the influence of a temperature of 30°C , the fading of the latent image of Ilford PM1 films over a period of 3 months was virtually non-existent at a rela-

tive humidity of 30%. But at 80% relative humidity, they reported the drop of density could be as high as 60%.

(iv) Explanation

It has been shown that the fading of the latent image is predominantly a chemical process, initiated by factors such as the humidity and the temperature in the environment (Ziegler and Chleck, 1960; Kathren and Brodsky 1963), but the actual mechanism has never been completely analyzed. It must also be understood that the relative importance of chemical or physical agents for the fading probably differs from emulsion to emulsion, in agreement with Buchignani and Howlett's observations.

Dudley (1968) suggested that the most likely reason for the fading is the oxidation of the latent image by the atmospheric oxygen. When the relative humidity increases, the emulsion of the film absorbs water containing dissolved oxygen from the atmosphere, thus inducing the oxidation reaction. But apparently, the boxes in which the films were stored in the present experiment served as a protection from the humidity which was fairly low already. Therefore, the fading of the latent image was not too significant. In the case of personnel monitoring by film badges, such low humidity conditions sometimes are not easily met; hence, the fading of the latent image could have a serious effect on the density obtained.

3.4 Thermoluminescent Dosimeter-Film Method

In some instances, the photographic method alone, because of its energy dependence, cannot provide results with the desirable degree of accuracy. Then it is necessary to introduce an energy independent dosimeter in place of film emulsion to measure the relative dose distribution. However, film emulsion can still serve as a complementary detector, i.e. for the mapping of information from areas not covered by the primary dosimeter.

A method of combining LiF, a considerably less energy dependent dosimeter, and film has been described in detail by Vacirac et al. (1972) to map out comprehensively the isodose distributions. The properties of a LiF dosimeter have been discussed by Sharma (1972) in his master's thesis and will not be duplicated here.

The present investigation, which was based extensively on the results of Vacirac et al., gave examples of dose distributions as obtained by this LiF-film method in the Rando Phantom Man. In order to relate the density of the film to the dose readings of LiF, a calibration curve is required. The method as used by Vacirac et al. to calibrate the densities of a film is given below.

Briefly, this calibration required the LiF dosimeters to be inserted between the sections of the Rando Phantom Man in the holes especially bored to hold the LiF capsules. The sensitivity of the LiF powder to cobalt

radiation was lower than that of the film. Therefore, it became necessary to expose the LiF dosimeters to a higher dose to obtain a sufficient LiF reading than that required to obtain a readable density. Different doses were delivered to different groups of LiF dosimeters.

The films were inserted in the same location where the LiF dosimeters were previously placed and doses given to the films were in the ratio as those given to the LiF, though considerably smaller in magnitude. Point measurements on the film were made at the same spots at which the LiF dosimeters had been placed. The readings for the LiF dosimeters were then scaled back to the same doses as given to the films.

The calibration graph was formed by combining the net densities of the films and the LiF readings. No attempts were made to measure the absolute doses delivered, as they were not necessary. All the LiF readings were obtained from the Con-Rad TLD Readout Instrument which was also described in Sharma's thesis.

3.5 Plotting of Isodose Distributions

3.5.1 Densitometric Plotting

One precise and straightforward method for obtaining the isodensity, and hence the isodose (linearity between dose and density being assumed), lines from the film is by means of direct measurements of the optical densities. This method is described in below.

The maximum density was first obtained from the film and defined as the 100% isodose. Then, a particular percentage depth dose to be plotted was decided upon and the density, D , of this percentage depth dose was calculated from the following expression:

$$(3) \quad \% \text{ depth dose} = (D - D_o) / (D_m - D_o) \times 100$$

where D_m is the maximum density, and

D_o the background fog.

Points of this density, D , were measured directly from the film by using the densitometer and spatially correspondent points were transferred onto a graph paper. These points, which were taken at a distance of radius 1 cm. from each other, when conjoined, formed the dose distribution for that particular percentage depth dose.

3.5.2 Automatic (Isodensity) Plotter

(i) Introduction

In contrast to the manual method of plotting isodose distributions as described in section 3.5.1, the isodensity lines of a film can also be plotted by means of an

automatic device. It has been mentioned in the introductory chapter that the device, usually referred to as an automatic isodose plotter, is sometimes used to plot the isodose distributions within a water phantom (Johns and Cunningham, 1974).

The isodose plotter utilizes an ionization chamber and a hunting mechanism in the phantom to locate points at which the dose rate is a certain percentage of the dose rate in the center of the radiation field, at the surface or at an equilibrium depth of the phantom. A printing mechanism follows the motion of the chamber and reproduces the isodose curves.

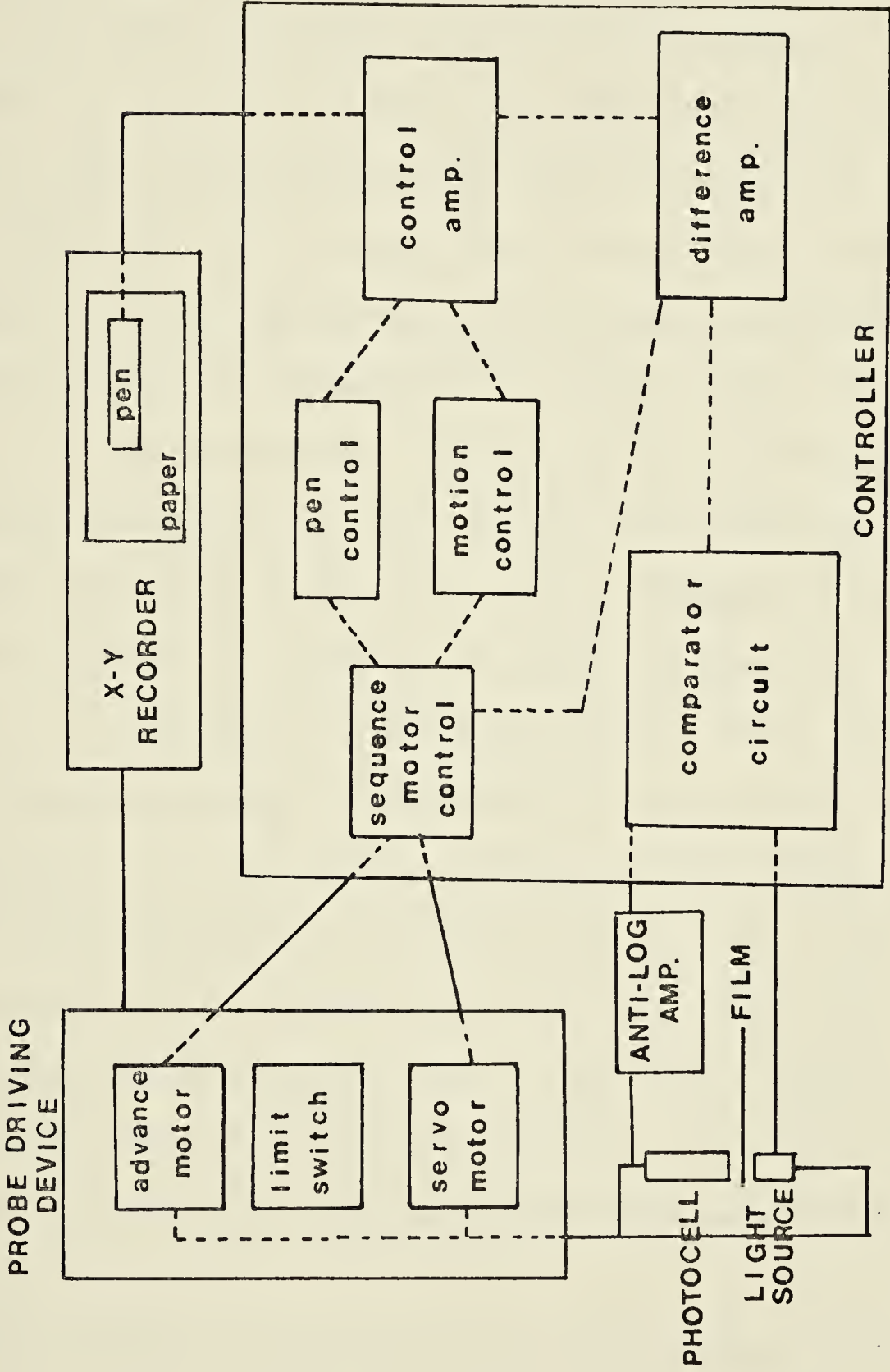
One such plotter, MRA 101-3, manufactured by Toshiba Tokyo Shibana Electric Co. Ltd. was originally available and its concepts are described below.

(ii) Basic Concepts of Plotter

To use the isodose plotter (partially shown in Fig. 19), radiation is first allowed to fall upon the water phantom contained in an acrylite box. Two thimble ionization chambers of the plotter, one serving as a monitor in air and the other as a probe in water, are placed inside the radiation field.

The monitor, fixed in a pre-selected position usually at the edge of the beam, acts to compensate for any fluctuation in the dose rate of the radiation source. The probe, controlled by two motors to move in the XY direc-

Fig. 19 Block Diagram of the Isodensity Plotter



tions in a given vertical plane, is lowered into the water phantom to search for and to measure the designated dose rate, i.e. the percentage isodose distribution.

Let it be presumed that the 80% dose level is the required dose distribution and that the probe is located at a depth which has a dose level other than the 80%. The input voltage generated by the probe is therefore different from that generated by the monitor. This results in a non-zero input voltage to the servo-amplifier.

This imbalance in input causes the servo-amplifier to drive the motor to move the probe along in an axial direction toward a location in which balance can be obtained. At the point of balanced input, the other motor, which causes movement of the probe in a direction at right angles to that of the previous motor, moves the probe into a location of different dose rate, and imbalance again occurs. The servo motor operates once more to move the probe axially back to the 80% isodose level. Hence, with this mechanical procedure, the probe always follows the required 80% dose rate curve until it is completed.

The motions of the probe are transmitted in a 1:1 ratio to the heat pen of the recorder. By following the exact motion and by drawing the points at which the balance of input voltages is obtained, the heat pen traces the outline of the isodose curve on a heat sensitive paper.

All other selected percentage levels can be plotted in a similar manner. This technique is referred to as tracing.

A technique of scanning is used whenever the situation occurs in which the isodose distributions consist of two or more peaks of the same percentage dose rate. In this mode of motion, the width of the area to be scanned is set by a limit switch. The two motors of motion control the movement of the probe and cause it to scan all points within the area selected. When the probe passes over the position at which the required percentage dose rate occurs, a balance of input voltages takes place and no signal is transmitted to the recorder. At this point, the heat pen operates and places a dot on the heat sensitive paper. After the whole area has been scanned, the conjoint dots constitute the selected isodose curve.

(iii) Modification of Plotter

In the present study, a film has replaced the probe as the measuring device for radiations. Therefore, modification of the isodose plotter became necessary.

The measurement of a film is characterized by its absorbance of light. To make use of this characteristic, a photocell (Hewlett-Packard 5082-4204) was installed to detect the light transmitted through the film. This photocell served the function of giving input voltage in a similar fashion to the probe. A light bulb (G.E. 327)

provided a constant light source and functioned in a similar way to the monitor in giving input voltage which served as a comparison for the input voltage produced by the photocell to the servo-amplifier.

The photocell was a photodiode which could provide electrical currents in the microampere range linear to the intensity of incident light (Malmstadt and Enke, 1969). To check for this linear property, the photocell was first connected to a linear, inverting amplifier (Analog Device 208) which could change the polarity of an input current or voltage.

The effect of this inversion was that zero reading with a full transmittance of light and 100% reading with a complete opaqueness of light could be obtained. This extreme range of transmittances effectively tested the entire response range of the photocell. The maximum reading, 100%, was set with an opaque film, while the 0% reading was obtained with no obstruction in the path of the light beam between the photocell and its source.

The intermediate points were obtained by using films of different densities, hence different transmittances, because D , the density, is defined as $-\log T$, T being the transmittance. The % reading of the meter of the amplifier was plotted as a function of the transmittance; a linear portion was obtained up to about 0.1% transmittance which corresponds to the optical density of about 3.

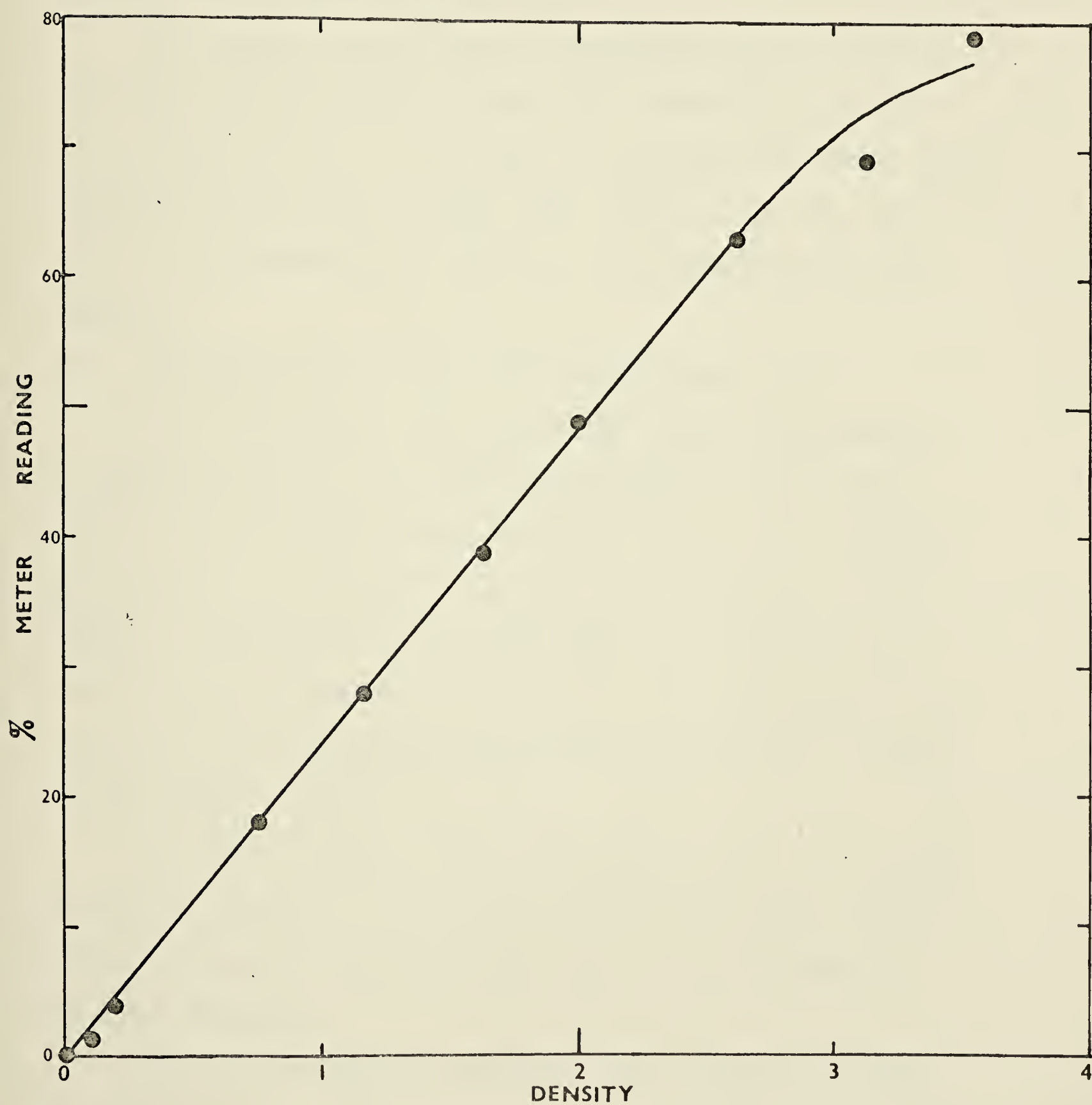
The final objective was to have a linear response between the density of the film and the electrical output from the linear amplifier. Therefore, this objective required an installation of an anti-log amplifier (Analog Device 755P) between the photocell and the linear, inverting amplifier to remove the logarithmic dependency in relating density to transmittance.

The eventual result of this conglomerate of devices was that the electrical output was directly proportional to density. To check for this linearity, the entire response range of these devices was again measured using the identical method employed in the checking of the photocell response.

The final calibration data are plotted in Fig. 20 between the % readings of the meter of the devices and the densities. This figure shows a linear function up to a density of about 3. Since no film used for the measurement of percentage depth doses was exposed to a quantity of radiation that would produce a density greater than 2.4, this linearity was quite adequate for the purpose of this present study.

To accomodate both the light source and the photocell so that they could move as one unit, the following structure was constructed to coordinate their movements. It is schematically depicted in the lower left hand corner of Fig. 19. Basically, the photocell was fixed at one end of a horizontal bar which, at the other end, was welded to

Fig. 20 Calibration Graph for the Isodensity Plotter



a vertical tube formerly employed to hold the probe ionization chamber of the isodose plotter. The light source, aligned directly beneath the photocell, was held by another horizontal bar which, at the other end, was also welded to the same vertical tube.

The motors controlling the movements of the vertical tube ensured motion between the photocell and its light source to be in one unit. A distance of about 4 cm. separated the two horizontal bars; this space was sufficient to accomodate the film and its transparent lucite support.

(iv) Plotting Method and Time Consumption

At the beginning of a plotting session, the region of maximum density on a film was arranged in the space between the photocell and its light source; this density was defined as the 100% isodose. The density of a processed but unexposed film of the same brand served to set the 0% isodose standard. The rest of the operational concepts of this isodensity plotter were identical to those of the isodose plotter.

The time consumed in the tracing process was between 15 and 30 minutes. By reading directly from the densitometer, single field isodensity lines could be obtained within 45 minutes.

The time consumed in scanning the isodensity curves as produced by two opposing radiation fields separated by the length of a film was estimated to be within 60 minutes.

Depending upon the amount of details required, the time taken for direct densitometric plotting of the same film was between 45 and 90 minutes.

(v) Problem of Accuracy

The accuracy of this isodensity plotter was checked using the densitometric readings as comparison. An overall discrepancy of about 4% in dose distribution was obtained when the result plotted by the plotter was compared with that using direct density measurement of the same film.

The inherent error of 4% became more apparent in the scanning technique. Again as a partial consequence of mechanical errors, the result was that lines instead of dots were drawn during scanning. This lack of unique definition for isodensity curves made this technique unusable. Attempts were made to reduce the inherent errors, but success was minimal.

Hence, in view of the fact that the use of the isodensity plotter gave less accurate results and saved little time, the plotting of dose distributions using direct density readings was preferred over the techniques as provided by the plotter. In this way, a better assessment of the accuracy of the photographic emulsion as a radiation detector could be obtained.

CHAPTER IV

RESULTS: APPLICATIONS

According to Murphy (1967), the steps involved in a plan for treatment with fixed radiation beams are as follows:

- 1) Determination of the location and the size of tumor to be treated and the sensitive structures around the tumor,
- 2) Determination of the dimensions of the treatment area,
- 3) Mapping of the anatomical site of tumor,
- 4) Determination of the quality of radiation to be used,
- 5) Marking of the outline of the isodose charts used,
- 6) Recording of the dose distributions,
- 7) Determination of the total tumor dose and the time of delivery.

Hence, the use of isodose charts is one of the integral parts of a regular treatment plan.

In using the photographic method to obtain isodose distributions, the major difficulty is energy dependence. The account that follows presents the results measured from films by means of the limited phantom method which reduces the effect of energy dependence. Most of the results presented hereunder are compared with the standard results, such as the isodose charts supplied by the manufacturer, data produced by computers, etc.

4.1 Uniform Beam, Homogenous Phantom

4.1.1 Single Radiation Field

Figs. 21-23 show the isodose charts of cesium-137 produced by the isodensity plotter from Kodak M films using a limited phantom of thickness of 1.5 cm. on each side of the film. Fig. 24 shows the isodose chart of a cobalt radiation field, using Kodak M film and a limited phantom of thickness of 2 cm. on each side of the film.

Due to the errors made by the plotter and by the energy dependence of Kodak M films, the results shown in the above figures are observed to be quite different from the charts supplied by the manufacturers.

The above figures therefore only serve as illustrations of the final products of the isodensity plotter. Kodak M films, because of their excessive energy dependence, were for this reason not used further in the measurement of depth doses and isodose distributions.

Figs. 25-26 show the isodose charts of cobalt-60 radiation fields using a phantom of 2.5 cm. on each side of Ilfoline films. In these two diagrams, the left half of the isodose charts is plotted by using the densitometric readings. The right half of the charts is redrawn from the AECL chart to give an indication of the errors as obtained from films.

The discrepancy of the best possible result from the central axis is not greater than 10%, corresponding to a

Fig. 21 Isodose Distribution for a 6 x 6 cm Field at 27 cm SSD for Cesium-137 Beam as plotted from Kodak M Film by the Automatic Isodensity Plotter

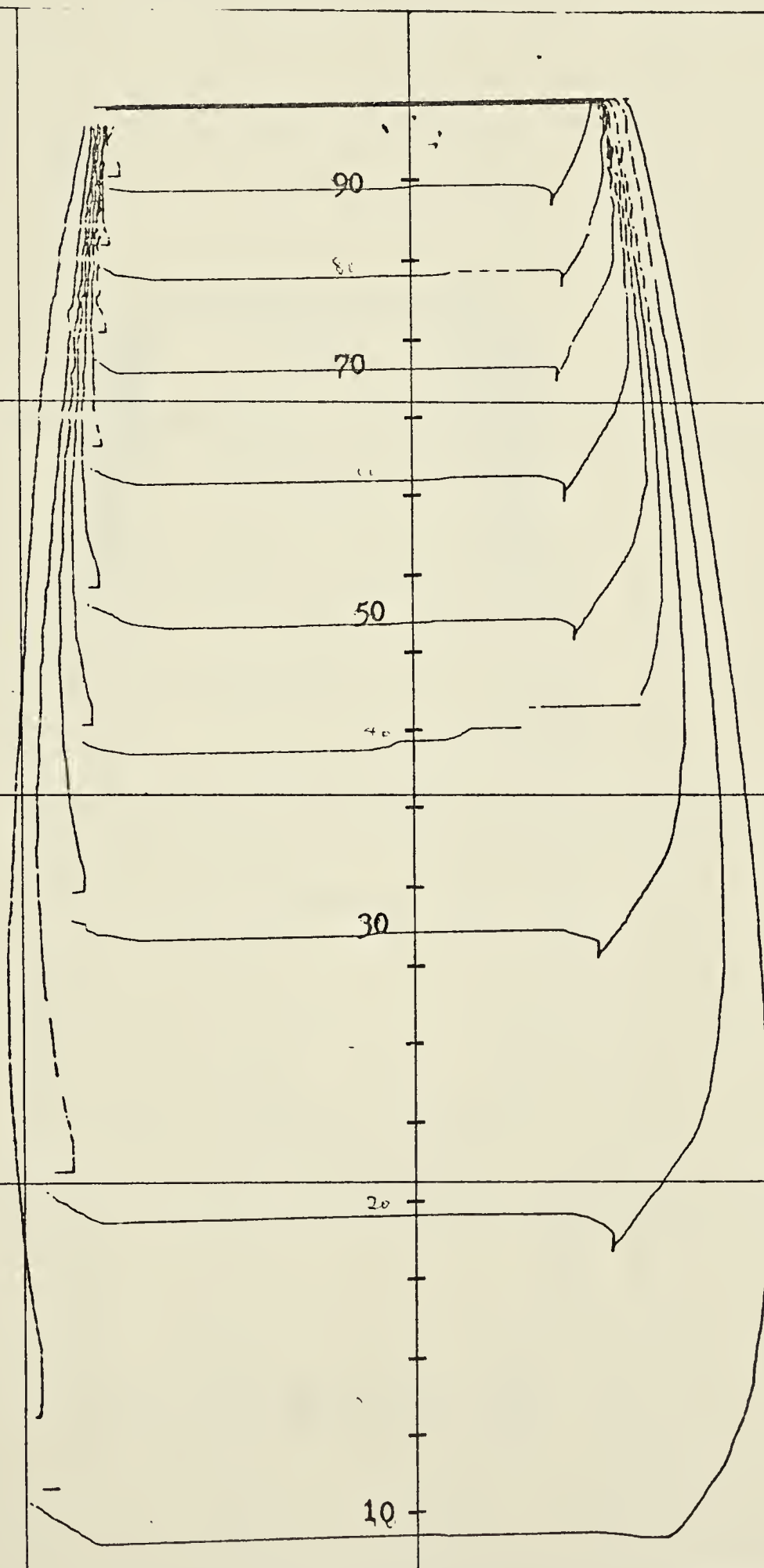


Fig. 22 Isodose Distribution for a 4 x 8 cm Field at 15 cm SSD for Cesium-137 Radiation as plotted from Kodak M Film by the Automatic Isodensity Plotter

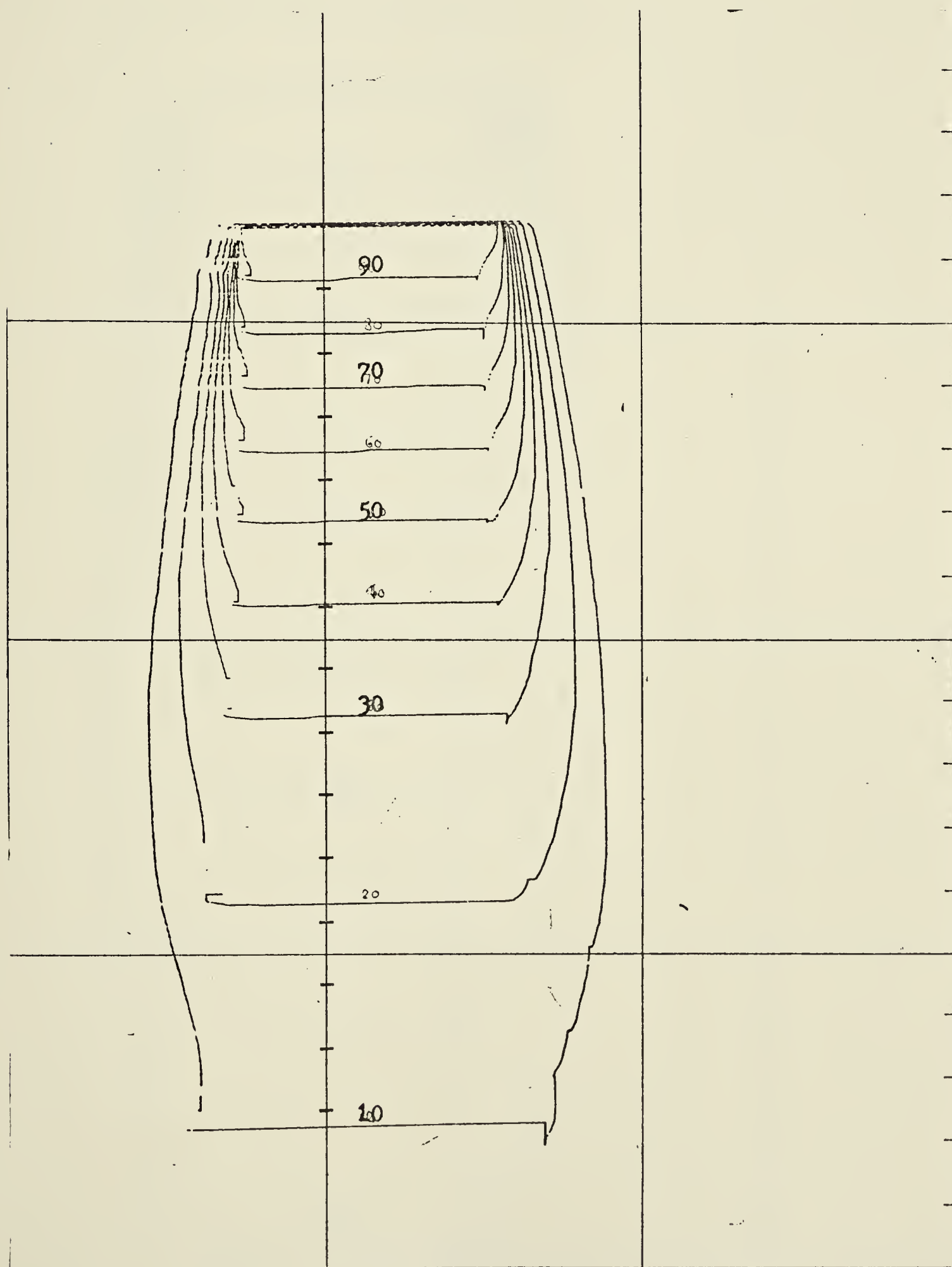
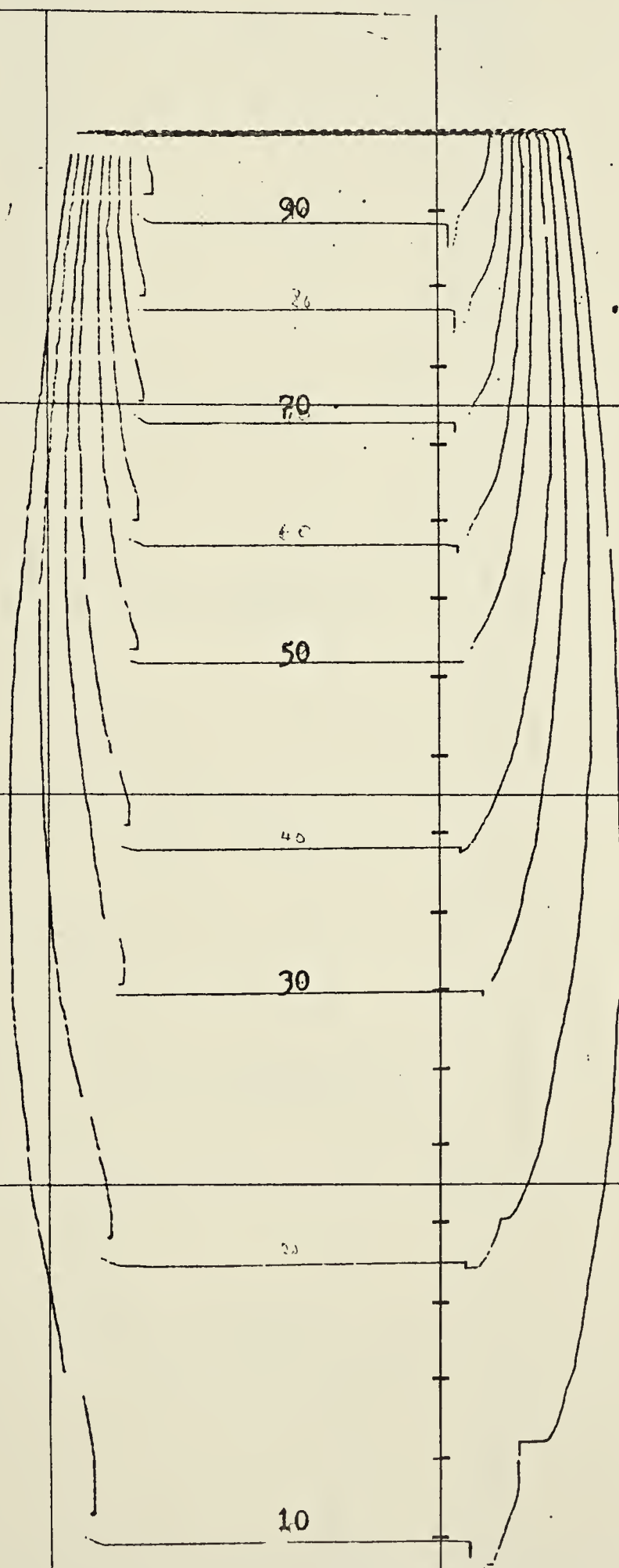


Fig. 23 Isodose Distribution for a 5 x 5 cm Field at 35 cm SSD for Cesium-137 Radiation as plotted from Kodak M Film by the Automatic Isodensity Plotter



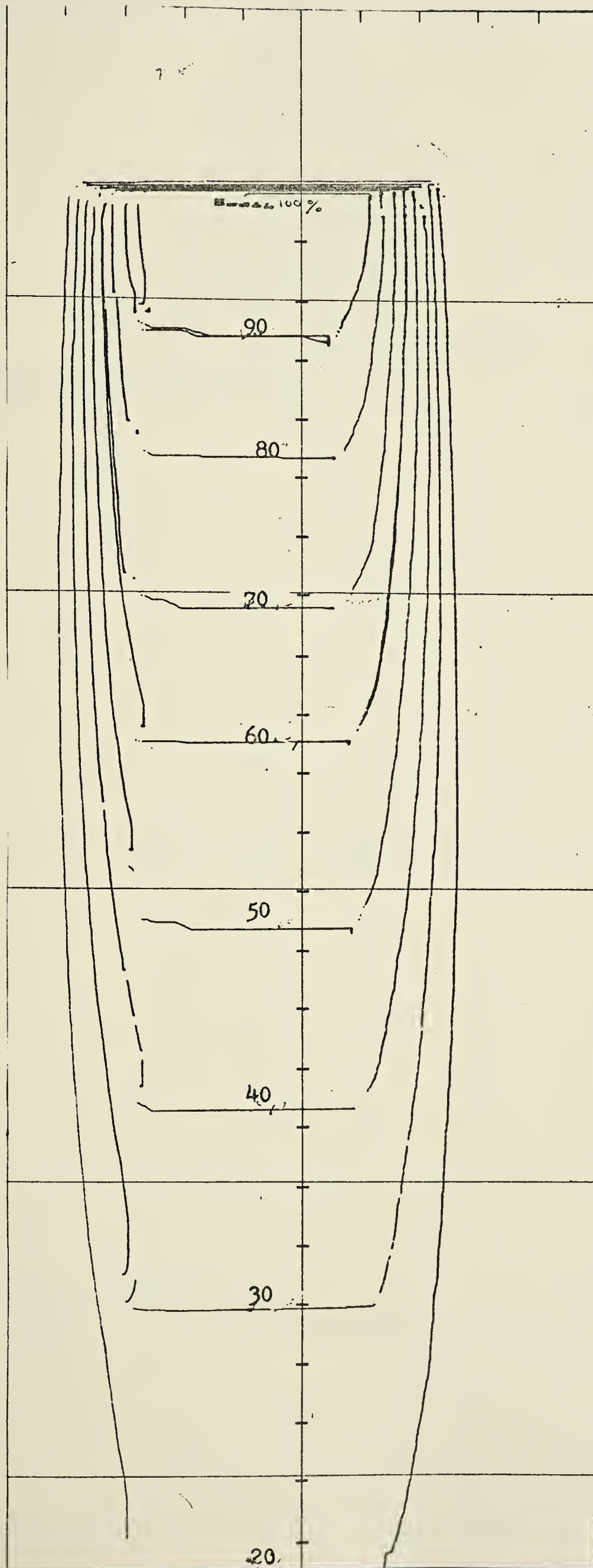


Fig. 24

Isodose Distribution
for a 5 x 5 cm Field
at 80 cm SSD for
Cobalt-60 Radiation
as plotted from
Kodak M Film
by the Automatic
Isodensity Plotter

Fig. 25
Isodose Distribution
for a 20 x 20 cm Field
at 80 cm SSD for Cobalt-60
Radiation as measured
from Ilfoline Film
and AECL chart

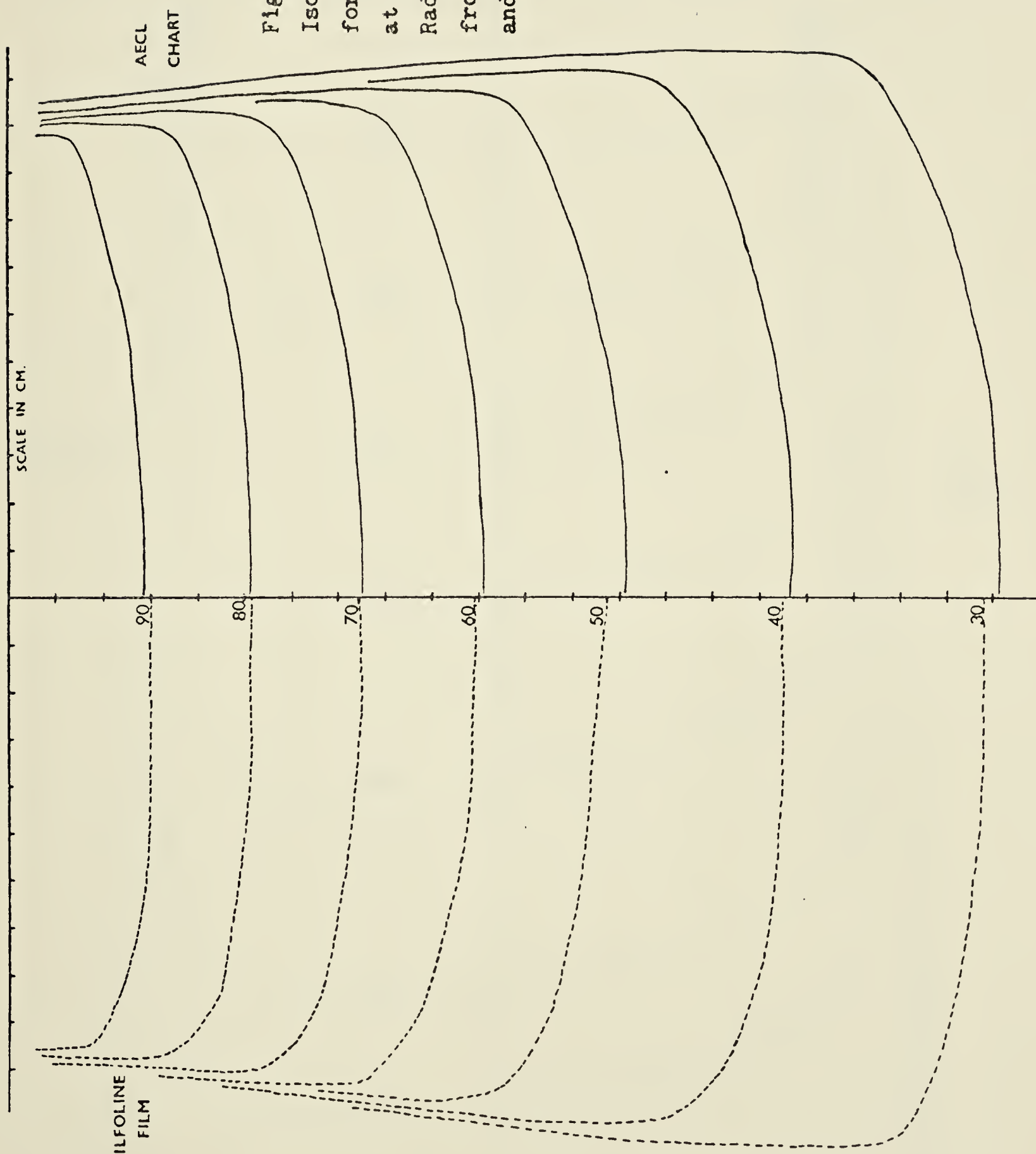
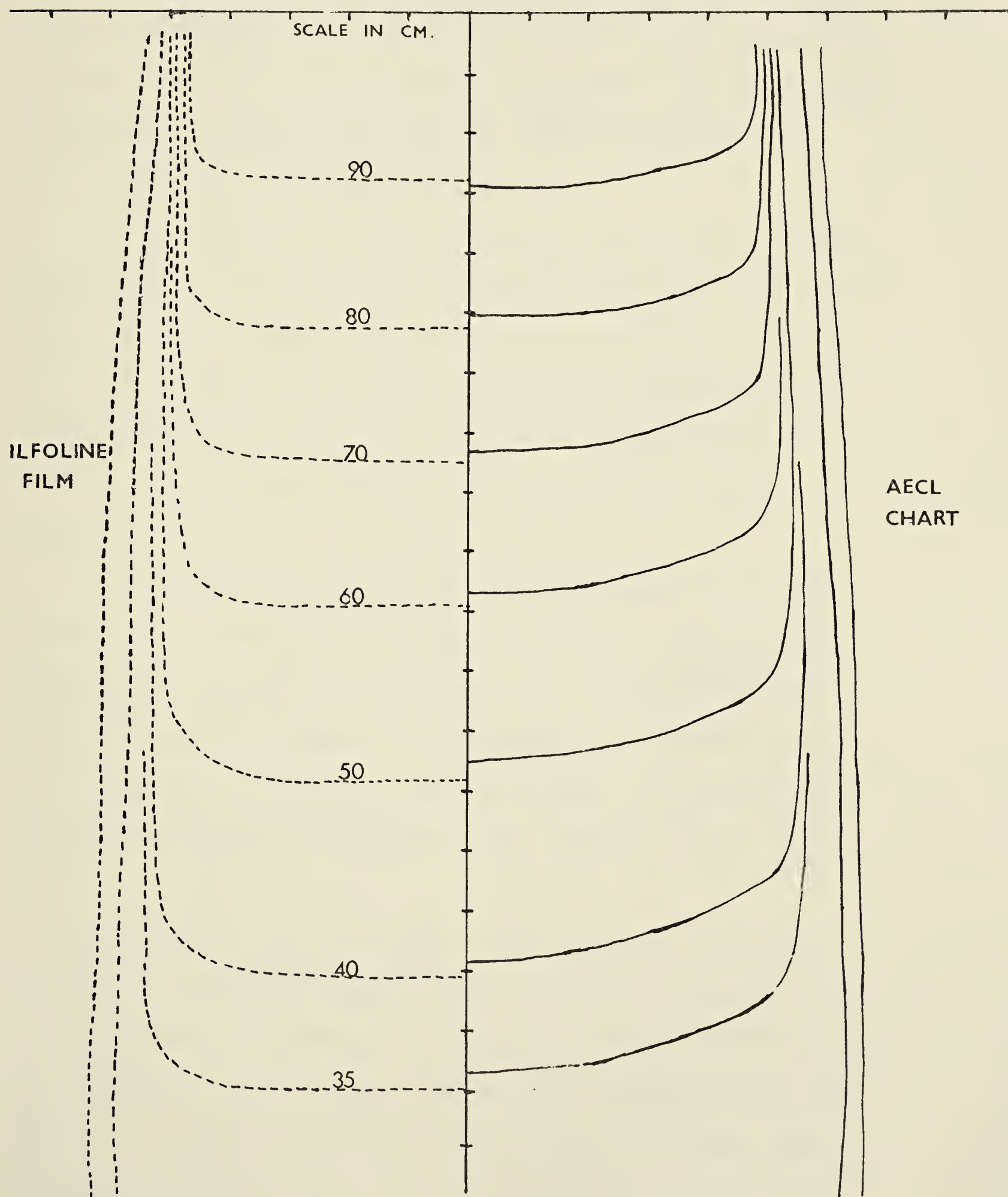


Fig. 26 Isodose Distribution for a 10x20 (10) cm
Field at 80 cm SSD for Cobalt-60 Radiation
as measured from Ilfoline Film and AECL chart



maximum displacement error (the error of the position of the isodose line detected by the film along the central axis in comparison with the AECL charts) of 5 mm. for the isodose lines which are greater than 50%. For doses lower than 50%, the displacement error could be quite large.

4.1.2 Multiple Radiation Fields

A tumor can sometimes be treated by a single radiation field. A majority of treatment plans call for two or more fields to provide an acceptable distribution of dose in the vicinity of the tumor. The dose distribution of these multiple fields can be evaluated by a simple addition of the isodose curves of the individual fields involved.

Using the photographic method, Loevinger and Spira (1957) first suggested that by obtaining a density-dose distribution from a film exposed by a single field and by superimposing films, it was possible to obtain multiple field distributions. This technique is essentially no different from the adding of the isodose charts manually.

Noda et al. (1970), using 10 MV x-rays, showed the possibility of utilizing one film multiply exposed by radiation fields to measure the multiple field distributions with Kodak M films. Onai et al. (1972) extended the procedure to cobalt-60 radiation for multiple fields using Fujilith Contact.

The lack of precise results derived from the addition of multiple fields in the same film is again mainly due to the energy dependence of film. With several fields exposing the same film, the errors can easily be augmented, especially around the penumbral regions. One solution to lessen the effect of energy dependence is to use a film known to be less sensitive to scattered radiation, to reduce the errors. Ilfoline films were chosen to measure the multiple field dose distributions.

In treatment planning, there are a very large number of ways of combining radiation fields to give the desirable tumor dose. The simplest combination of multiple fields is that of two opposing fields with coincident axes.

Figs. 27 and 28, using data obtained from Ilfoline films, show the isodose distributions of two opposing fields with different radiation fields: a 100 cm.² field of SSD 27 cm. cesium radiation with the limited phantom of thickness of 2 cm. on each side of the film, and a 200 cm.² (10x20) field of SSD 80 cm. cobalt radiation with the limited phantom of 2.5 cm. thick on each side of the film, respectively.

The isodoses produced by the addition of manufacturer's isodose charts and by PC-12 computer have been inserted on the opposite sides of each diagram for comparison. In each of the examples, the best possible result gives a displacement error along the central axis of about 5 mm.

Fig. 27

Resultant Isodose
Distribution
obtained by combining
Two Cesium-137 Fields
(10 x 10 cm, 27 cm SSD)
in Opposition 20 cm
Apart

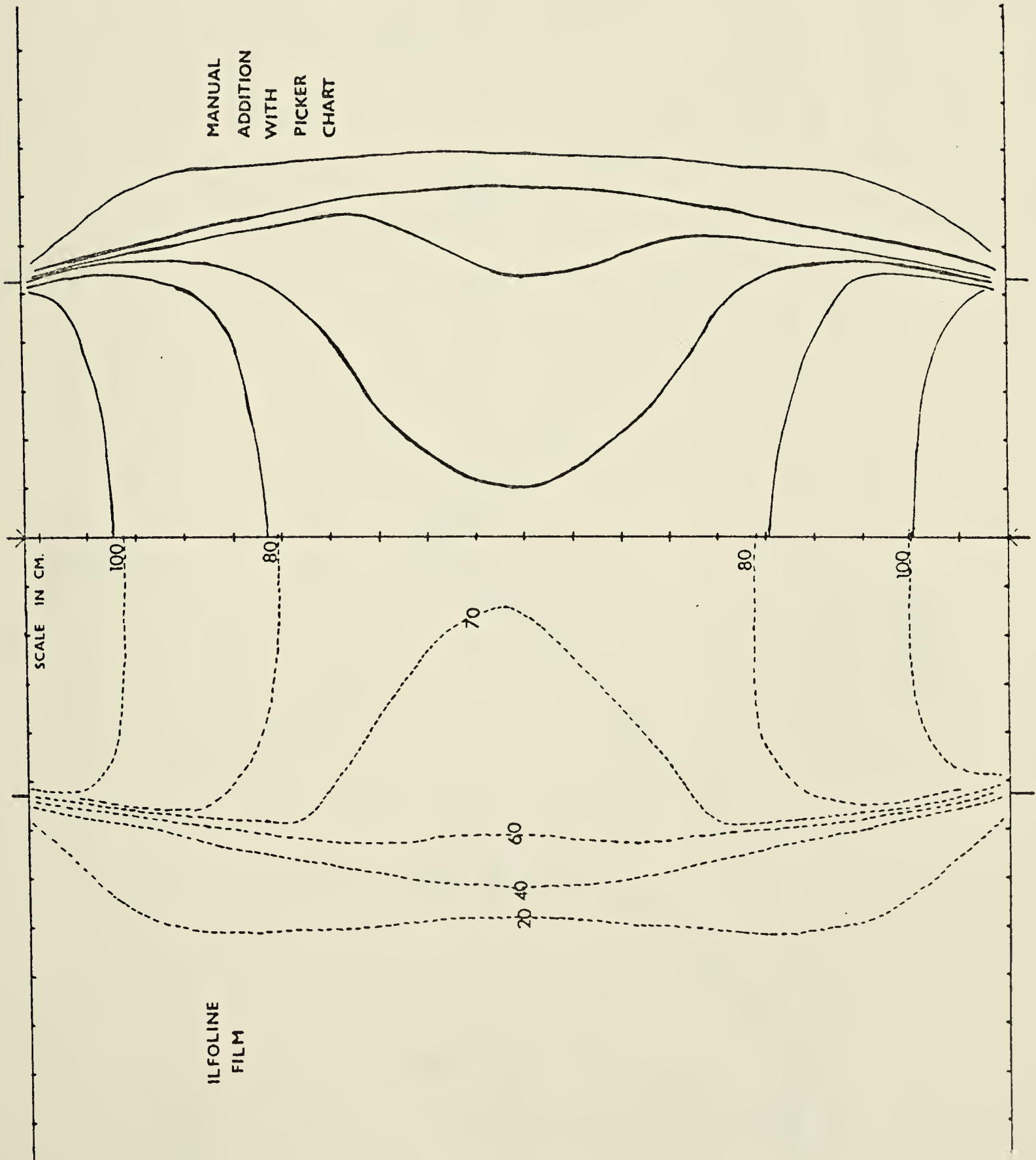
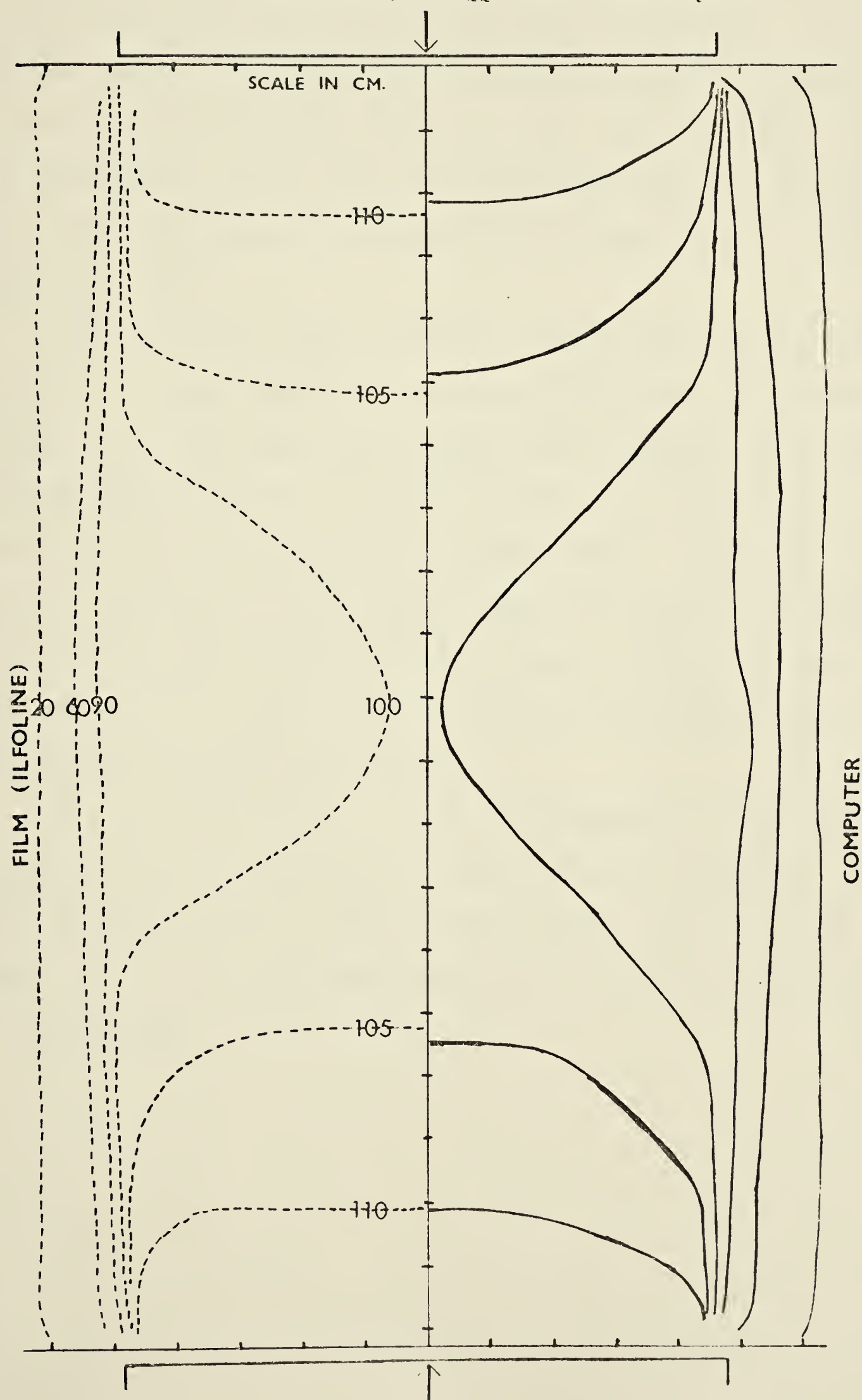


Fig. 28 Resultant Isodose Distribution obtained by combining Two Cobalt-60 Fields (10x20 (10) cm, 80 cm SSD) in Opposition 20 cm Apart



Also using data obtained from Ilfoline films, Figs. 29 and 30 show the results of more complex multiple fields: triple and quadruple fields with cobalt radiation. In the triple fields, the field size used was 36 cm.^2 with angulations of the radiation beams at 45° , 180° and 315° . In the quadruple fields, the field size used was 8×15 (8), with the angulations of the radiation beams at 52° , 122° , 238° , and 302° .

These results serve as good illustrations of the use of films to approximate the dose distributions of multiple fields. For the quadruple fields, the treatment plan was originally identified by Murphy (1967) as a method of treatment for the cancer of uterine cervix. However, it was not possible to find in the Rando Phantom Man an exact duplicate of the anatomical site shown in Murphy's text. Therefore, the results shown in the present example and in Murphy's are not identical.

The results for the triple and quadruple fields are compared with the isodose produced by PC-12 computer. The best possible result gives a displacement error of less than 1 cm. in the high dose region, i.e. at the junction of the fields.

Fig. 29

Resultant Isodose
Distribution
for three 6 x 6 cm
Cobalt-60 Fields
at SSD 80 cm. The
Fields are placed
at 45° , 180° and
 315° .

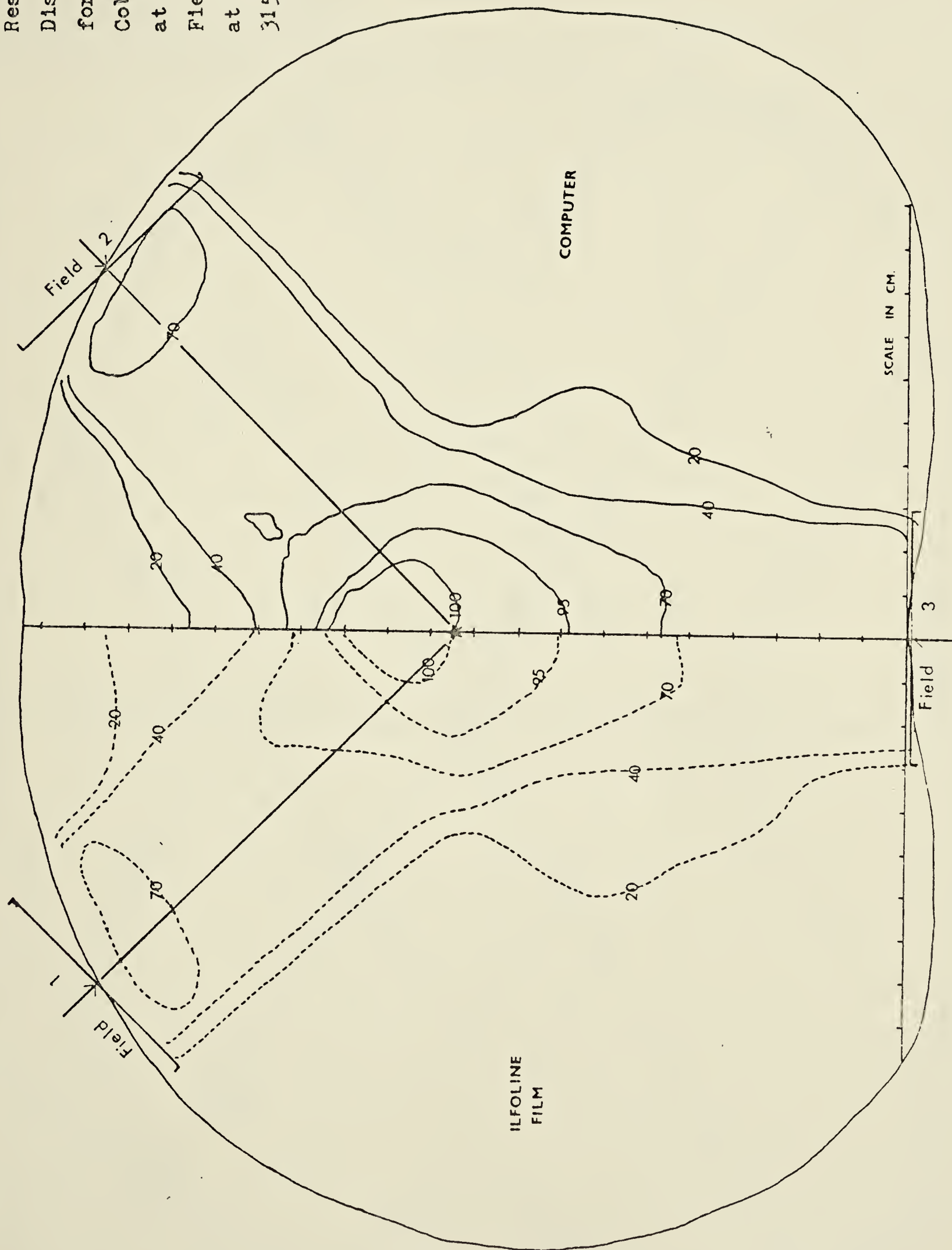


Fig. 30

Resultant Isodose

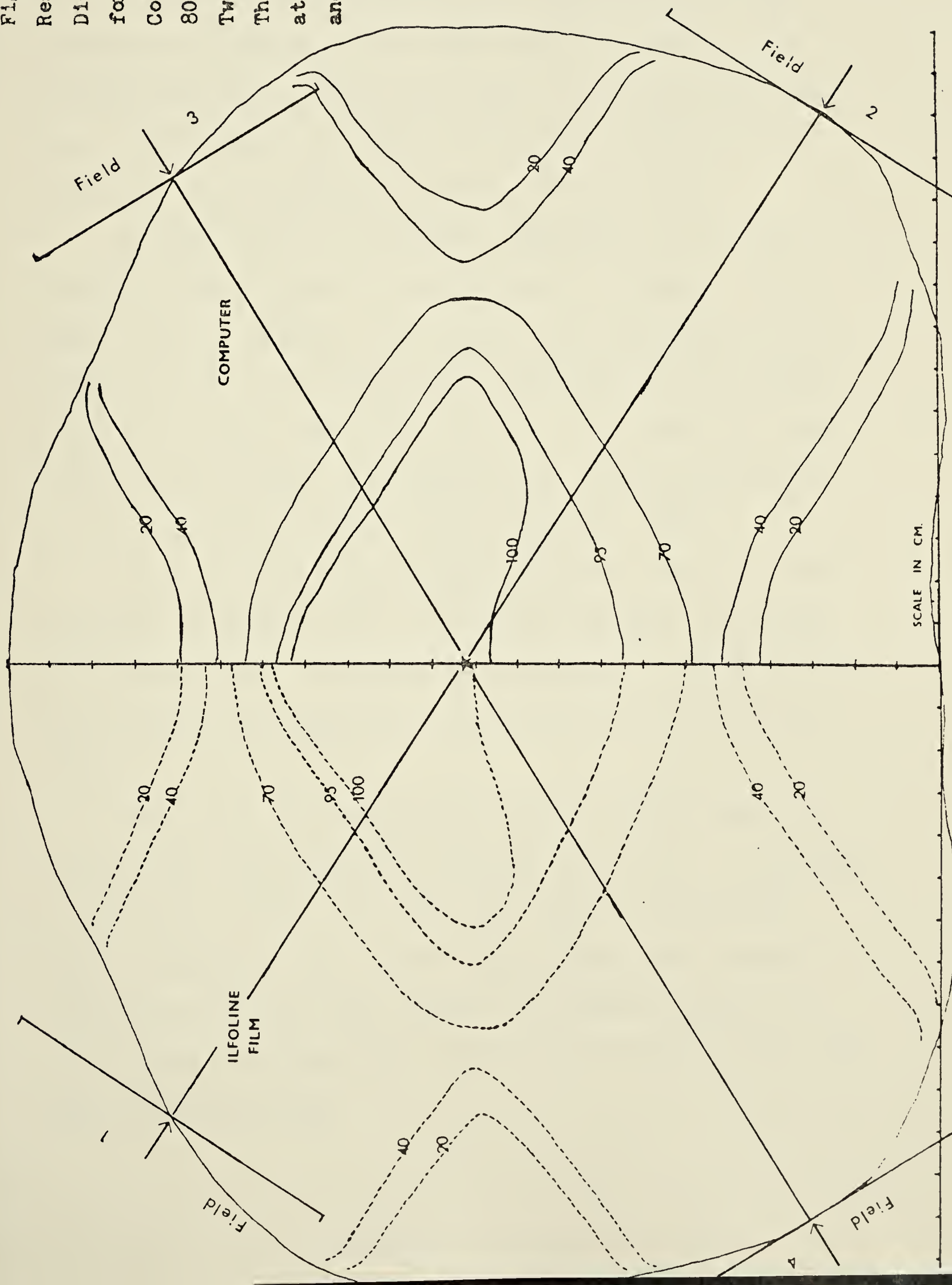
Distribution

for Four 8 x 15 cm

Cobalt-60 Fields at

80 cm SSD arranged as

Two Opposing Pairs.

The Fields are placed
at 52° , 122° , 238° ,
and 302° .

4.2 Non-uniform Beam, Homogenous Phantom

4.2.1 Wedge Filter

In some clinical situations, especially for the treatment of cancer in the head and neck regions, the introduction of a third field may not be desirable (Murphy, 1967). Instead, wedge filters may be used to improve the dose uniformity over the tumor volume.

A wedge filter is normally employed to alter the normal isodose curves to ones which are angled to the axis of the radiation beam (Johns and Cunningham, 1974). Wedged fields make possible the irradiation of a target volume of tissue near the surface of the body to a high and uniform extent, the minimum dose being directed on-to the contiguous normal tissue (Murphy, 1967).

There are two wedge angles available for the Theratron-80 cobalt-60 unit: 45 and 60 degrees. The angle of a wedge filter is defined as the angle, θ , made by the 50% isodose curve and the perpendicular to the central axis.

Using data obtained from Ilfoline films, Figs. 31 and 32 show the results of isodose curves for a 10x8(w)cm wedge field with a 45° and a 60° angle respectively. These results of the central axis depth doses compare favorably with the AECL charts. The best possible result gives a displacement error of less than 0.5 cm. for most isodose curves.

Fig. 31 Isodose Distribution for a 10 x 8(w) cm, 80 cm SSD,
Cobalt-60 Beam modified by a 45° wedge filter

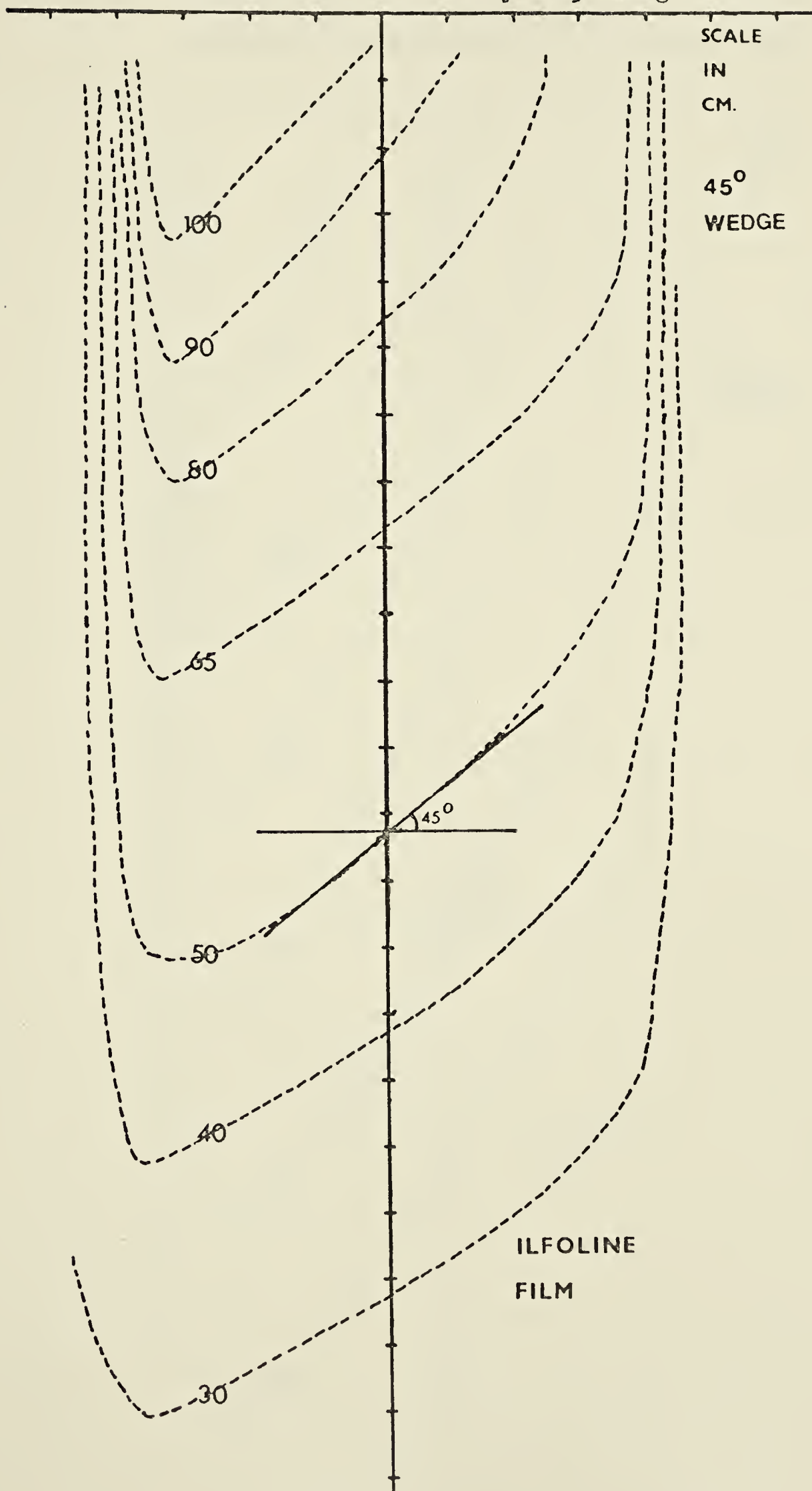
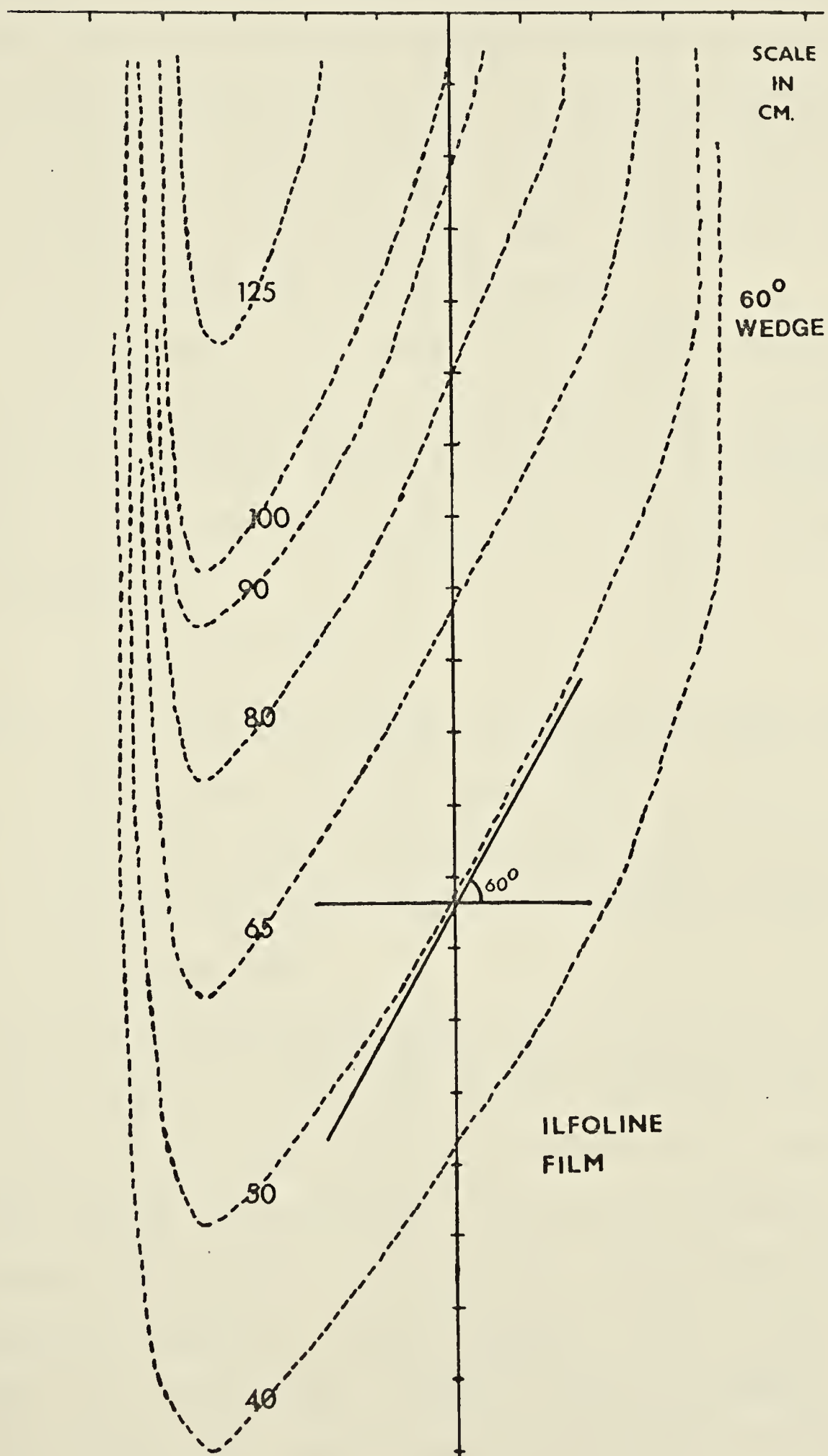


Fig. 32 Isodose Distribution for a 10 x 8(w) cm, 80 cm SSD,
Cobalt-60 Beam modified by a 60° wedge filter



4.2.2 Application of Wedge Filter

In some instances, even the wedge angles of 45° and 60° cannot give an acceptable uniform dose distribution. Thatcher (1970) and Mansfield et al. (1974) described a simple technique of fragmenting the total dose administered to produce a different wedge angle from which a more uniform dose distribution can be obtained.

In this technique, the area to be treated is irradiated partly with and partly without the wedge filter, and a spectrum of wedge angles smaller than the original angle can be effected. In general, the effective wedge angle is given as:

$$(1) \quad \theta_{\text{eff}} = (1 - F)\theta_0$$

where θ_{eff} is the resultant or effective wedge angle, θ_0 the original wedge angle, and F the fraction of the given dose delivered without the wedge filter in relation to the total given dose.

For the following experiments, the limited phantom used was 2.5 thick on each side of the Ilfoline films. Figs. 33 and 34 show two very similar results of $10 \times 8(w)$ cm, 30° wedge isodose distributions respectively obtained from the original 45° and 60° wedge filters. The central axis depth doses of these 30° wedge isodoses do not differ by more than 1 cm. from those of the 45° and 60° wedges.

Figs. 35 and 36 further show the results of using two

Fig. 33 Isodose Distribution for a 10 x 8(w) cm, 80 cm SSD, Cobalt-60 Wedge Field with an Effective angle of 30° as obtained from a 45° Wedge and an open Field. Ratio of Given Dose with and without 45° Wedge 2:1.

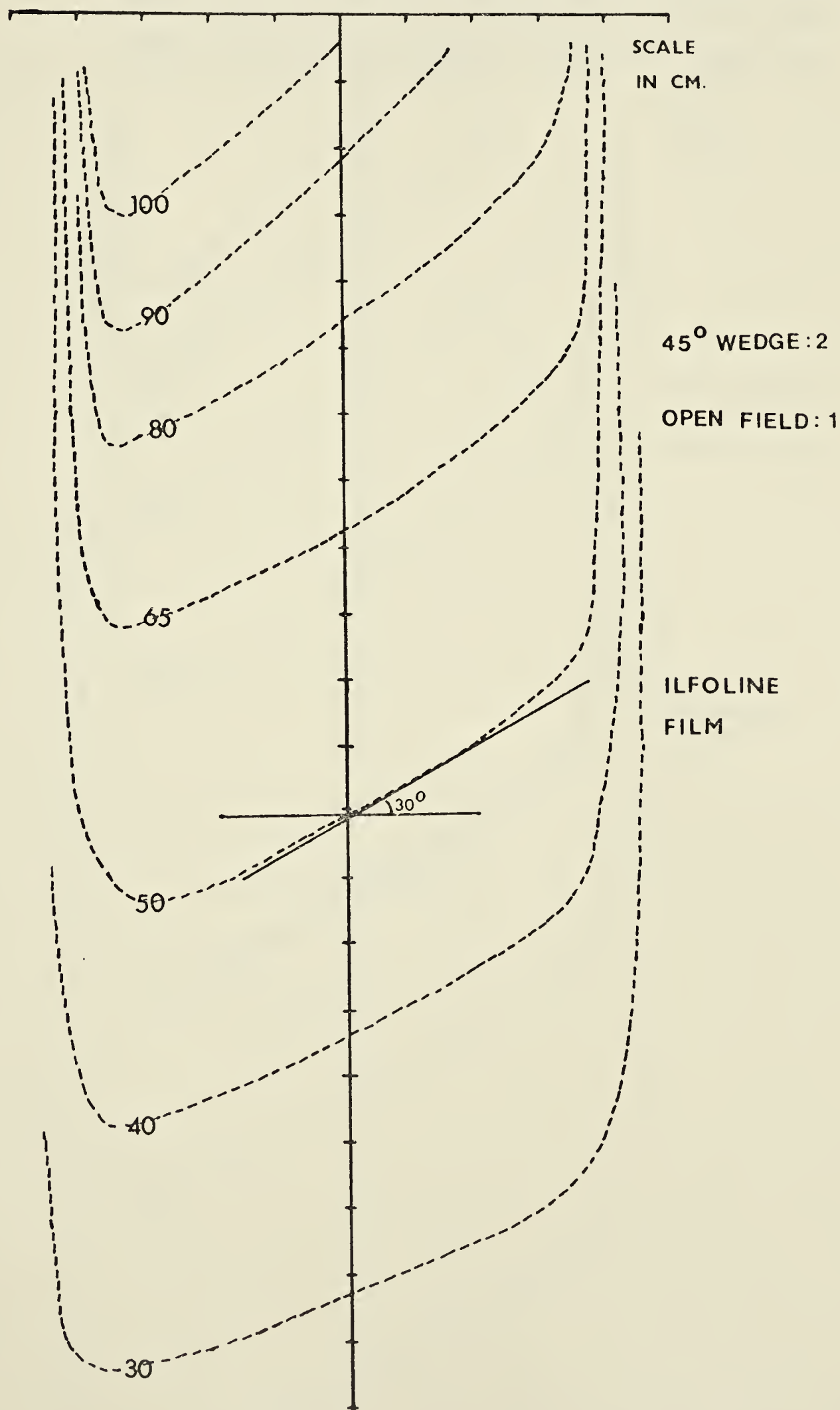


Fig. 34 Isodose Distribution for a 10 x 8(w) cm, 80 cm SSD, Cobalt-60 Wedge Field with an Effective angle of 30° as obtained from a 60° Wedge and an open Field. Ratio of Given Dose with and without 60° Wedge 1:1.

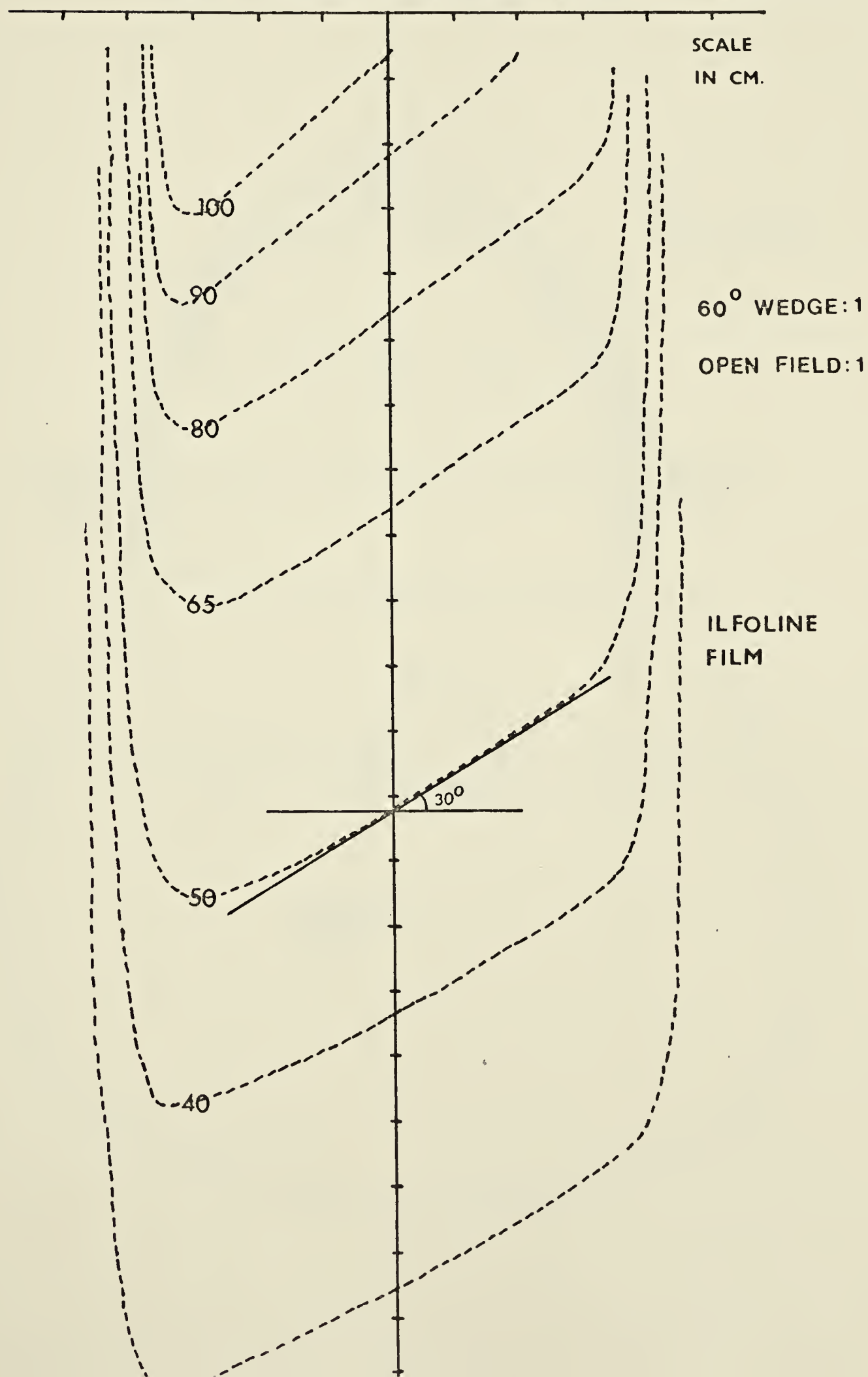


Fig. 35 Resultant Isodose Distribution for Two Opposing 8 x 8(w) cm, 80 cm SSD, Cobalt-60 Beams modified by a 45° wedge filter at the level of the tonsil area of the Rando Phantom

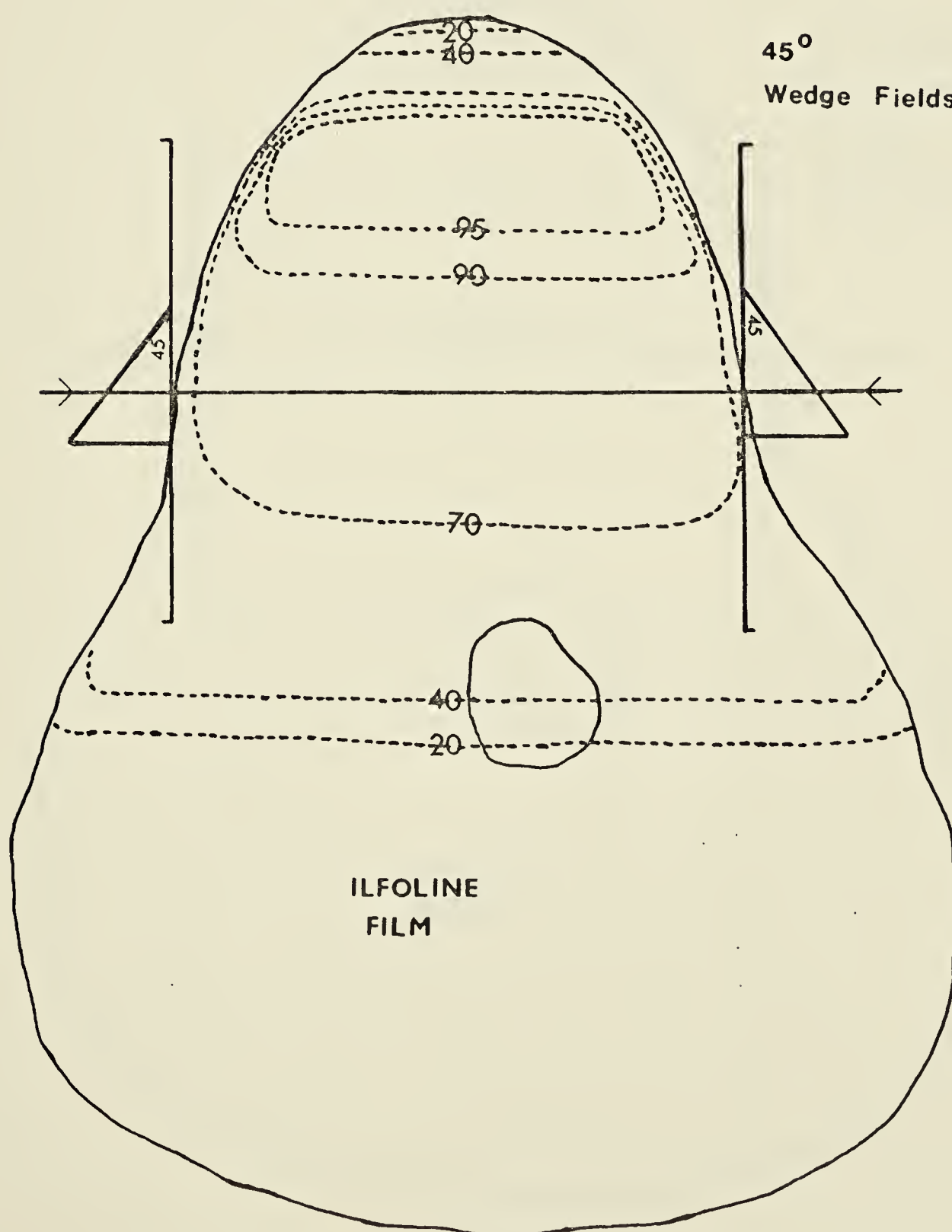
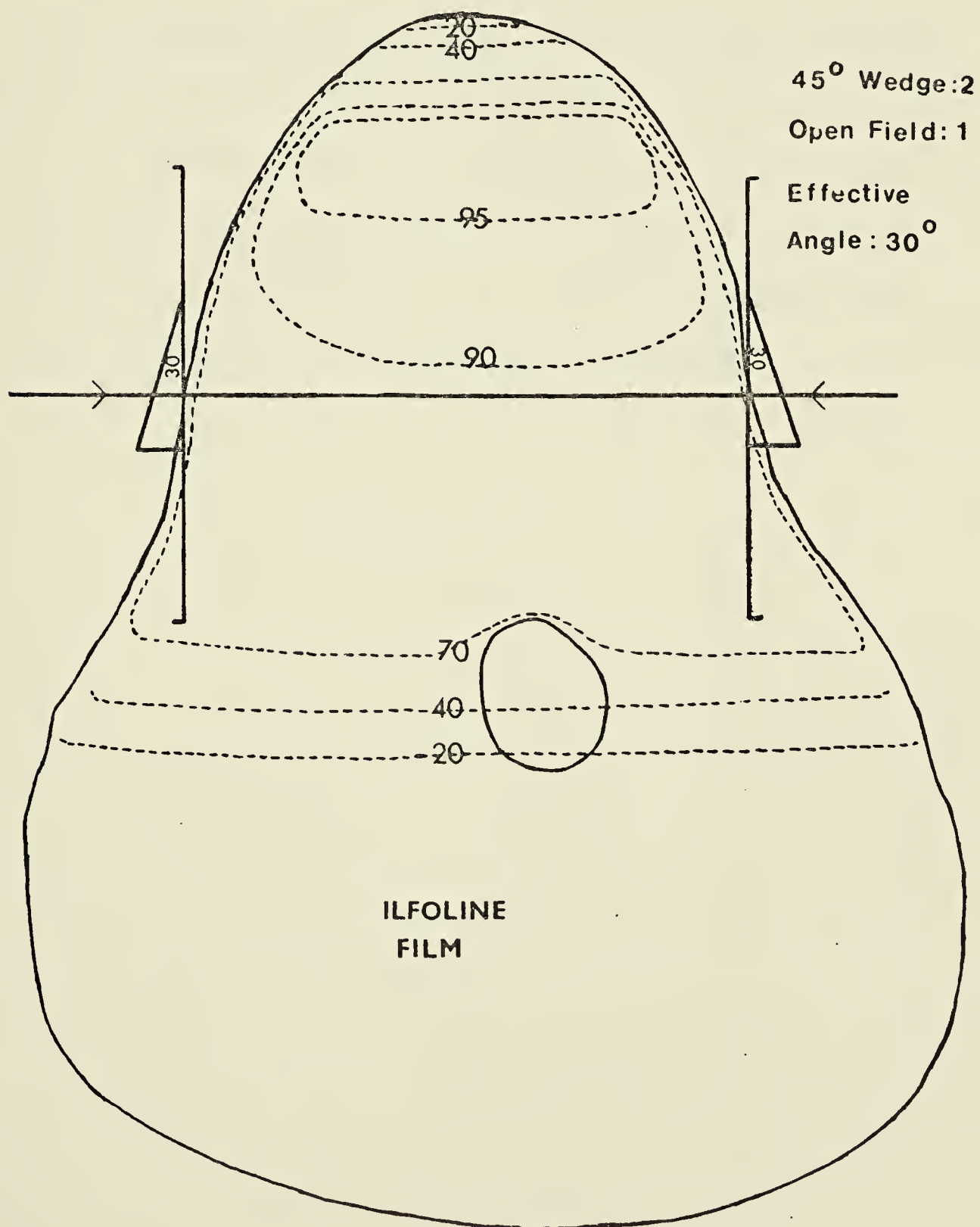


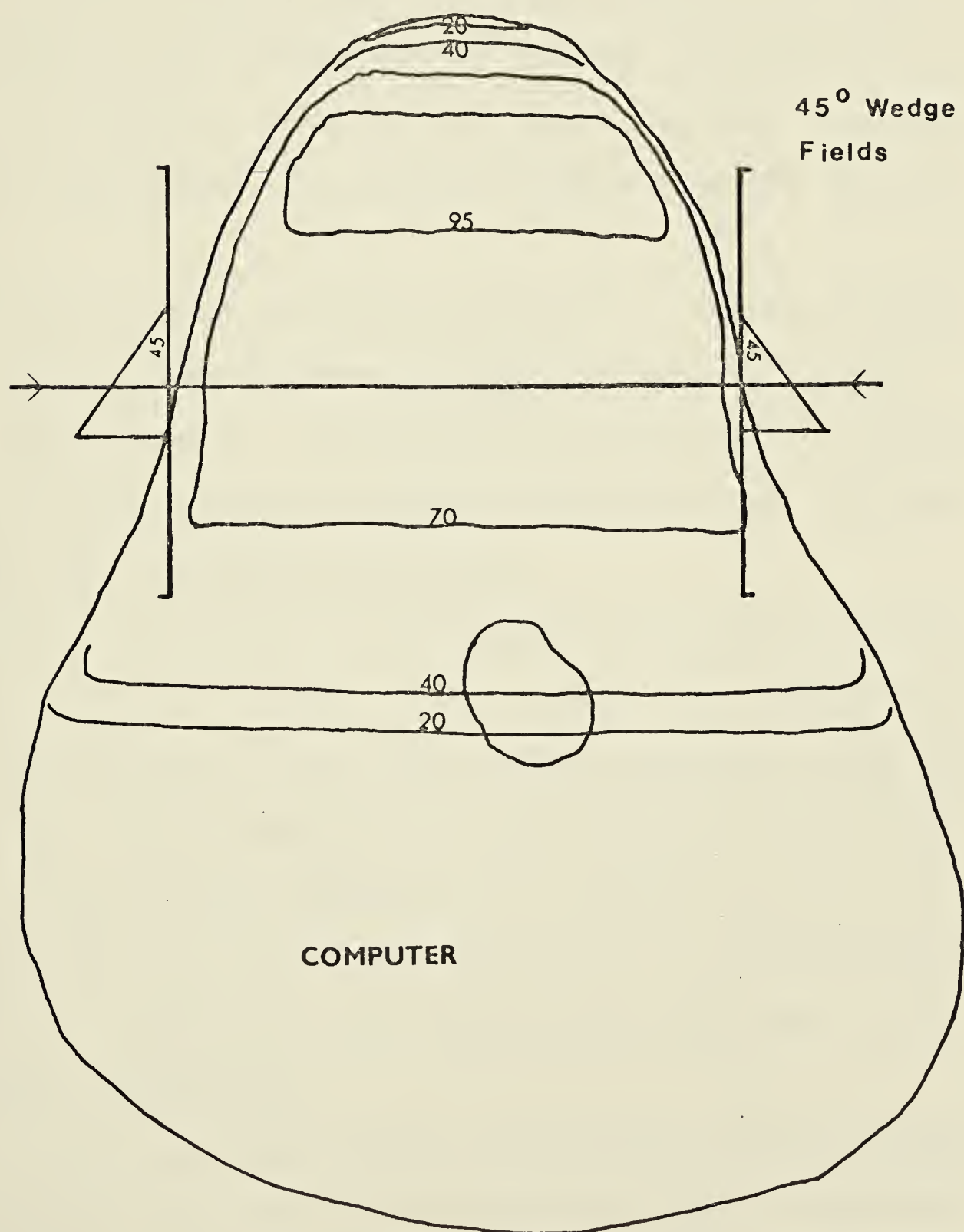
Fig. 36 Resultant Isodose Distribution for Two Opposing 8 x 8(w) cm, 80 cm SSD, Cobalt-60 30° Wedge Fields for the same contour and target volume as in Fig. 35. The 30° Wedge derived from the 45° Wedge. Ratio of Given Dose with and without 45° Wedge 2:1.



opposing wedge fields, 8x8(w), with the 45° and 30° angles on the level of the tonsil of the Rando Phantom. Fig. 37 shows the isodose distributions for the 45° wedge produced by the PC-12 computer and can serve as a comparison.

In the examples presented, the particular section of Rando Phantom Man which contains the tonsil area was chosen to illustrate the chief advantage of film emulsion, viz. its resolution aspect, as there is only one dosimetric point available over the entire region for either LiF dosimeter or ionization chamber.

Fig. 37 Resultant Isodose Distribution for Two Opposing 8 x 8(w) cm, 80 cm SSD, Cobalt-60 Beams modified by a 45° Wedge Filter for the same contour and target volume as in Fig. 35. The diagram shown here is redrawn from the one produced by the PC-12 Computer and serves as a comparison.



4.3 Uniform Beam, Inhomogenous Phantom

So far the phantom into which the film is inserted has been assumed to be homogenous. In an actual treatment situation, air gaps and tissues of different density exist in the human body. When an inhomogenous phantom, the Rando Phantom Man, is used, the scatter dose contributions may exaggerate the energy dependence of the film emulsion; when this is taken together with the angular dependence, the results obtained can be unreliable.

However, film emulsions can still serve the purpose of giving a comprehensive qualitative mapping despite these difficulties. To obtain more quantitative results, a less energy dependent detector should be used to complement the readings of the film.

The combination of LiF dosimeter and film emulsion can be fruitful (Vacirca et al., 1972). LiF dosimeter was used because of its lower energy dependence than film emulsion. In the case of LiF, the relative sensitivity ratio of low energy radiation to 1.25 MeV is about 1.4 to 1, while in the case of film emulsion, it is between 30 to 80 to 1, depending upon the emulsion type and the development conditions.

In the following example illustrating this LiF-film combination, the film was NDT 55 which shows a relative sensitivity ratio of low energy radiation to 1.25 MeV of about 50 to 1.

The example used the head region of the Rando Phantom Man; the whole phantom, in fact, resembles the situation of a limited phantom. A reduction in the scattered radiation reaching the film, therefore, can give a linear response for the film. Fig. 38 gives the calibration graph which, indeed, shows a linear function between the net density and LiF readings.

With this linearity, the measurements can be taken directly from the film. Fig. 39 shows the isodose distribution with a 36 cm.² field, SSD of 80 cm., cobalt radiation beam traversing near the section of the tonsil area. The dose reading from the film compares favorably with that from LiF, the discrepancy being less than 3% in the central region of the fields.

However, in the penumbral region, the results obtained from both the film and the LiF dosimeter can be in error. The LiF dosimeter gives an ambiguous resolution since its physical dimension covers the area of isodose of 50-30% at the penumbral region as measured by the film. The discrepancy between the two detectors at the penumbral region is within 30%.

This technique of LiF-film combination can be further extended to mapping out the isodose distributions in such irregular fields as the Mantle and the Inverted Y fields in the treatment of Hodgkin's Disease.

In such treatment, fields with sizes greater than

Fig. 38 Calibration Graph for Lithium Fluoride (TLD) and Film (NDT 55)

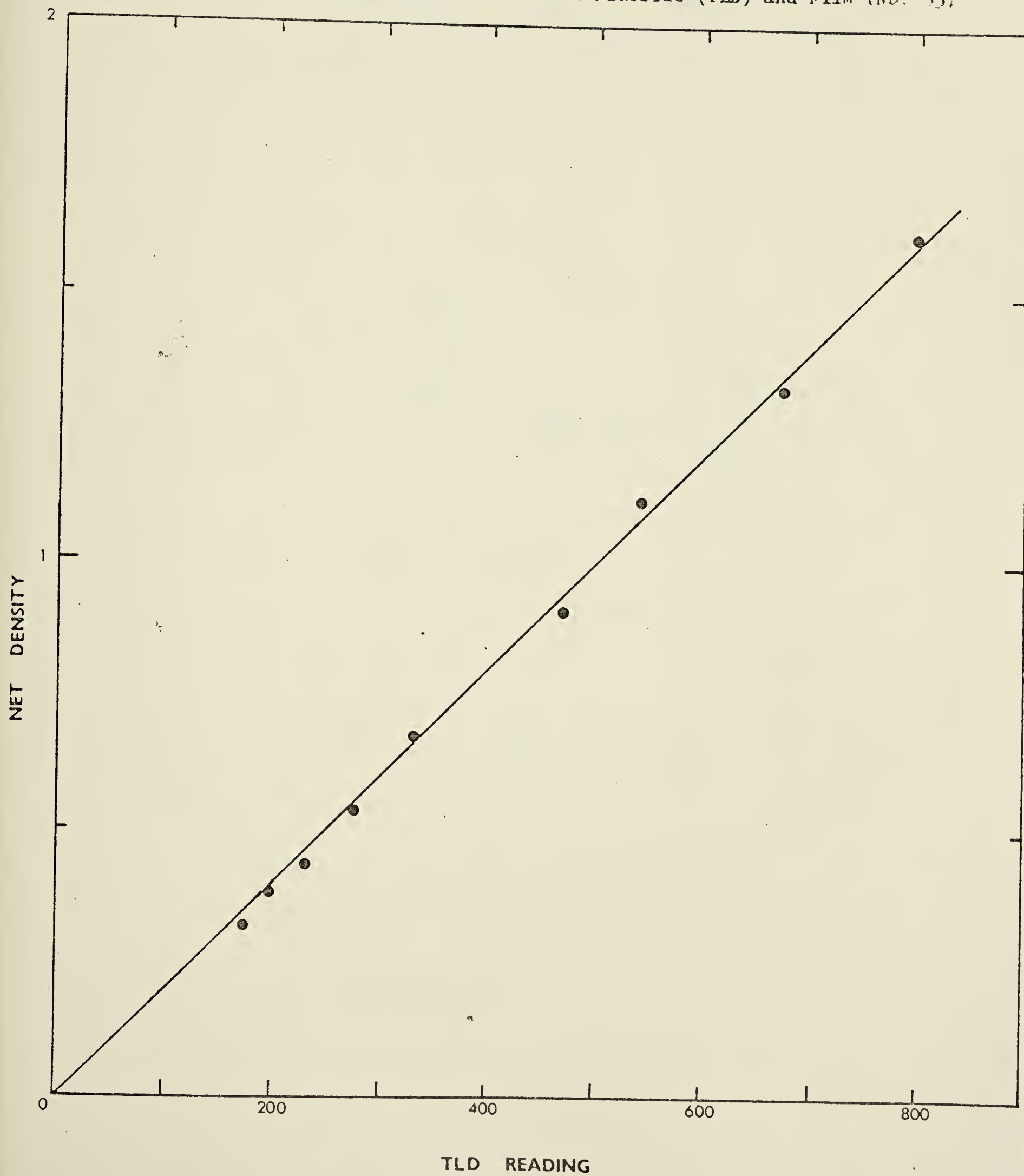
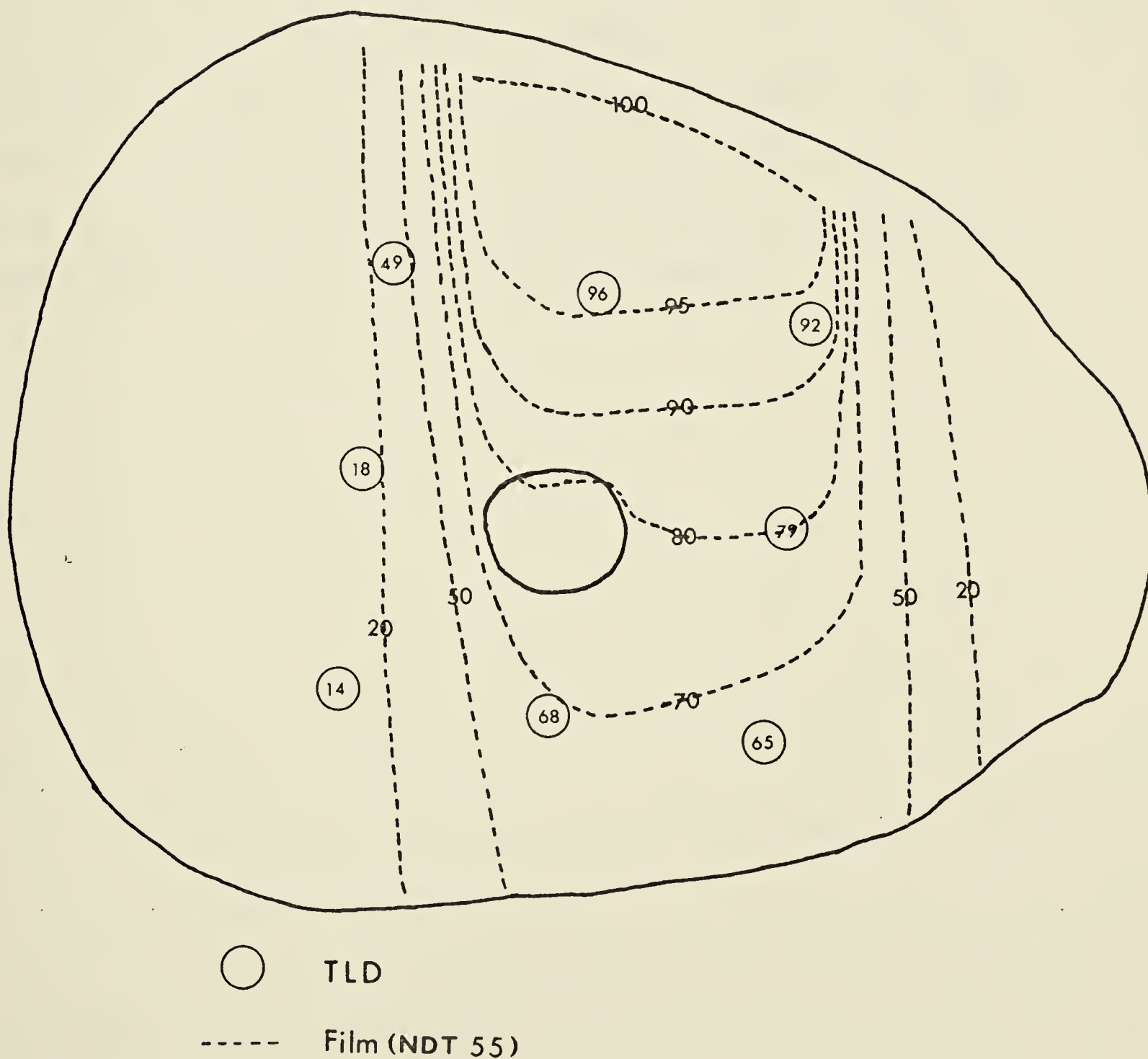


Fig. 39 Isodose Distribution for a 6 x 6 cm Field at 80 cm SSD for Cobalt-60 Radiation at the level of the tonsil area. This Figure illustrates the result of the method of combining LiF (TLD) and Film.



900 cm.² are used; the energy dependence of the film becomes excessive. With the use of a LiF dosimeter, the measurements should still be sufficiently accurate. In this situation, a different calibration graph is required; but the linearity of the film response is not necessary, as long as the density of the film can be correlated with the LiF readings on a one-to-one basis. The spatial resolution of the LiF dosimeter is insufficient to give the complete picture inside the Rando Phantom Man, but suitable combinations of LiF dosimeters and films may map out every small detail of the dose distribution.

CHAPTER V

CONCLUSIONS

5.1 Discussions and Observations

5.1.1 Energy Dependence

The lack of accuracy of film in photographic gamma ray dosimetry arises mainly from its energy dependence. By comparison, the angular dependence and the factors involved in the development conditions make a relatively small contribution to the inaccuracy of this method.

The energy dependence of photographic emulsion is reflected in the measurements of percentage depth doses in which the results as obtained from film are higher than the accepted values. This dependence can be directly demonstrated by the relative sensitivity graph (Fig. 10) which displays a greatly enhanced response per rad of absorbed dose for low energy radiation.

The enhancement of response of the emulsion arises from the fact that an emulsion contains silver halide grains which are of higher atomic number than soft tissue. This, then, implies that the emulsion undergoes a greater photoelectric process and absorbs a greater dose than tissue at low energy radiations.

Films, such as Fuji Medical and Kodak M, demonstrate different relative sensitivities towards low energy radiations. This difference is the result of different emulsion properties, which depend upon such diverse parameters as emulsion thickness, contents of impurities, concentration

of silver halide, size of individual grain, etc. Hence, the energy absorption of an emulsion does not depend solely upon the silver halide grains, but is a resultant of the composite functions of the above parameters.

The selection of a less energy dependent film for dosimetric purposes obviously demands favorable combinations of the above parameters, so that a ratio of the energy absorption in the emulsion to that in tissue can approximate the value of 1 for most radiation energies.

In a theoretical semi-qualitative analysis, Greening (1951), using a film model consisting of gelatin and pure silver bromide, pointed out that much of the energy transferred by x-rays to electrons within the bromide crystals is expended outside the grains in the gelatin -- it can be as high as 90% in the case of 0.1 MeV x-rays.

Therefore, in order to reduce the absorption of low energy radiation by the emulsion, Greening suggested two possible solutions: either reducing the emulsion thickness so that low energy radiation can escape without being totally absorbed, or decreasing the ratio of the concentration of silver halide to gelatin.

The compatibility of the theory and the experimental results in the determination of a less energy dependent film has been pointed out by Mauderli et al. (1960) and Onai et al. (1972).

Mauderli et al. showed that Kodak Fine Grain Positive

film, of thinner emulsion than Kodak M, demonstrated better percentage depth doses than the latter film. From their experimental data, Onai et al. further pointed out that, in addition to emulsion thickness, the concentration of silver halide also controlled the degree of energy dependence of a film.

The difference between Kodak M and Ilfoline films in their relative sensitivities towards low energy radiations can be explained.

In the present study, it was found that the thickness of Kodak M film is 30.7 mg./cm.^2 , compared to the values reported as 29 and 24.5 mg./cm.^2 by Mauderli et al. and Onai et al. respectively. The thickness of Ilfoline film is 16.9 mg./cm.^2 . The emulsion thickness of Kodak M films on one side of the film base is 3.1 mg./cm.^2 ; that of Ilfoline is 1.6 mg./cm.^2 . Kodak M film has emulsions on both sides of the base, while Ilfoline film has a single coating.

The concentration of silver halide grains in Kodak M film is approximately 2.0 mg./cm.^2 , whereas that in Ilfoline is about 0.4 mg./cm.^2 (both are manufacturers' data). The ratio of the concentrations of silver halide to gelatin is 0.47 for Kodak M and 0.33 for Ilfoline. Hence, the greater energy dependency of Kodak M than Ilfoline is understandable.

5.1.2 Techniques to reduce the Effect of Energy Dependence

Even though a lesser energy dependent film has been

selected, the results obtained from it are still insufficiently accurate to approximate the accepted values of percentage depth doses of large field sizes in a semi-infinite phantom.

Various operational techniques have been proposed to minimize the inaccuracy of this photographic method:

1. Granke et al. (1954) suggested that the published central axis depth doses could be used to interpret the density on an individual film. At any depth along the central axis of any single field, the density corresponding to the percentage depth dose could be used to plot that particular percentage isodose curve.

The usefulness of Granke's technique is based upon the premise that, anywhere within the radiation field, equal densities on the film represent equal doses received.

However, in the penumbral region, the contribution of dose to a particular point is primarily scattered radiation. Therefore, the components of the dose in the penumbral region are significantly different from those constituting the central axis depth dose.

The implication of this difference in components is that, since film shows excessive response towards scattered low energy radiation, identical densities measured along the central axis and at the penumbral region cannot be simply inferred to be the same dose.

Thus, Granke's method of interpretation of isodose curves in the penumbral region can lead to serious errors. This technique can be a good approximation with small field sizes where the contribution of scattered radiations is still small.

With large field sizes, the greatly exaggerated penumbral depth doses due to the scattered radiation simply cannot be overlooked. Moreover, this technique cannot be employed to determine the isodose distributions of multiple fields, since no accepted percentage depth dose values are usually published. Here, an ionization chamber or some other energy independent detectors are required to corroborate the film density.

If Granke's technique is to be used for the measurement of multiple fields, an alternative would be to attempt Loevinger and Spira's (1957) method of adding the densities of films together, as mentioned in section 4.1.2.

2. Mauderli et al. (1960) were the first to recognize that better approximations could be obtained from film by reducing the phantom materials surrounding the film.

In the perpendicular method, they reported that the difference in sensitivity between minimum and maximum thickness of phantom backing the film (Kodak M) showed a difference of 40% for the film, but of 5% for the ionization chamber with the same experimental set-up. This result serves as an indication of the magnitude of the sensitivity of the film to the backscattered radiation.

To reduce the energy dependence of film, they further proposed to reduce the phantom material backing the film in order to eliminate any possible backscattered radiation. However, in the case of large field sizes, this particular technique failed to approximate the accepted values. This was due to the fact that enlargement of the field sizes increased the amount of low energy forward scattered radiation. An increase in discrepancy can be expected, especially with films of the type of Kodak M, when the results are compared with the accepted values.

3. Instead of removing phantom materials backing the film, Stanton (1962), in the parallel method, reduced the materials on both sides of the film.

His method has been shown in this study to be quite useful for obtaining approximations to the best possible results with less than 10% error.

This limited phantom technique has been extended to find the isodoses of multiple fields. With the proper phantom thickness for a particular film, the results in the high dose region of the multiple fields, i.e. at the junction of all the fields on the target areas, could produce a displacement error of, at best, less than 1 cm. However, the junction of the penumbral regions contained the largest error: the displacement error was sometimes greater than 1 cm.

If exact results are required, then an ionization chamber is needed to corroborate the film density in this

limited phantom technique.

5.1.3 Angular Dependence

On the subject of angular dependence, its exact mechanism in photographic gamma ray dosimetry is still uncertain. The theoretical considerations given in section 2.5 cannot fully predict the angular dependence as displayed by films of the Kodak M type.

One possible explanation in the underestimation of angular dependence for Kodak M involves the role of the exposing actions imparted by the secondary electrons which the theoretical consideration fails to take into account.

To simplify the discussion, a parallel beam of electrons incident at an angle θ to the plane of the film is considered. With high energy electrons, the energy removal from the beam by the emulsion resembles that of x- or gamma rays. Hence, the important parameters determining the amount of angular dependence are similar to those for x- or gamma rays, i.e. μ , mass energy-absorption coefficient, and d , thickness of emulsion, as shown in section 2.5.

With μ not varying radically from emulsion to emulsion at high energy radiation, d becomes essentially the factor determining angular dependence. This conclusion that emulsion thickness plays an important role in angular dependence has already been deduced in the experiment for cobalt radiation.

With low energy electrons which, as pointed out in section 2.2.4, cannot fully penetrate the emulsion layer, complete energy absorption per unit area of emulsion may be expected. Then, the situation of angular dependence is considerably more complicated than in the case of high energy electrons. As experimental data are still insufficient, any discussion of angular dependence of low energy radiations will tend to be of a highly speculative nature.

However, one experimental fact is clear; a single emulsion film displays somewhat less angular dependence than a double emulsion one for low energy radiation, as supported by the results from Ilfoline film when compared to those from Kodak M film.

Since photographic gamma ray dosimetry is probably more frequently used for high energy radiation, the problem of angular dependence can be reduced by considering the choice of a thin emulsion film. Hence, angular dependence should create less inaccuracy than energy dependence.

5.1.4 Film as a Supplementary Detector

In a situation where both angular dependence and multiple scattered radiations cannot be avoided, an ionization chamber or other detector known to be independent of both angular and energy dependences has to be introduced as the only quantitative measuring detector. Film can only be supplementary as a continuous qualitative mapping device, but may be able to provide quantitative information if used with another detector.

5.1.5 Comparisons among Films

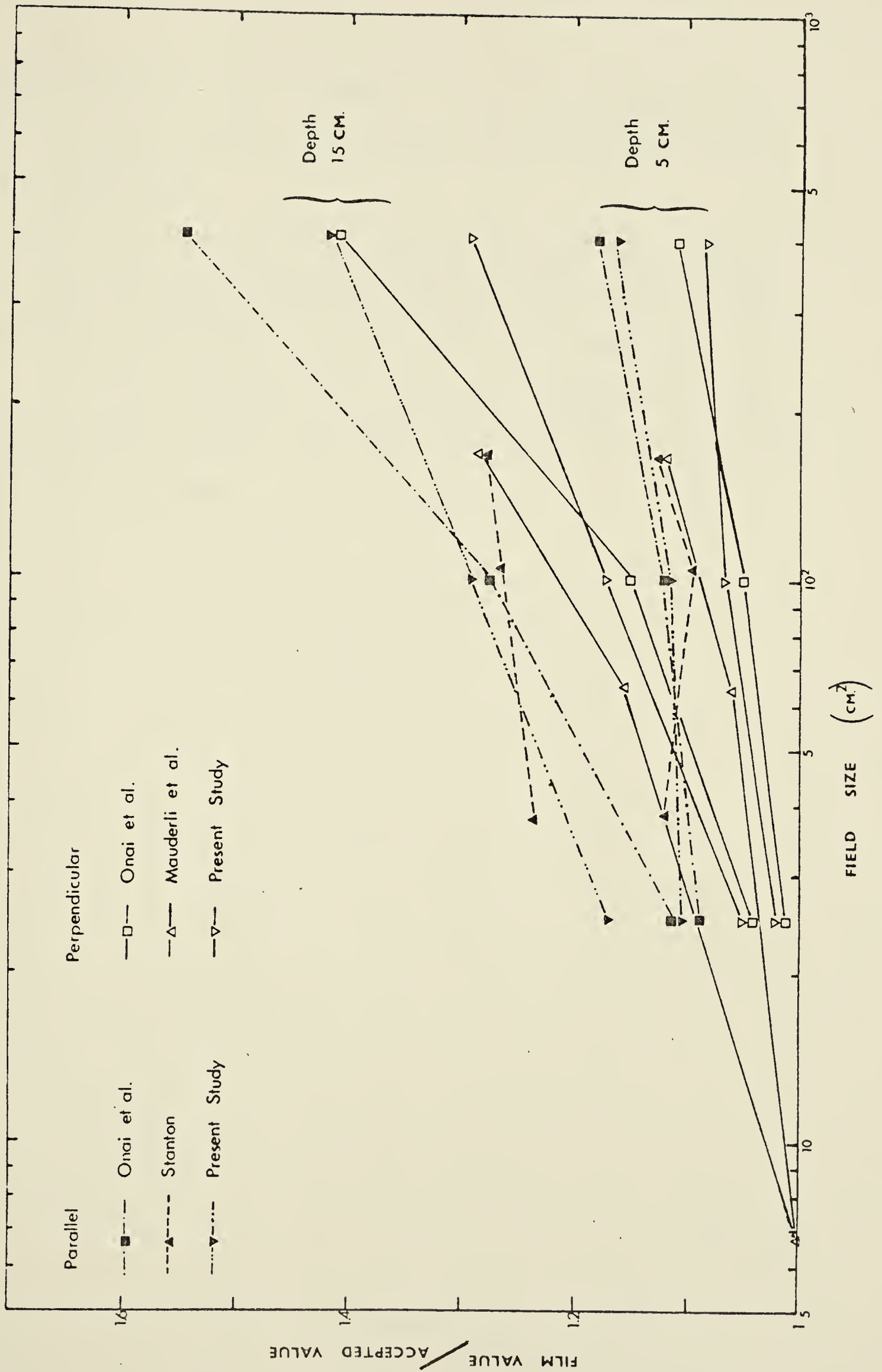
Mauderli et al. (1960), Stanton (1962), and Onai et al. (1972) have all utilized Kodak M films for the purpose of depth dose measurements with a semi-infinite phantom for cobalt radiation (in the case of Stanton's experiment, a semi-infinite phantom implies only a 8.8 cm. thick tissue-equivalent material on each side of the film).

The comparison of their results with those of the present study is demonstrated in Fig. 40 which plots the ratio of the percentage depth doses as measured by film to the accepted values, against the field sizes at the depths of 5 and 15 cm. With Mauderli et al. and Onai et al., the SSD is 50 cm., whereas Stanton and the present study use the SSD of 70 and 80 cm. respectively.

From Fig. 40, it is apparent that no absolute agreement among the data previously reported and presented in this study is obtained. This discrepancy is partially due to the processing conditions and the experimental materials, with the complexity of energy and angular dependences also playing an essential role. Here, one basic conclusion can be drawn, that the use of photographic emulsion as an accurate dosimeter is virtually impossible because of all the factors previously considered.

Onai et al. also used the single emulsion film, Fujilith Contact, to measure the percentage depth doses of

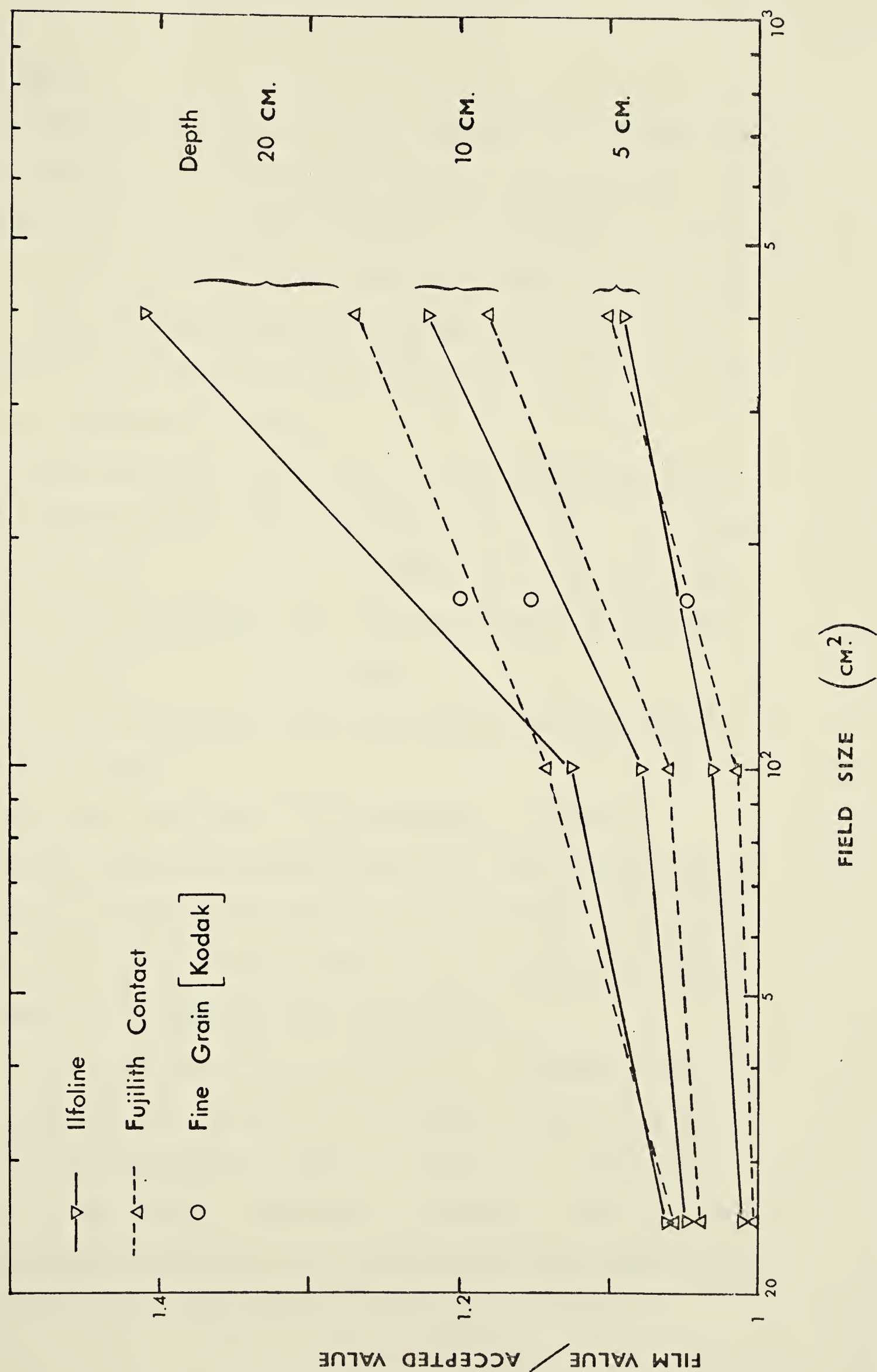
Fig. 40 Comparisons of Depth Doses as measured from Kodak M Films
by Different Investigators



cobalt radiation, while Mauderli et al. used Kodak Fine Grain Positive, also single-coated, for only one field size of 166 cm.²

The comparison of the results obtained with these two films and with Ilfoline in the present study by the perpendicular method is shown in Fig. 41 which plots the ratio of the percentage depth doses as measured by film to the accepted values, against the field sizes at depths of 5, 10 and 20 cm.

Fig. 41 Comparisons of Depth Doses as measured from
Different Single Emulsion Films



5.2 Summary

A mathematical model has been proposed to explain the energy dependence of photographic gamma ray dosimetry. The measurements of depth doses, because of the enhanced sensitivity of the silver halide grains to low energy as compared to high energy radiation, usually are higher than the conventional values as measured by an ionization chamber or an equivalent device.

However, manipulations of the processing conditions and the scattering material quantity can alter the results obtained from the film to approximate the conventionally accepted values of depth doses, thus giving both qualitative and quantitative information.

The following conclusions from the experimental results can be made:

1. Photographic Emulsion is a secondary dosimeter.
2. A single emulsion usually indicates both lesser degree of energy and angular dependences to radiation than double emulsion film, provided that the former possesses thinner total emulsion thickness than the latter.
3. No film, regardless of its emulsion thickness, will be able to measure the precise depth doses as well as a less energy dependent detector, except in the case where the presence of low energy radiation is minimal. With the proper processing conditions, the percentage depth doses will always exceed the conventionally accepted values.

In a semi-infinite phantom, the single-emulsion film can give good results of less than 10% error with small fields, up to 25 cm.² for cobalt radiation. With large fields where scattered radiation increases, a discrepancy of more than 40% can be expected.

4. Because of the angular dependence to the primary radiation, the depth dose measurement obtained by the parallel method with a large angular dependent (thick emulsion) film shows a difference in the results from those obtained by the perpendicular method.

5. With a suitable choice of film, good approximations to the accepted values of percentage depth doses can be obtained by using the limited phantom technique for the simple and the multiple fields. The displacement errors of the best possible results are less than 1 cm. in the high dose region of the multiple fields.

6. For more precise results, the technique of combining LiF and photographic emulsion can be useful in giving reliable dose readings and comprehensive information of the radiation fields. It is also relatively simple and convenient for routine use.

BIBLIOGRAPHY

- Attix, F. H. (1968). Health Phys. 15, 49.
- Bagne, F. (1974). Medical Phys. 1, 266.
- Barkas, W. H. (1963). Nuclear Research Emulsions, Part I: Techniques and Theory, p. 45. (Academic Press, New York).
- Becker, K. (1966). Photographic Film Dosimetry (The Focal Press, London and New York).
- British Journal of Radiology Supplement 11. (1972). Central Axis Depth Dose Data for Use in Radiotherapy, M. Cohen, D.E.A. Jones and D. Greene (Eds). (British Institute of Radiology, London).
- Bromley, D. and Herz, R. H. (1950). Proc. Phys. Soc. (London), B63, 90.
- Bruce, W. R. and Pearson, M. L. (1962). Rad. Res. 17, 555.
- Buchignani, J. S. and Howlett, P. (1973). Radiology, 108, 213.
- Charlesby, A. (1940). Proc. Phys. Soc., (London), 52, 657.
- Clarkson, J. R. (1941). Brit. J. Radiol., 14, 265.
- Derbowka, R. M. and Cormack, D. V. (1965). Brit. J. Radiol. 38, 653.
- Dudley, R. A. (1954). Nucleonics, 12, No. 5, 24.
- Dudley, R. A. (1968). Dosimetry with Photographic Emulsion in F. H. Attix and W. C. Roesch (Eds.) Radiation Dosimetry II (Academic Press, New York).
- Ehrlich, M. (1954). Photographic Dosimetry of X- and Gamma Rays, N. B. S. Handbk. 57.
- Farnell, G. C. (1966). The Relationship between Density and Exposure in C.E.K. Mees and T. H. James (Eds.) The Theory of the Photographic Process (The Macmillan Co., New York).
- Farnell, G. C. and Solman, L. R. (1963). J. Photo. Sci., 11, 347.

Bibliography

- Frey, K. W. (1957). Fortschr. Geb. Roentgestr. Nuklearmed., 87, 378.
- Golden, R. and Tochilin, E. (1959). Health Phys., 2, 199.
- Granke, R. C., Wright, K. A., Evans, W. W., Nelson, J.E. and Trump, J.G. (1954). Am. J. Roent. & Rad. Ther., 72, 302.
- Greening, J. R. (1951). Proc. Phys. Soc., (London), B64, 977.
- Gurney, R. W. and Mott, N. R. (1938). Proc. Roy. Soc. A164, 151.
- Hamilton, J. F. (1966). Photographic Effects of Electron Beams, X-Rays and Gamma Rays in C.E.K. Mees and T.H. James (Eds.) The Theory of the Photographic Process (The MacMillan Co., New York).
- Heard, M. J., Cook, J. E. and Holt, P. D. (1960). Photographic Emulsion Dosimetry and the A.E.R.E. Dosimeter. A.E.R.E. - R 3300.
- Hendee, W. R. (1973). Medical Radiation Physics. (Year Book Medical Publishers, Inc., Chicago).
- Herz, R. H. (1969). Photographic Action of Ionizing Radiation. (Wiley-Interscience, New York).
- Hettinger, G. and Svensson, H. (1967). Acta Radiol. Ther. Phys. Biol., 6, 74.
- Hine, G. J. (1950). Nucleonics, 7, No. 4, 18.
- Hine, G. J. (1954). Am. J. Roent. & Rad. Ther., 72, 293.
- Hoerlin, H. (1949). J. Opt. Soc. Am., 39, 891.
- Hurter, F. and Driffield, V. C. (1890). J. Soc. Chem. Ind., 9, 455.
- I.C.R.U. (1968). Radiation Quantities and Units, I.C.R.U. Report 11, Washington, D.C.
- Jacobi, C.A. and Paris D. Q. (1968). Textbook of Radiologic Technology (The C.V. Mosby Co., St. Louis).

Bibliography

- Jacobson, C.I. and Jacobson, R.E. (1972). Developing.
(The Focal Press, New York
& London).
- Johns, H. E. and Cunningham, J. R. (1974). The Physics
of Radiology (Charles C.
Thomas, Springfield, Ill.).
- Kathren, R. L. and Brodsky, A. (1963). Part III. Health
Phys., 9, 769.
- Kirchner, R. A. and Ryan, T. L. (1967). Health Phys., 13,
810.
- Kodak (1968). Photographic Material for the Graphic Arts:
A Kodak Graphic Arts Data Book. (Eastman
Kodak Co.).
- Lawrence, D. J. (1973). Med. Radiogr. Photogr., 49, 2.
- Lescrenier, C., Stacey, A.J. and Jones, C.H. (1965). Phys.
Med. Biol., 10,
567.
- Loevinger, R., Karzmark, C.J. and Weissbluth, M. (1960).
Radiology, 77, 906.
- Loevinger, R. and Spira, J. (1957). Am. J. Roent. and
Rad. Ther., 77, 869.
- Malmstadt, H.V. and Enke, C.G. (1969). Digital Electrons
for Scientists (W.A. Benja-
min, Inc., New York and Am-
sterdam).
- Mansfield, C. M., Suntharalingam, N. and Chow, M. (1974).
Am. J. Roent. and Rad. Ther., 120, 699.
- Mathewson, D.S. (1956). Brit. J. Radiol., 29, 63.
- Mauderli, W., Gould, D.M. and Lane, J.W. (1960). Am. J.
Roent. and Rad. Ther., 83, 520.
- McLaughlin, W. L. and Ehrlich, M. (1954). Nucleonics, 12,
No. 10, 34.
- Meredith, W.J. and Neary, G.J. (1944). Part I and II.
Brit. J. Radiol.,
17, 75 and 126.

Bibliography

- Mitchell, J.W. (1957). J. Photo. Sc., 5, 49.
- Murphy, W.T. (1967). Radiation Therapy. (W. B. Saunders Co., Philadelphia & London).
- Natrella, M.G. (1963). Experimental Statistics. N. B. S. Handbk. 91 p. 1-10.
- Neufeld, J. (1971). Health Phys., 21, 317.
- Noda, H., Ono, Y. and Umesaki, N. (1970). Nippon Acta Radiol., 30, 1.
- Nutting, P.G. (1913). Phil. Mag. 26, 423.
- Okrent, D. and Solomon, A. K. (1951). Phys. Rev., 83, 826.
- Onai, Y., Tomaru, T., Irifune, T. and Uchida, I. (1970). Nippon Acta Radiol., 29, 1474.
- Onai, Y., Tomaru, T., Irifune, T. and Uchida, I. (1972). Nippon Acta Radiol., 31, 1224.
- Paic, V. and Paic, M. (1971). Health Phys., 20, 259.
- Payne, W.H., Waggoner, R.G., Levy, L.B. and Russell, J.R. (1974). Medical Phys., 1, 277.
- Pelc, S. R. (1945). Proc. Phys. Soc., (London). 57, 523.
- Pniewski, J. (1951). Acta Phys. Polonica, 11, 230.
- Price, C. (1973). Brit. J. Radiol., 46, 719.
- Piret, P., LeMaire, M. and Garsou, J. (1972). J. Belge Radiol., 55, 5, 533.
- Quimby, E.H., Cohen, B.S., Castro, V., and Meredith, W.J. (1956). Radiology 66, 667.
- Sharma, P. H. (1972). Master's thesis. University of Alberta, Edmonton.
- Silberstein, L. (1922). Phil. Mag. (6) 44, 257.
- Silberstein, L. and Trivelli, A.P.H. (1930). Phil. Mag. 2, 787.
- Stanton, L. (1960). Radiology 75, 416.

Bibliography

- Stanton, L. (1962). Radiology 78, 445.
- Tatcher, M. (1970). Radiology 97, 132.
- Tatcher, M., Barnea, I., and Loevinger, E. (1970). Brit. J. Radiol. 43, 664.
- Tellez-Plasencia, H. (1954). Sci. Ind. Phot. (2) 25, 425.
- Tochilin, E. (1955). Am. J. Roent. & Rad. Ther. 73, 265.
- Tochilin, E. and Golden, R. (1953). Nucleonics 11, #8, 26.
- Tochilin, E. and Golden, R. (1961). Health Phys. 4, 244.
- Tsien, K. C., and Robbins, R. (1966). Brit. J. Radiol. 39, 1.
- Tsunemoto, Koike, Ogawa, Kusumoto and Kurihara. (1966). Nippon Acta Radiol. 26, 876.
- Vacirca, S. J., Thompson, D. L., Pasternack, B. S., and Blatz, H. (1972). Phys. Med. Biol. 17, 71.
- Watson, E. G. (1959). Health Phys. 2, 207.
- Webb, J. H. (1939). J. Opt. Soc. Am. 29, 309.
- Webb, J. H. (1948). J. Opt. Soc. Am. 38, 312.
- Wilsey, R. B. (1934). Am. J. Roent. & Rad. Ther. 32, 789.
- Wilsey, R. B., Strangeways, D. H., and Corney, G. M. (1956). Part I and II, Radiology 66, 408 and 418.
- Wilson, F.C., Waggener, R.G., Rogers, L.F., Goff, D.L., and Zanca, P. (1972). Am.J. Roent. & Rad. Ther. 114, 610.
- Winkler, K. G. and Levin, S. G. (1966). Health Phys. 12, 345.
- Wyckoff, H. O., Allisy, A., and Lidén, K. (1976). Radiology 118, 233.
- Ziegler, C.A. and Chleck, D.J. (1960). Health Phys. 4, 32.

APPENDIX I
PHOTOGRAPHIC EMULSIONS

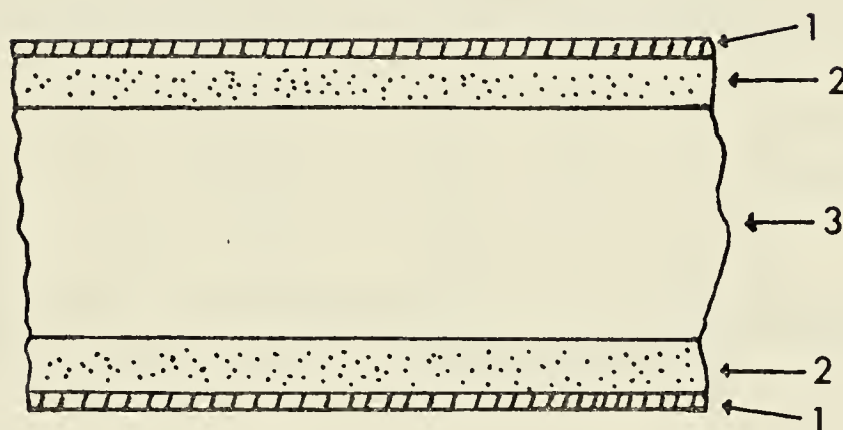
Since there are great varieties of films available for use in the measurement of radiation doses, the choice of a suitable film depends on the particular objective(s) of the experiments. Some of the more common films employed for the measurement of radiation dose in a phantom, especially for high energy radiations, are listed, according to the manufacturers, as follows:

- 1) Kodak: Industrial Type A (Granke et al., 1954), Type K (Tochilin and Golden, 1953) and Type M (Mauderli et al., 1960; Tochilin, 1959; Stanton, 1960 and 1962; Loevinger et al., 1960; Thatcher et al., 1970; Onai et al., 1970 and 1972; Noda et al., 1970);
- 2) Ilford: Ilford Line film (Thatcher et al., 1970; Lescrenier et al., 1965);
- 3) Fuji: Fujilith Contact film (Onai et al., 1972);
- 4) Gevaert-Agfa: Structurix D2 (Priest et al., 1972), HD 75 (Wilson et al., 1972) and Ansco-Superay HD (Tsien et al., 1966);
- 5) Dupont: Adlux (Loevinger and Spira, 1957).

APPENDIX II

STRUCTURE OF A DOUBLE

EMULSION FILM



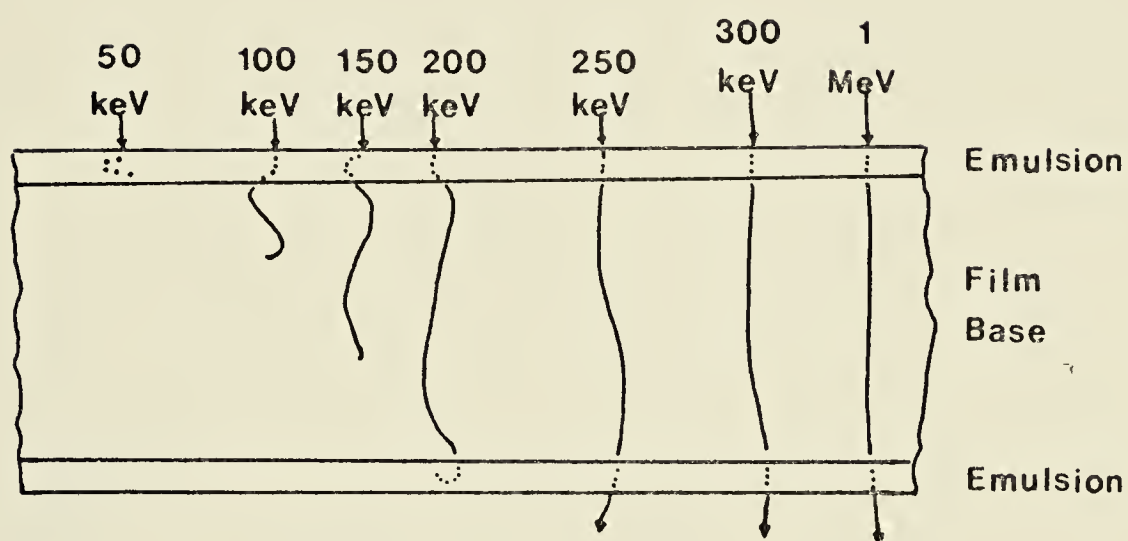
1. T COAT (Protective Layer)
2. EMULSION (With Silver Halide Grains)
3. FILM BASE

Cross Section of a Double Emulsion x-ray
Film. The Emulsion Layer consists of
Silver Halide suspended in gelatin.
(After Hendee, 1973)

APPENDIX III

PATHS OF ELECTRONS

THROUGH THE EMULSION

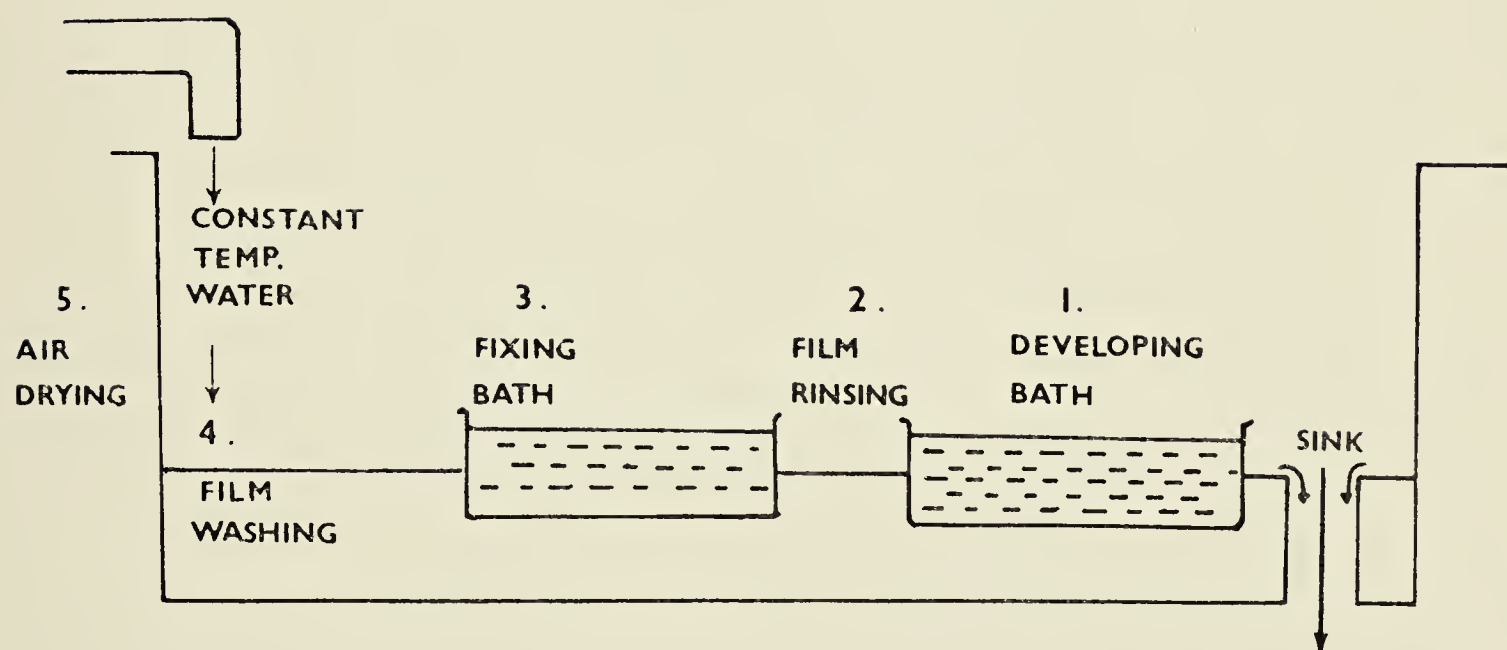


..... Grains Rendered Developable

↓ Path of Electron

The Paths of Electrons of Different
Radiation Energies perpendicularly
incident on a Double Emulsion Film
(After Hine, 1954).

APPENDIX IV
TRAY METHOD OF
PROCESSING FILMS



The Steps involved in the Manual (Tray)
Method of Processing Films in the
present study.

B30185